



Lawrence Berkeley Laboratory

UNIVERSITY OF CALIFORNIA

CHEMICAL SCIENCES DIVISION

Submitted to Macromolecules

An Equation-of-State Analysis of Binary Copolymer Systems:

1. Screening Effect
2. Homopolymer and Copolymer Mixtures
3. Miscibility Maps

T. Hino, Y. Song, and J.M. Prausnitz

January 1995



REFERENCE COPY
Does Not Circulate
Bldg. 50 Library.
LBL-36817
Copy 1

DISCLAIMER

This document was prepared as an account of work sponsored by the United States Government. While this document is believed to contain correct information, neither the United States Government nor any agency thereof, nor the Regents of the University of California, nor any of their employees, makes any warranty, express or implied, or assumes any legal responsibility for the accuracy, completeness, or usefulness of any information, apparatus, product, or process disclosed, or represents that its use would not infringe privately owned rights. Reference herein to any specific commercial product, process, or service by its trade name, trademark, manufacturer, or otherwise, does not necessarily constitute or imply its endorsement, recommendation, or favoring by the United States Government or any agency thereof, or the Regents of the University of California. The views and opinions of authors expressed herein do not necessarily state or reflect those of the United States Government or any agency thereof or the Regents of the University of California.

LBL-36817
UC-401
Preprint

An Equation-of-State Analysis of Binary Copolymer Systems:
1. Screening Effect
2. Homopolymer and Copolymer Mixtures
3. Miscibility Maps

Toshiaki Hino, Yuhua Song, and John M. Prausnitz*

Department of Chemical Engineering
University of California, Berkeley

and

Chemical Sciences Division
Lawrence Berkeley Laboratory
University of California
Berkeley, California 94720

January 1995

*To whom correspondence should be addressed.

This work was supported by the Director, Office of Energy Research, Office of Basic Energy Sciences, Chemical Sciences Division, of the U.S. Department of Energy under Contract No. DE-AC03-76SF00098.

AN EQUATION-OF-STATE ANALYSIS OF BINARY COPOLYMER SYSTEMS 1. SCREENING EFFECT

*Toshiaki Hino, Yuhua Song, and John M. Prausnitz **

Department of Chemical Engineering
University of California, Berkeley
and
Chemical Sciences Division
Lawrence Berkeley Laboratory
Berkeley, CA 94720

ABSTRACT

The screening effect is introduced into the recently presented perturbed hard-sphere-chain (PHSC) equation of state for copolymer systems. Using reactivity ratios of copolymerization kinetics, the model first computes the number of specific monomer sequences in the copolymer consisting of monomers A and B. Some of the AB and BA monomer sequences are then replaced by BB sequences to represent the screening effect of segment B on segment A in AB and BA sequences. The essential characteristic of the screening effect is the assumption that the solution properties of a copolymer correspond to those of another copolymer whose composition differs from that of the true copolymer. The screening effect theory is used to calculate miscibility maps for several poly(styrene-co-methyl methacrylate) random copolymers which exhibit lower-critical-solution-temperature phase behavior and significant deviation from the classical Flory-Huggins model. For a fixed temperature, there is good agreement between the theoretical miscibility map and experiment. The temperature dependence of the miscibility map, however, cannot be predicted using the same set of intersegmental parameters.

(Keywords: copolymer blend; equation-of-state; lower critical solution temperature; phase equilibria)

* To whom correspondence should be addressed.

INTRODUCTION

Song *et al.*¹⁻⁴ and Hino *et al.*⁵ recently presented a perturbed hard-sphere-chain (PHSC) equation of state applicable to mixtures of large heteronuclear chain molecules, i.e., copolymers. The PHSC equation of state for real copolymer mixtures⁵ is based on a modified form of Chiew's equation of state⁶ for athermal mixtures of heteronuclear hard-sphere chains by Song *et al.*¹ The PHSC equation of state also employs a van-der-Waals perturbation whose parameters are related to the intermolecular potential as suggested by Song and Mason². The sequence distribution in a copolymer was introduced only into the hard-sphere-chain reference state which represents repulsive interactions. The perturbation term which accounts for attractive forces was given in terms of segmental interaction energies. The segmental interaction energies depend only on the pair of segments of interest, independent of the type of segment adjacent to the segments of interest. The PHSC equation of state is able to represent lower critical solution temperature (LCST) phenomena as well as partial immiscibility with an upper critical solution temperature (UCST).

Comparison of the PHSC equation of state for copolymer systems with experiment was made for random copolymer systems containing two kinds of segments; these systems are denoted as $(A_X B_{1-X})_{r_1} / (A_Y B_{1-Y})_{r_2}$ where r_i is the number of effective hard spheres per molecule of component i and X and Y are segment number fractions for segment A in components 1 and 2, respectively⁵. Using the same set of intersegmental parameters at two different temperatures, calculated and experimental miscibility maps showed good agreement for the system containing poly(methyl methacrylate-*co*-butyl methacrylate) which does not exhibit screening effect. For the system containing poly(styrene-*co*-butyl methacrylate) which exhibits moderate screening effect, however, theory and experiment showed only semiquantitative agreement. In these systems, immiscibility is caused by LCST behavior.

A fundamental task in the development of molecular-thermodynamic models for copolymer systems is inclusion of the screening effect, an effect due to sequence distribution. To explain this effect, consider mixtures of random copolymers containing two kinds of segments. In the classical Flory-Huggins theory⁷⁻⁹, a unique interaction energy is assigned to a segment pair A and B. It is, however, conceivable that the interaction energy between a segment A in an AB or BA sequence (i.e., dyad) and a segment B in an AB or BA sequence can be different from that between a segment A in an AA sequence and a segment B in an AB or BA sequence. Their difference may follow from the screening effect of segment B on segment A in AB and BA dyads which is not present in an AA sequence. The screening effect in the liquid-liquid equilibria of copolymer systems was recently reported for several systems containing two kinds of segments: mixtures of poly(styrene-*co*-methyl methacrylate) random copolymers differing in copolymer compositions¹⁰.

In this work we present a simple method to include the screening effect into the previously presented PHSC equation of state for copolymer systems⁵. Theoretical miscibility maps with screening effect are computed for the system $(A_X B_{1-X})_{r_1} / (A_Y B_{1-Y})_{r_2}$. Comparison with experiment was made for mixtures containing poly(styrene-*co*-methyl methacrylate) random copolymers¹⁰ which exhibits LCST behavior and significant deviation from the classical Flory-Huggins model⁷⁻⁹.

THEORY

Equation of State for Copolymer Mixtures. Details of the perturbed hard-sphere-chain (PHSC) equation of state are given in References 1 to 5. The PHSC equation of state requires three parameters to describe the normal fluids including homopolymers: number of effective hard spheres per molecule, r ; segmental diameter, σ ; and non-bonded segment pair-interaction energy, ϵ . These parameters were regressed from available volumetric and vapor-pressure data for a variety of normal fluids and several

homopolymers; they are tabulated in Reference 2. For a homopolymer, one of the regressed characteristic quantities is r/M , where M is the molecular weight of polymer. The procedure to define the equation-of-state parameters for copolymer systems is discussed later. The PHSC equation of state also requires at least one or two adjustable intersegmental parameters for a given pair of dissimilar segments. Intersegmental parameters can be obtained from the critical points of mixtures and from the miscibility/immiscibility boundaries of miscibility maps.

The PHSC equation of state for mixtures of heteronuclear polymer molecules is⁵

$$\frac{p}{\rho k_B T} = 1 + \rho \sum_{i=1}^m \sum_{j=1}^m x_i x_j \left[\sum_{k=1}^{r_i} \sum_{l=1}^{r_j} b_{ij,kl} g_{ij,kl} \right] - \sum_{i=1}^m x_i \sum_{k=1}^{r_i-1} [g_{ii,k,k+1} - 1] - \frac{\rho}{k_B T} \sum_{i=1}^m \sum_{j=1}^m x_i x_j \left[\sum_{k=1}^{r_i} \sum_{l=1}^{r_j} a_{ij,kl} \right] \quad (1)$$

where p is the pressure, number-density $\rho=N/V$ (N is the number of molecules and V is the volume), k_B is the Boltzmann constant, T is the absolute temperature, m is the number of components; r_i and x_i are the number of effective hard spheres per molecule and the mole fraction, respectively, of component i ; and subscripts k and l denote the k -th and l -th segments, respectively, of hard-sphere chains. Equation (1) obeys the ideal-gas limit as $\rho \rightarrow 0$. In Eq. (1) $a_{ij,kl}$ is a parameter which reflects the strength of attractive forces between k -th effective hard sphere of component i and l -th effective hard sphere of component j ; $b_{ij,kl}$ represents the second virial coefficient of hard spheres or the van der Waals covolume for effective hard spheres that accounts for the excluded volume due to the repulsive forces in the Song-Mason theory²; and $g_{ij,kl}$ is the pair radial distribution function of hard spheres when k -th and l -th segments of components i and j , respectively, are at contact. These parameters are temperature-dependent, as discussed later. The perturbation term in Eq. (1) assumes random mixing of molecules. Equation (1) is for the

mixture of hard-sphere chains consisting of arbitrary numbers of chemically different segments. The segments in the chain need *not* have the same size.

We consider binary mixtures of copolymers consisting of two types of segments A and B:

$$(A_X B_{1-X})r_1 / (A_Y B_{1-Y})r_2 \quad (2)$$

The number of segments of type A per hard-sphere chain of component 1 is given by $r_{1,A}$ and that of type B per hard-sphere chain of component 1 is given by $r_{1,B}$:

$$r_{1,A} = r_1 X \quad (3)$$

$$r_{1,B} = r_1 (1 - X) \quad (4)$$

Similarly, the number of segments of type A and that of type B per hard-sphere chain of component 2 are given by $r_{2,A}$ and $r_{2,B}$, respectively:

$$r_{2,A} = r_2 Y \quad (5)$$

$$r_{2,B} = r_2 (1 - Y) \quad (6)$$

For binary mixtures of copolymers, Eq. (1) is⁵

$$\begin{aligned}
\frac{p}{\rho k_B T} = & 1 + \rho \sum_{i=1}^2 \sum_{j=1}^2 x_i x_j \left[r_{i,A} r_{j,A} b_{ij,AA} g_{ij,AA} + r_{i,A} r_{j,B} b_{ij,AB} g_{ij,AB} \right. \\
& \left. + r_{i,B} r_{j,A} b_{ij,BA} g_{ij,BA} + r_{i,B} r_{j,B} b_{ij,BB} g_{ij,BB} \right] \\
& - \sum_{i=1}^2 x_i \left[n_{i,AA} (g_{ii,AA} - 1) + n_{i,AB} (g_{ii,AB} - 1) + n_{i,BA} (g_{ii,BA} - 1) + n_{i,BB} (g_{ii,BB} - 1) \right] \\
& - \frac{\rho}{k_B T} \sum_{i=1}^2 \sum_{j=1}^2 x_i x_j \left[r_{i,A} r_{j,A} a_{ij,AA} + r_{i,A} r_{j,B} a_{ij,AB} + r_{i,B} r_{j,A} a_{ij,BA} + r_{i,B} r_{j,B} a_{ij,BB} \right] \quad (7)
\end{aligned}$$

where $n_{i,\alpha\beta}$ ($i=1,2$; $\alpha,\beta=A,B$) is the number of $\alpha\beta$ sequences per molecule in component i and

$$n_{i,AA} + n_{i,AB} + n_{i,BA} + n_{i,BB} = r_i - 1 \quad (i=1,2) \quad (8)$$

The subscript $ij,\alpha\beta$ ($i,j=1,2$; $\alpha,\beta=A,B$) of parameters and the pair distribution function in Eq. (7) denotes a pair of segment α of component i and segment β of component j . With a substitution of appropriate segments into segments A and B, Eq. (7) is also applicable to mixtures of type $(A_X B_{1-X})_{r_1} / (C_Y B_{1-Y})_{r_2}$ and $(A_X B_{1-X})_{r_1} / (C_Y D_{1-Y})_{r_2}$. For mixtures of type $(A_X B_{1-X})_{r_1} / (C_Y B_{1-Y})_{r_2}$ we replace segment A of component 2 by segment C. Similarly, for mixtures of type $(A_X B_{1-X})_{r_1} / (C_Y D_{1-Y})_{r_2}$ we replace segments A and B of component 2 by segments C and D, respectively.

For a mixture of type $(A_X B_{1-X})_{r_1} / (A_Y B_{1-Y})_{r_2}$, parameters $a_{ij,\alpha\beta}$ and $b_{ij,\alpha\beta}$ and the radial distribution function $g_{ij,\alpha\beta}$ ($i,j=1,2$; $\alpha,\beta=A,B$) are⁵

$$a_{ii,\alpha\alpha} = \frac{2}{3} \pi \sigma_{i,\alpha}^3 \varepsilon_{i,\alpha} F_a(\tilde{T}_{i,\alpha}) \quad (9)$$

$$a_{ij,\alpha\beta} = a_{ji,\beta\alpha} = \frac{2}{3} \pi \sigma_{ij,\alpha\beta}^3 \varepsilon_{ij,\alpha\beta} \sqrt{F_a(\tilde{T}_{i,\alpha}) F_a(\tilde{T}_{j,\beta})} \quad (10)$$

$$b_{ii,\alpha\alpha} = b_{i,\alpha} = \frac{2}{3} \pi \sigma_{i,\alpha}^3 F_b(\tilde{T}_{i,\alpha}) \quad (11)$$

$$b_{ij,\alpha\beta} = b_{ji,\beta\alpha} = \frac{1}{8} (b_{i,\alpha}^{1/3} + b_{j,\beta}^{1/3})^3 \quad (12)$$

$$g_{ij,\alpha\beta} = g_{ji,\beta\alpha} = \frac{1}{1-\eta} + \frac{3}{2} \frac{\xi_{ij,\alpha\beta}}{(1-\eta)^2} + \frac{1}{2} \frac{\xi_{ij,\alpha\beta}^2}{(1-\eta)^3} \quad (13)$$

where η is the packing fraction

$$\eta = \frac{\rho}{4} \sum_{i=1}^2 x_i (r_{i,A} b_{i,A} + r_{i,B} b_{i,B}) \quad (14)$$

Variable η is a particular form of the reduced density. Similarly, variable ξ is a more general reduced density

$$\xi_{ij,\alpha\beta} = \xi_{ji,\beta\alpha} = \frac{\rho}{4} \left[\frac{b_{i,\alpha} b_{j,\beta}}{b_{ij,\alpha\beta}} \right]^{1/3} \sum_{i=1}^2 x_i (r_{i,A} b_{i,A}^{2/3} + r_{i,B} b_{i,B}^{2/3}) \quad (15)$$

In Eqs. (9) to (11), $\sigma_{i,\alpha}$ and $\sigma_{ij,AB}$ are the separation distances between similar and dissimilar segments, respectively, at the minimum potential energies $\varepsilon_{i,\alpha}$ and $\varepsilon_{ij,AB}$, respectively, in the segment-segment pair potential. We use the following combining rules to obtain parameters $\sigma_{ij,\alpha\beta}$ and $\varepsilon_{ij,\alpha\beta}$:

$$\sigma_{ij,\alpha\beta} = \sigma_{ji,\beta\alpha} = \frac{1}{2} (\sigma_{i,\alpha} + \sigma_{j,\beta}) \quad (16)$$

$$\varepsilon_{ij,\alpha\beta} = \varepsilon_{ji,\beta\alpha} = \sqrt{\varepsilon_{i,\alpha} \varepsilon_{j,\beta}} (1 - \kappa_{ij,\alpha\beta}) \quad (17)$$

and

$$\sigma_{ii,\alpha\alpha} = \sigma_{i,\alpha} \quad (18)$$

$$\varepsilon_{ii,\alpha\alpha} = \varepsilon_{i,\alpha} \quad (19)$$

where $\kappa_{ij,\alpha\beta}$ is an adjustable intersegmental parameter whenever $\alpha \neq \beta$.

Equation (12) assumes additivity of effective hard-sphere diameters of unlike segments and that of similar segments in different components. In Eqs. (9) to (11) F_a and F_b are the universal functions of reduced temperature defined as

$$\tilde{T}_{i,\alpha} = \frac{k_B T}{\varepsilon_{i,\alpha} s(r_i)} \quad (20)$$

where $s(r_i)$ is a scaling parameter that depends only on r_i . The scaling parameter $s(r_i)$ in the reduced temperature arises from the scaling of F_a and F_b from single-sphere systems to systems containing polymer molecules; $s(r)$ is given in Reference 2.

Equations (9) and (11) follow from the Song-Mason method² which scales the effective van der Waals covolume, b , (i.e., second virial coefficient of hard spheres) and the attractive energy parameter, a , in terms of the well depth of the pair potential, ε , and the distance of separation at minimum potential energy, σ . The universal functions F_a and F_b account for the temperature dependences of parameters a and b , respectively. Equation (10) assumes a geometric mean of F_a for a segment A and that for a segment B to calculate the temperature dependence of the attractive energy parameter between a pair of dissimilar segments A and B . Equation (10) also assumes a geometric mean of F_a for a pair of similar segments in different components. The universal functions are obtained from volumetric and vapor-pressure data for argon and for methane as indicated previously². They are represented by the following empirical relations²:

$$F_a(\tilde{T}_{i,\alpha}) = 0.7170 + 1.9003 \exp(-0.5152 \tilde{T}_{i,\alpha}) \quad (21)$$

$$F_b(\tilde{T}_{i,\alpha}) = 0.5849 \exp(-0.4772 \tilde{T}_{i,\alpha}) + (1 - 0.5849) \left[1 - \exp(-1.0669 \tilde{T}_{i,\alpha}^{-1/4}) \right]. \quad (22)$$

Finally, an additional adjustable parameter $\zeta_{ij,\alpha\beta}$ can be introduced if necessary to relax the additivity of effective hard-sphere diameters of unlike segments such that

$$b_{ij,\alpha\beta}^{1/3} = b_{ji,\beta\alpha}^{1/3} = \frac{(b_{i,\alpha}^{1/3} + b_{j,\beta}^{1/3})}{2} (1 - \zeta_{ij,\alpha\beta}) \quad (23)$$

where $\zeta_{ij,\alpha\beta}$ is an adjustable intersegmental parameter whenever $\alpha \neq \beta$. The PHSC equation of state therefore requires at least one ($\kappa_{ij,\alpha\beta}$) and sometimes as many as two ($\kappa_{ij,\alpha\beta}$ and $\zeta_{ij,\alpha\beta}$) adjustable intersegmental parameters for a given pair of unlike segments.

Characteristic Parameters for Systems Containing Two Kinds of Segments. We consider mixtures of random copolymers of type $(A_X B_{1-X})_{r_1} / (A_Y B_{1-Y})_{r_2}$ containing two kinds of segments. For these systems the characteristic parameters in Eqs. (16) to (19) and (23) are:

$$\begin{aligned} \sigma_{i,A} &= \sigma_A, \quad \sigma_{i,B} = \sigma_B, \quad \varepsilon_{i,A} = \varepsilon_A, \quad \varepsilon_{i,B} = \varepsilon_B \\ \varepsilon_{ij,AB} &= \varepsilon_{ij,BA} = \varepsilon_{AB}, \quad \kappa_{ij,AB} = \kappa_{ij,BA} = \kappa_{AB}, \quad \zeta_{ij,AB} = \zeta_{ij,BA} = \zeta_{AB} \quad (i,j=1,2) \end{aligned} \quad (24)$$

where

$$\varepsilon_{AB} = \sqrt{\varepsilon_A \varepsilon_B} (1 - \kappa_{AB}) \quad (25)$$

$$b_{ij,AB}^{1/3} = b_{ji,BA}^{1/3} = \frac{(b_{i,A}^{1/3} + b_{j,B}^{1/3})}{2} (1 - \zeta_{AB}) \quad (i,j=1,2). \quad (26)$$

As shown in the Appendix, Eq. (7) and its relevant equations are applicable to mixtures of type $(A_X B_{1-X})_{r_1} / (C_Y B_{1-Y})_{r_2}$ and $(A_X B_{1-X})_{r_1} / (C_Y D_{1-Y})_{r_2}$ with appropriate substitutions of characteristic parameters for these system into those for the mixture of type $(A_X B_{1-X})_{r_1} / (A_Y B_{1-Y})_{r_2}$.

Calculation of Monomer Sequence Distribution from Reactivity Ratios. Copolymers exhibiting the screening effect behave as if they have copolymer compositions (i.e., pseudo copolymer compositions) different from those of the true copolymers. Therefore, a method to include the screening effect is to replace the true copolymer composition by the pseudo copolymer composition in the PHSC equation of state. In this paper we present a systematic method to calculate the pseudo copolymer composition from the true copolymer composition using information from copolymerization kinetics.

Consider a real copolymer of type $(A_X B_{1-X})_r$, where r is the number of total monomers per molecule and X is the number fraction of monomer of type A, in which one of the monomers in the AB and BA dyads (i.e., sequences) is screened by the other monomer. Since the degree-of-screening effect depends on the number of AB and BA dyads in a copolymer, the important question is how to determine the numbers of specific sequences. For a truly random copolymer, the numbers of $\alpha\beta$ sequences, $n_{\alpha\beta}$ ($\alpha, \beta = A, B$), can be calculated from a statistical average as

$$n_{AA} = X^2(r-1); \quad n_{AB} = n_{BA} = X(1-X)(r-1); \quad n_{BB} = (1-X)^2(r-1). \quad (27)$$

The monomer sequences of real copolymers, however, may deviate from those given by Eq. (27). From an appropriate copolymerization-kinetic model, the monomer sequence distribution can be determined from the study of copolymerization kinetics.

Consider the terminal model of copolymerization¹¹. We apply the terminal model

to the copolymerization of monomers A and B which yields the copolymer of type $(A_x B_{1-x})_r$. Kinetic equations for the terminal model are:



where $\sim A \cdot$ and $\sim B \cdot$ are the monomer-A and monomer-B ended polymeric radicals, respectively, and $k_{\alpha\beta}$ ($\alpha, \beta = A, B$) is the reaction-rate constant of monomer β to the polymeric radical ended by monomer α .

We also define the reactivity ratios as

$$\mathfrak{R}_1 = \frac{k_{AA}}{k_{AB}} \quad (32)$$

$$\mathfrak{R}_2 = \frac{k_{BB}}{k_{BA}} \quad (33)$$

In the terminal model, truly random copolymers are obtained only if $\mathfrak{R}_1 = \mathfrak{R}_2 = 1$. On the other hand, copolymers exhibit high alternation in the monomer sequence when $\mathfrak{R}_1 \ll 1$ and $\mathfrak{R}_2 \ll 1$. For copolymerizations in a batch reactor, the reactivity ratios are obtained from a plot of initial copolymer composition against the monomer composition in the feed.

For sufficiently low conversions where the monomer concentrations in a batch reactor remain nearly constant, the terminal model predicts that the ratio of number

fraction of segment A to that of segment B in the copolymer, \bar{X} , is related to the ratio of the molar concentration of monomer A to that of monomer B in the feed, Θ , by

$$\bar{X} = \frac{X}{1-X} = \frac{\mathfrak{R}_1 \Theta + 1}{\mathfrak{R}_2 / \Theta + 1} \quad (34)$$

For a known copolymer composition X , Eq. (34) is solved for Θ :

$$\Theta = \frac{-(1-\bar{X}) + \sqrt{(1-\bar{X})^2 + 4\mathfrak{R}_1\mathfrak{R}_2\bar{X}}}{2\mathfrak{R}_1} \quad (35)$$

We define $P_{\alpha\beta}$ the probability of monomer α reacting with the monomer- β ended polymeric radical; it follows that $P_{\alpha A} + P_{\alpha B} = 1$ ($\alpha, \beta = A, B$). For a system with two monomers (A and B), we have four probabilities:

$$P_{AA} = \frac{\mathfrak{R}_1 \Theta}{\mathfrak{R}_1 \Theta + 1} \quad (36)$$

$$P_{AB} = 1 - P_{AA} = \frac{1}{\mathfrak{R}_1 \Theta + 1} \quad (37)$$

$$P_{BB} = \frac{\mathfrak{R}_2 / \Theta}{\mathfrak{R}_2 / \Theta + 1} \quad (38)$$

$$P_{BA} = 1 - P_{BB} = \frac{1}{\mathfrak{R}_2 / \Theta + 1} \quad (39)$$

Therefore

$$\frac{n_{AA}}{n_{AB}} = \frac{P_{AA}}{P_{AB}} = \mathfrak{R}_1 \Theta \quad (40)$$

$$\frac{n_{BB}}{n_{BA}} = \frac{P_{BB}}{P_{BA}} = \mathfrak{R}_2 / \Theta \quad (41)$$

where $n_{\alpha\beta}$ ($\alpha, \beta = A, B$) is the number of α - β sequences. In addition, by neglecting the end effect (i.e., assuming that $r - 1 \cong r$)

$$r_A = rX = \frac{2n_{AA} + n_{AB} + n_{BA}}{2} \quad (42)$$

$$r_B = r(1 - X) = \frac{2n_{BB} + n_{AB} + n_{BA}}{2} \quad (43)$$

where r_α ($\alpha = A, B$) is the number of monomer α per molecule. Equations (40) to (43) are then solved for $n_{\alpha\beta}$:

$$n_{AB} = \frac{r_A(2\mathfrak{R}_2/\Theta + 1) - r_B}{2\mathfrak{R}_1\mathfrak{R}_2 + \mathfrak{R}_1\Theta + \mathfrak{R}_2/\Theta} \quad (44)$$

$$n_{AA} = n_{AB}\mathfrak{R}_1\Theta \quad (45)$$

$$n_{BA} = \frac{r_B(2\mathfrak{R}_1\Theta + 1) - r_A}{2\mathfrak{R}_1\mathfrak{R}_2 + \mathfrak{R}_1\Theta + \mathfrak{R}_2/\Theta} \quad (46)$$

$$n_{BB} = n_{BA}\mathfrak{R}_2/\Theta \quad (47)$$

When the measured monomer sequence distribution is used as the hard-sphere sequence distribution in the PHSC equation of state, the PHSC equation-of-state

parameters must be obtained such that one monomer unit is represented by a single hard sphere in the model.

Screening Effect. Consider a heteronuclear hard-sphere chain which represents a real copolymer of type $(A_x B_{1-x})_r$. The rigorous approach to introduce the screening effect into the model is to represent a copolymer consisting of segments A and B by a terpolymer consisting of segments A, B, and C which represent AA, BB, and AB and BA sequences, respectively, of the copolymer. Figure 1b shows the hard-sphere sequence of the terpolymer which represents the copolymer having the hard-sphere sequence shown in Figure 1a. The numbers of segment of type A, B, and C in a terpolymer are given by r'_A , r'_B , and r'_C , respectively; they are related to the numbers of α - β sequences $n_{\alpha\beta}$ ($\alpha, \beta = A, B$) of a copolymer, Eqs. (44) to (47), by

$$r'_A = n_{AA} \quad (48)$$

$$r'_B = n_{BB} \quad (49)$$

$$r'_C = n_{AB} + n_{BA} \quad (50)$$

To keep the hard-core volume of a terpolymer equal to that of a copolymer, the diameter of segment C, σ_C , is given by

$$\sigma_C = \left[\frac{\sigma_A^3 + \sigma_B^3}{2} \right]^{1/3} \quad (51)$$

Representation of a copolymer by a terpolymer, however, is not practical because three sets of intersegmental parameters are required to describe the phase behavior of the

mixture of type $(A_X B_{1-X})r_1 / (A_Y B_{1-Y})r_2$. To simplify the problem, we replace the fraction ψ of segments C in a terpolymer by segments B and the fraction $1-\psi$ by segments A. Figure 1c shows the hard-sphere sequence of the copolymer obtained by replacing all segments C in the terpolymer shown in Figure 1b by segments B, i.e., $\psi=1$ which corresponds to the complete screening of segment A by segment B in AB and BA dyads. After replacing segments C by segments A and B, the number of segments of type A and that of type B are given by r_A'' and r_B'' , respectively:

$$r_A'' = r_A' + r_C' (1 - \psi) \left(\frac{\sigma_C^3}{\sigma_A^3} \right) \quad (52)$$

$$r_B'' = r_B' + r_C' \psi \left(\frac{\sigma_C^3}{\sigma_B^3} \right) \quad (53)$$

The factors σ_C^3/σ_A^3 and σ_C^3/σ_B^3 in Eqs. (52) and (53), respectively, are introduced to keep the hard-core volume of a molecule constant. When $\psi = (\sigma_B^3/\sigma_C^3)/2$, there is no screening effect.

In the presence of screening effect, the copolymer of type $(A_X B_{1-X})r$ is assumed to have the total number of segments, r^* , and the number fraction of segment of type A, X^* , given by

$$r^* = r_A'' + r_B'' \quad (54)$$

$$X^* = r_A''/r \quad (55)$$

where r_A'' and r_B'' are given by Eqs. (52) and (53), respectively.

CALCULATION PROCEDURE

Critical Conditions. The critical points and coexistence curves of mixtures can be found from the Helmholtz energy of the mixture, $A(T, N_i, \rho)$, where N_i is the number of molecules of component i . The Helmholtz energy of the mixture A should not be confused with segment type A. The Helmholtz energy of the mixture is calculated from the equation of state for the mixture¹², Eq. (1); it is

$$\begin{aligned}
 \frac{A}{Nk_B T} &= \sum_{i=1}^m x_i \frac{A_i^{\circ}}{Nk_B T} + \int_0^{\rho} \left(\frac{p}{\rho k_B T} - 1 \right) \frac{d\rho}{\rho} + \sum_{i=1}^m x_i \ln(x_i \rho k_B T) \\
 &= \sum_{i=1}^m x_i \frac{A_i^{\circ}}{Nk_B T} + \rho \sum_{i=1}^m \sum_{j=1}^m x_i x_j \left[\sum_{k=1}^{r_i} \sum_{l=1}^{r_j} b_{ij,kl} W_{ij,kl} \right] - \sum_{i=1}^m x_i \sum_{k=1}^{r_i-1} Q_{ii,k,k+1} \\
 &\quad - \frac{\rho}{k_B T} \sum_{i=1}^m \sum_{j=1}^m x_i x_j \left[\sum_{k=1}^{r_i} \sum_{l=1}^{r_j} a_{ij,kl} \right] + \sum_{i=1}^m x_i \ln(x_i \rho k_B T) \quad (56)
 \end{aligned}$$

where A_i° is the Helmholtz energy of component i in the reference state and

$$W_{ij,kl} = \frac{1}{\rho} \int_0^{\rho} g_{ij,kl} d\rho \quad (57)$$

$$Q_{ii,k,k+1} = \int_0^{\rho} [g_{ii,k,k+1} - 1] \frac{d\rho}{\rho} \quad (58)$$

The reference state is taken to be the pure ideal gas at unit pressure and at the temperature of the mixture containing the same number of molecules as the total number of molecules in the mixture.

For binary mixtures, the critical conditions are given by³

$$\rho^2 \left(\frac{\partial^2 A}{\partial x^2} \right)_{T, \rho} \left(\frac{\partial p}{\partial \rho} \right)_{T, x} - \left(\frac{\partial p}{\partial x} \right)_{T, \rho}^2 = 0 \quad (59)$$

$$\begin{aligned} & \rho^3 \left(\frac{\partial^3 A}{\partial x^3} \right)_{T, \rho} \left(\frac{\partial p}{\partial \rho} \right)_{T, x}^3 - 3\rho \left(\frac{\partial p}{\partial x} \right)_{T, \rho} \left(\frac{\partial^2 p}{\partial x^2} \right)_{T, \rho} \left(\frac{\partial p}{\partial \rho} \right)_{T, x}^2 \\ & + 3\rho \left(\frac{\partial p}{\partial x} \right)_{T, \rho}^2 \left(\frac{\partial^2 p}{\partial x \partial \rho} \right)_{T, \rho} \left(\frac{\partial p}{\partial \rho} \right)_{T, x} - \left[2 \left(\frac{\partial p}{\partial \rho} \right)_{T, x} + \rho \left(\frac{\partial^2 p}{\partial \rho^2} \right)_{T, x} \right] \left(\frac{\partial p}{\partial x} \right)_{T, \rho}^3 = 0 \end{aligned} \quad (60)$$

where x is the mole fraction of component 1 or 2. Equation (59) also gives the spinodal curve which defines the boundary between unstable and metastable regions.

The theoretical miscibility map at constant temperature computed in this paper gives the boundary between total miscibility and partial miscibility. In the mixture where immiscibility is caused by LCST behavior, the LCST of a pair of miscible copolymers in the theoretical miscibility map is higher than the temperature of system. Conversely, the UCST of a pair of miscible copolymers is lower than the temperature of system in the mixture where immiscibility is caused by UCST behavior. A theoretical miscibility map, therefore, tells us that if the copolymer compositions of a pair of copolymers are in the miscible region, mixtures of these copolymers form a single homogeneous phase in all proportions.

An experimental miscibility map is usually obtained for binary equi-mass mixtures. The difference between the miscibility map which provides the boundary between total and partial miscibilities and the miscibility map for a fixed mixture composition, however, is small because the phase diagrams of polymer blends are flat near the critical point. As a first approximation, the measured phase separation temperature of an equi-mass mixture can be taken as the critical temperature of the mixture.

In this paper all the theoretical calculations were performed for liquids at zero pressure, an excellent approximation when the systems of interest are in the liquid state near atmospheric pressure.

Equation-of-State Parameters. In comparing theory with experiment, the equation-of-state parameters for copolymer mixtures are obtained as follows. Consider component 1, a copolymer of type $(A_x B_{1-x})_{r_1}$. We use the regressed parameters ϵ_A , σ_A , and r/M of homopolymer consisting of segment A reported in Reference 2 as the characteristic parameters of segment A in copolymers; here M is the molecular weight. These parameters were obtained from pure-component pressure-volume-temperature (PVT) data.

For monodisperse polymers, the choice of average molecular weight has little effect on the calculation of phase equilibria. For polydisperse systems, however, it is not obvious which average molecular weight to use. The effect of molecular-weight distribution of polystyrene on the cloud points of the system poly(vinyl methyl ether) / polystyrene (PVME/PS) was reported by Nishi and Kwei¹³. The system PVME/PS is known to exhibit LCST-type phase behavior. These authors simulated the effect of molecular-weight distribution of PS on the cloud points of equi-mass blends by mixing different amounts of monodisperse PS of known molecular weights. Although PVME was polydisperse, Nishi and Kwei showed that, for a given weight-average molecular weight, M_w , of PS, the cloud points in the system PVME/PS containing polydisperse PS agree well with those containing monodisperse PS. Therefore, we use the weight-average molecular weight of polymer to compute the equation-of-state parameters.

When the copolymer composition in weight fraction and the weight-average molecular weight are known, simple stoichiometry gives Ω_A , the total mass of segment A per mole of copolymer; Ω_A is then multiplied by r/M of homopolymer consisting of

segment A to obtain $r_{1,A}$, the number of effective hard spheres of type A. A similar calculation is performed to obtain $r_{1,B}$, the number of effective hard spheres of type B.

RESULTS AND DISCUSSION

Screening Effect on Theoretical Miscibility Map. Within the framework of incompressible Flory-Huggins theory⁷⁻⁹, Braun *et al.*¹⁰ have discussed the screening effect on the miscibility map for the mixture of type $(A_X B_{1-X})_{r_1} / (A_Y B_{1-Y})_{r_2}$ containing two kinds of segments. The systems $(A_X B_{1-X})_{r_1} / (A_Y B_{1-Y})_{r_2}$ which exhibit a screening effect are mixtures containing poly(styrene-*co*-methyl methacrylate), poly(styrene-*co*-butyl methacrylate), and poly(*p*-chlorostyrene-*co*-butyl methacrylate) random copolymers¹⁰. For the system containing poly(styrene-*co*-butyl methacrylate) random copolymers, the theoretical miscibility map computed by the PHSC equation of state and experiment showed semi-quantitative agreement without introducing the screening effect⁵.

Braun *et al.*¹⁰ suggest that the screening effect is more apparent in the mixture of type $(A_X B_{1-X})_{r_1} / (A_Y B_{1-Y})_{r_2}$ than in more complicated systems such as mixtures of type $(A_X B_{1-X})_{r_1} / (C_Y B_{1-Y})_{r_2}$ and $(A_X B_{1-X})_{r_1} / (C_Y D_{1-Y})_{r_2}$ containing three and four kinds of segments, respectively. This suggestion probably follows because in the systems $(A_X B_{1-X})_{r_1} / (C_Y B_{1-Y})_{r_2}$ and $(A_X B_{1-X})_{r_1} / (C_Y D_{1-Y})_{r_2}$, a variety of miscibility maps can be obtained by simply adjusting the intersegmental parameters. In the system $(A_X B_{1-X})_{r_1} / (A_Y B_{1-Y})_{r_2}$, however, the classical Flory-Huggins⁷⁻⁹ theory predicts only one kind of miscibility map: a pair of copolymers is miscible when the copolymer composition difference $|X-Y|$ is less than the critical copolymer composition difference $|X-Y|_c$ which is independent of the copolymer compositions X and Y . Therefore, any effect which violates the assumptions of Flory-Huggins theory would cause deviation of observed miscibility maps from those predicted of Flory-Huggins theory.

Figure 2 shows the screening effect on the theoretical miscibility map at constant temperature for a mixture of type $(A_X B_{1-X})_{r_1} / (A_Y B_{1-Y})_{r_2}$. If a pair of X and Y are in the miscible region, a pair of copolymers with these compositions form a single homogeneous phase in all proportions. The copolymers in this system are assumed to be truly random copolymers. The numbers of α - β hard-sphere sequences, $n_{\alpha\beta}$ ($\alpha, \beta = A, B$), are therefore given by Eq. (27). For known total number of monomers, r , and number fraction of segment of type A, X , the copolymer of type $(A_X B_{1-X})_r$ is assumed to have the total number of monomer, r^* , and the number fraction of segment of type A, X^* , given by Eqs. (54) and (55), respectively. Since the hard-sphere diameter of segment A is equal to that of segment B, $\psi=0.5$ represents the system where there is no screening effect. On the other hand, $\psi=1$ and $\psi=0$ correspond to the complete screening of segment A by segment B and that of segment B by segment A, respectively, in AB and BA dyads in a copolymer. Theory predicts that immiscibility is caused by LCST-type phase behavior.

In the miscibility map for a mixture of type $(A_X B_{1-X})_{r_1} / (A_Y B_{1-Y})_{r_2}$, there is always a miscible region near the diagonal line $X=Y$; when $X=Y$, component 1 is identical to component 2 and there is complete miscibility. A pair of copolymers is therefore miscible when the copolymer composition difference $|X-Y|$ is less than the critical copolymer composition difference $|X-Y|_c$. In the system shown in Figure 2, $|X-Y|_c$ is nearly independent of the copolymer compositions X and Y in the absence of a screening effect (i.e., when $\psi=0.5$), in accord with the prediction of Flory-Huggins theory⁷⁻⁹. For $\psi=1$, the screening effect results in a significantly wider miscible area for small X and Y . Conversely, the miscible area becomes wider at large X and Y for $\psi=0$. The screening effect results in strong dependence of $|X-Y|_c$ on the copolymer compositions.

As discussed by Koningsveld *et al.*¹⁴, the dependence of critical copolymer composition difference $|X-Y|_c$ on the copolymer compositions can also be caused by the difference in the segmental interaction surface areas. Koningsveld *et al.*¹⁴ modified the Flory-Huggins theory such that the interaction surface area per segment depends on the

type of segment comprising the copolymer. The resulting model is able to explain the dependence of $|X-Y|_c$ on the copolymer composition. In the modeling calculations shown in Reference 14, however, $|X-Y|_c$ is nearly a linear function of copolymer composition. In the miscibility maps with a screening effect shown in Figure 2, $|X-Y|_c$ increases sharply as $X \rightarrow 1$ for $\psi=0$ and as $X \rightarrow 0$ for $\psi=1$.

A miscibility map similar to that for the system $\psi=1$ in Figure 2 was also obtained by Braun *et al.*¹⁰ who modified the incompressible Flory-Huggins model (which predicts UCST type phase behavior) by replacing AB and BA dyads by BB dyads. The PHSC equation of state is able to explain the screening effect in the system where immiscibility is caused by LCST behavior.

Comparison with Experiment

Systems Containing Styrene and Methyl Methacrylate. Figure 3 compares a theoretical miscibility map with experimental data reported by Braun *et al.*¹⁰ for a mixture of type $(A_X B_{1-X})_{r_1} / (A_Y B_{1-Y})_{r_2}$ containing poly(styrene-co-methyl methacrylate) random copolymers ($M_w \approx 150000$, $M_w/M_n \approx 1.7$; $M_n \approx$ number-average molecular weight). Poly(styrene-co-methyl methacrylate) random copolymers are denoted as (S-co-MMA) where S and MMA represent styrene and methyl methacrylate segments, respectively. The PHSC equation-of-state parameters for polystyrene and poly(methyl methacrylate) are given in Table I. Let segments A and B represent styrene and methyl methacrylate, respectively. In this system, immiscibility is caused by LCST behavior. Open and solid circles are the pairs of copolymers which are miscible and immiscible, respectively, at both 25 and 180 °C. Open triangles denote the pairs of copolymers which are miscible at 25 °C but are immiscible at 180 °C. The miscible area decreases as the temperature rises because a pair of miscible copolymers eventually becomes immiscible as the temperature is raised above the LCST of the mixture. The experimental miscibility map shown in Figure 3 is similar to that shown in Figure 2 with $\psi=1$; in this system segment A

(styrene) is completely screened by segment B (methyl methacrylate) in AB and BA sequences.

The intersegmental parameters for the styrene-methyl methacrylate (S-MMA) pair, parameter set 1, were obtained as follows. We first preset ζ_{S-MMA} to -0.02 and then solve for κ_{S-MMA} assuming that at $25\text{ }^\circ\text{C}$ the boundary between miscible and immiscible regions at $\omega_{1,A}=1.0$ lies at $\omega_{2,A}=0.85$ where $\omega_{i,A}$ is the weight fraction of styrene in component i . Intersegmental parameters are given in Table II. With these parameters, theory predicts that immiscibility is caused by LCST behavior. Agreement between theory and experiment is good in the styrene-rich region of the miscibility map at both 25 and $180\text{ }^\circ\text{C}$. Parameter set 1 therefore may be used as the intersegmental parameters for the S-MMA pair in the systems PVME/(MMA-co-S) and (tetramethyl bisphenol A polycarbonate)/(MMA-co-S) where the mixtures exhibit phase separation in the experimentally accessible temperature range when methyl methacrylate content in the MMA-co-S copolymer is less than about 35 % by weight.

Better agreement between theory and experiment is obtained if the screening effect is considered. For the copolymerization of styrene with methyl methacrylate at $60\text{ }^\circ\text{C}$, the reactivity ratios, Eqs. (32) and (33), are¹⁰

$$\mathfrak{R}_1 = \frac{k_{AA}}{k_{AB}} = 0.522 \quad (61)$$

$$\mathfrak{R}_2 = \frac{k_{BB}}{k_{BA}} = 0.482 \quad (62)$$

where subscripts A and B represent styrene and methyl methacrylate monomers, respectively. Using these reactivity ratios, for known copolymer composition and total number of monomers per molecule, the numbers of α - β ($\alpha, \beta = A, B$) monomer sequences per molecule of component i , $n_{i, \alpha\beta}$ ($i=1,2; \alpha, \beta = A, B$), are computed by Eqs. (44) to (47).

To use the monomer sequences calculated from the reactivity ratios as the hard-sphere sequences in the PHSC equation of state, equation-of-state parameters of homopolymers must be obtained assuming that one monomer is represented by a single sphere in the model. The PHSC equation-of-state parameters ϵ and σ for polystyrene and poly(methyl methacrylate) were regressed from the same *PVT* data used in reference 2 by presetting r/M to $1/M^*$ where M^* is the molecular weight of monomer. The PHSC equation-of-state parameters for polystyrene and poly(methyl methacrylate) obtained in this manner are given in parentheses in Table I.

Figure 4 compares a theoretical miscibility map (with screening effect) with experiment for a mixture of type $(A_X B_{1-X})_{r_1} / (A_Y B_{1-Y})_{r_2}$ containing S-co-MMA random copolymers. The theoretical miscibility map was calculated assuming complete screening of styrene segment by methyl methacrylate segment in the S-MMA and MMA-S sequences (i.e., $\psi=1$). The temperature dependence of the miscibility map is not predicted using the same set of intersegmental parameters. Parameter set 2 was obtained by assuming that $\zeta_{S-MMA} = -0.004$ and that at 25 °C the boundary between miscible and immiscible regions at $\omega_{1,A} = 1.0$ lies at $\omega_{2,A} = 0.85$. Similarly, parameter set 3 was obtained by assuming that $\zeta_{S-MMA} = -0.04$ and that at 180 °C the boundary between miscible and immiscible regions at $\omega_{1,A} = 1.0$ lies at $\omega_{2,A} = 0.94$. Theory predicts that immiscibility is caused by LCST behavior at both 25 and 180 °C.

Upon introducing the screening effect, theory and experiment show good agreement in the entire copolymer composition range. The temperature dependence of the miscibility map, however, is not predicted by using the same set of intersegmental parameters. These observations imply that the intersegmental parameters for the S-MMA pair may be temperature-dependent. Another possible implication is that the degree of screening depends on the copolymer composition. As shown in Figure 3, theory and experiment can show good agreement in the styrene-rich region of miscibility map without introducing the screening effect.

A remaining question is whether the screening effect is observed in mixtures of S-*co*-MMA with another copolymer such as poly(acrylonitrile-*co*-styrene). The screening effect in systems containing three kinds of segments is discussed in the subsequent paper.

CONCLUSIONS

Reactivity ratios of copolymerization kinetics are used to introduce the screening effect into the perturbed hard-sphere-chain-(PHSC) equation of state for copolymer systems. The theory with screening effect is able to explain the strong dependence of the critical copolymer composition difference on the copolymer compositions in the system where immiscibility is caused by phase behavior due to a lower critical solution temperature (LCST). For a mixture containing poly(styrene-*co*-methyl methacrylate) random copolymers differing in copolymer compositions, the theory with screening effect and experimental miscibility map show good agreement at constant temperature. Although the theory is able to predict the immiscibility due to LCST-type phase behavior in the system poly(styrene-*co*-methyl methacrylate), the temperature dependence of the miscibility map is not predicted using a temperature-independent set of intersegmental parameters.

ACKNOWLEDGMENT

This work was supported by the Director, Office of Energy Research, Office of Basic Energy Sciences, Chemical Sciences Division of the U.S. Department of Energy under Contract No. DE-AC03-76SF0098. Additional funding was provided by E.I. du Pont de Nemours & Co. (Philadelphia, PA) and Koninklijke Shell (Amsterdam, The Netherlands). The authors thank S.M. Lambert for performing the regression of equation-of-state parameters.

Appendix. Characteristic Parameters for Systems Containing Three and Four Kinds of Segments.

Consider mixtures of random copolymers of type $(A_X B_{1-X})_{r_1} / (C_Y B_{1-Y})_{r_2}$ containing three kinds of segments. Equation (7) and its relevant equations are applicable to a mixture of type $(A_X B_{1-X})_{r_1} / (C_Y B_{1-Y})_{r_2}$ with the following substitutions of characteristic parameters for this system into those for the mixture of type $(A_X B_{1-X})_{r_1} / (A_Y B_{1-Y})_{r_2}$:

$$\begin{aligned} \sigma_{1,A} &= \sigma_A, \quad \sigma_{i,B} = \sigma_B, \quad \sigma_{2,A} = \sigma_C, \quad \varepsilon_{1,A} = \varepsilon_A, \quad \varepsilon_{i,B} = \varepsilon_{12,BB} = \varepsilon_B, \quad \varepsilon_{2,A} = \varepsilon_C \\ \varepsilon_{11,AB} &= \varepsilon_{12,AB} = \varepsilon_{AB}, \quad \varepsilon_{12,AA} = \varepsilon_{AC}, \quad \varepsilon_{12,BA} = \varepsilon_{22,BA} = \varepsilon_{BC} \\ \kappa_{11,AB} &= \kappa_{12,AB} = \kappa_{AB}, \quad \kappa_{12,AA} = \kappa_{AC}, \quad \kappa_{12,BA} = \kappa_{22,BA} = \kappa_{BC} \\ \zeta_{11,AB} &= \zeta_{12,AB} = \zeta_{AB}, \quad \zeta_{12,AA} = \zeta_{AC}, \quad \zeta_{12,BA} = \zeta_{22,BA} = \zeta_{BC} \quad (i,j=1,2) \end{aligned} \quad (A.1)$$

where

$$\varepsilon_{AB} = \sqrt{\varepsilon_A \varepsilon_B} (1 - \kappa_{AB}), \quad \varepsilon_{AC} = \sqrt{\varepsilon_A \varepsilon_C} (1 - \kappa_{AC}), \quad \varepsilon_{BC} = \sqrt{\varepsilon_B \varepsilon_C} (1 - \kappa_{BC}) \quad (A.2)$$

$$b_{ij,\alpha\beta}^{1/3} = b_{ji,\beta\alpha}^{1/3} = \frac{(b_{i,\alpha}^{1/3} + b_{j,\beta}^{1/3})}{2} (1 - \zeta_{\alpha\beta}) \quad (i,j=1,2; \alpha,\beta=A,B,C; \alpha \neq \beta) \quad (A.3)$$

For a mixture of type $(A_X B_{1-X})_{r_1} / (C_Y D_{1-Y})_{r_2}$ the following substitutions of characteristic parameters for this system into those for a mixture of type $(A_X B_{1-X})_{r_1} / (A_Y B_{1-Y})_{r_2}$ are required:

$$\begin{aligned} \sigma_{1,A} &= \sigma_A, \quad \sigma_{1,B} = \sigma_B, \quad \sigma_{2,A} = \sigma_C, \quad \sigma_{2,B} = \sigma_D, \quad \varepsilon_{1,A} = \varepsilon_A, \quad \varepsilon_{1,B} = \varepsilon_B, \quad \varepsilon_{2,A} = \varepsilon_C, \quad \varepsilon_{2,B} = \varepsilon_D \\ \varepsilon_{11,AB} &= \varepsilon_{AB}, \quad \varepsilon_{12,AA} = \varepsilon_{AC}, \quad \varepsilon_{12,AB} = \varepsilon_{AD}, \quad \varepsilon_{12,BA} = \varepsilon_{BC}, \quad \varepsilon_{12,BB} = \varepsilon_{BD}, \quad \varepsilon_{22,AB} = \varepsilon_{CD} \\ \kappa_{11,AB} &= \kappa_{AB}, \quad \kappa_{12,AA} = \kappa_{AC}, \quad \kappa_{12,AB} = \kappa_{AD}, \quad \kappa_{12,BA} = \kappa_{BC}, \quad \kappa_{12,BB} = \kappa_{BD}, \quad \kappa_{22,AB} = \kappa_{CD} \end{aligned}$$

$$\zeta_{11,AB} = \zeta_{AB}, \zeta_{12,AA} = \zeta_{AC}, \zeta_{12,AB} = \zeta_{AD}, \zeta_{12,BA} = \zeta_{BC}, \zeta_{12,BB} = \zeta_{BD}, \zeta_{22,AB} = \zeta_{CD} \quad (\text{A.4})$$

where

$$\varepsilon_{\alpha\beta} = \sqrt{\varepsilon_{\alpha}\varepsilon_{\beta}}(1 - \kappa_{\alpha\beta}) \quad (\alpha, \beta = A, B, C, D; \alpha \neq \beta) \quad (\text{A.5})$$

$$b_{ij,\alpha\beta}^{1/3} = \frac{(b_{i,\alpha}^{1/3} + b_{j,\beta}^{1/3})}{2} (1 - \zeta_{\alpha\beta}) \quad (i, j = 1, 2; \alpha, \beta = A, B, C, D; \alpha \neq \beta) \quad (\text{A.6})$$

References

1. Song, Y.; Lambert, S.M.; Prausnitz, J.M. *Macromolecules* **1994**, *27*, 441.
2. Song, Y.; Lambert, S.M.; Prausnitz, J.M. *Ind. Eng. Chem. Res.* **1994**, *33*, 1047.
3. Song, Y.; Lambert, S.M.; Prausnitz, J.M. *Chem. Eng. Sci.* **1994**, *49*, 2765.
4. Song, Y.; Lambert, S.M.; Prausnitz, J.M. paper presented at the AIChE meeting in St. Louis, November 1993.
5. Hino, T.; Song, Y.; Prausnitz, J.M. *Macromolecules* **1994**, *27*, 5681.
6. Chiew, Y.C. *Mol. Phys.* **1990**, *70*, 129.
7. Kambour, R.P.; Bendler, J.T.; Bopp, R.C. *Macromolecules* **1983**, *16*, 753.
8. Paul, D.R.; Barlow, J.W. *Polymer* **1984**, *25*, 487.
9. ten Brinke, G.; Karasz, F.E.; MacKnight, W.J. *Macromolecules* **1983**, *16*, 1827.
10. Braun, D.; Yu, D.; Kohl, P.R.; Gao, X.; Andradi, L.N.; Manger, E.; Hellmann, G.P. *J. Polym. Sci., Polym. Phys. Edn.* **1992**, *30*, 577.
11. Mayo, F.R.; Lewis, F.M. *J. Amer. Chem. Soc.* **1944**, *66*, 1594.
12. Prausnitz, J.M.; Lichtenthaler, R.N.; de Azevedo, E.G. "Molecular Thermodynamics of Fluid-Phase Equilibria", 2nd ed.; Prentice-Hall Inc.: Englewood Cliffs, N.J., 1986; Chapter 3.
13. Nishi, T.; Kwei, T.K. *Polymer* **1975**, *16*, 285.
14. Koningsveld, R.; Kleintjens, L.A. *Macromolecules* **1985**, *18*, 243.

Figure Captions

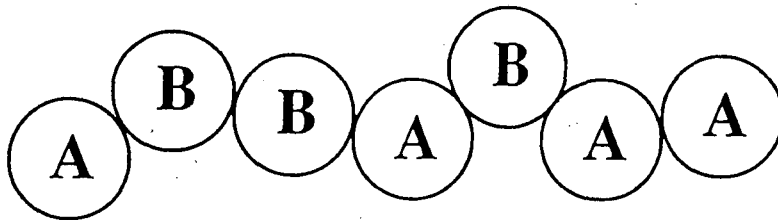
Figure 1. (a) Hard-sphere sequence of a copolymer consisting of segments A and B, (b) Hard-sphere sequence of a terpolymer consisting of segments A, B, and C which represent AA, BB, and AB and BA sequences, respectively, of a copolymer shown in Figure 1a, (c) Hard-sphere sequence of a copolymer obtained by replacing all the segments C in the terpolymer shown in Figure 1b by segments B, i.e., complete screening of segment A by segment B in AB and BA dyads.

Figure 2. Screening effect on the miscibility map for mixtures of type $(A_X B_{1-X})_{r_1} / (A_Y B_{1-Y})_{r_2}$: $r_1 = r_2 = 10000$, $\sigma_B / \sigma_A = 1.0$, $\varepsilon_B / \varepsilon_A = 1.05$, $\kappa_{AB} = 0.00345$, $\zeta_{AB} = -0.002$, $p = 0$, $\tilde{T}_A = k_B T / \varepsilon_A = 0.7$, $\mathfrak{R}_1 = \mathfrak{R}_2 = 1$; (—) $\psi = 0.5$, no screening; (- - -) $\psi = 1$, complete screening of segment A by segment B in AB and BA dyads; (- · · ·) $\psi = 0$, complete screening of segment B by segment A in AB and BA dyads. Theory predicts that immiscibility is caused by LCST behavior.

Figure 3. Comparison of theoretical miscibility maps with experiment for mixtures of type $(A_X B_{1-X})_{r_1} / (A_Y B_{1-Y})_{r_2}$ containing poly(styrene-co-methyl methacrylate) random copolymers ($M_w \cong 150000$, $M_w / M_n \cong 1.7$): $M_1 = M_2 = 150000$, parameter set 1; $\kappa_{S-MMA} = -0.02125$, $\zeta_{S-MMA} = -0.02$. Poly(styrene-co-methyl methacrylate) copolymers are denoted as S-co-MMA where S and MMA represent styrene and methyl methacrylate segments, respectively. Theory predicts that immiscibility is caused by LCST behavior. Data are from Braun *et al.*¹⁰: (o) miscible at 25 and 180 °C, (Δ) miscible at 25 °C but immiscible at 180 °C, (\bullet) immiscible at 25 and 180 °C.

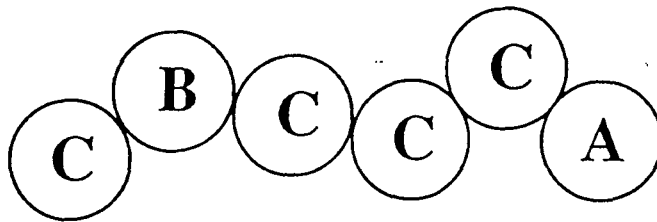
Figure 4. Comparison of theory (with screening effect) with experiment for mixtures of type $(A_X B_{1-X})_{r_1} / (A_Y B_{1-Y})_{r_2}$ containing poly(styrene-*co*-methyl methacrylate) random copolymers¹⁰ ($M_1=M_2=150000$): parameter set 2; $\kappa_{S-MMA}=-0.00566$, $\zeta_{S-MMA}=-0.004$, parameter set 3; $\kappa_{S-MMA}=-0.05627$, $\zeta_{S-MMA}=-0.04$. Poly(styrene-*co*-methyl methacrylate) copolymers are denoted as S-*co*-MMA where S and MMA represent styrene and methyl methacrylate segments, respectively. Theoretical miscibility maps assume complete screening of S segment by MMA segment in the S-MMA and MMA-S sequences. Theory predicts that immiscibility is caused by LCST behavior.

Figure 1



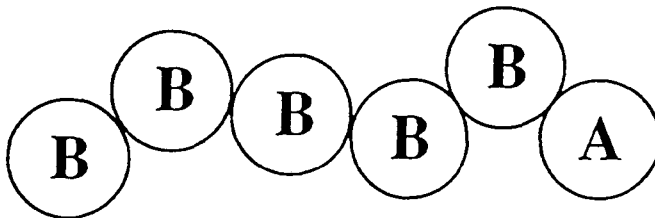
ABBABAA

a



CBCCCA

b



BBBBBA

c

Figure 2

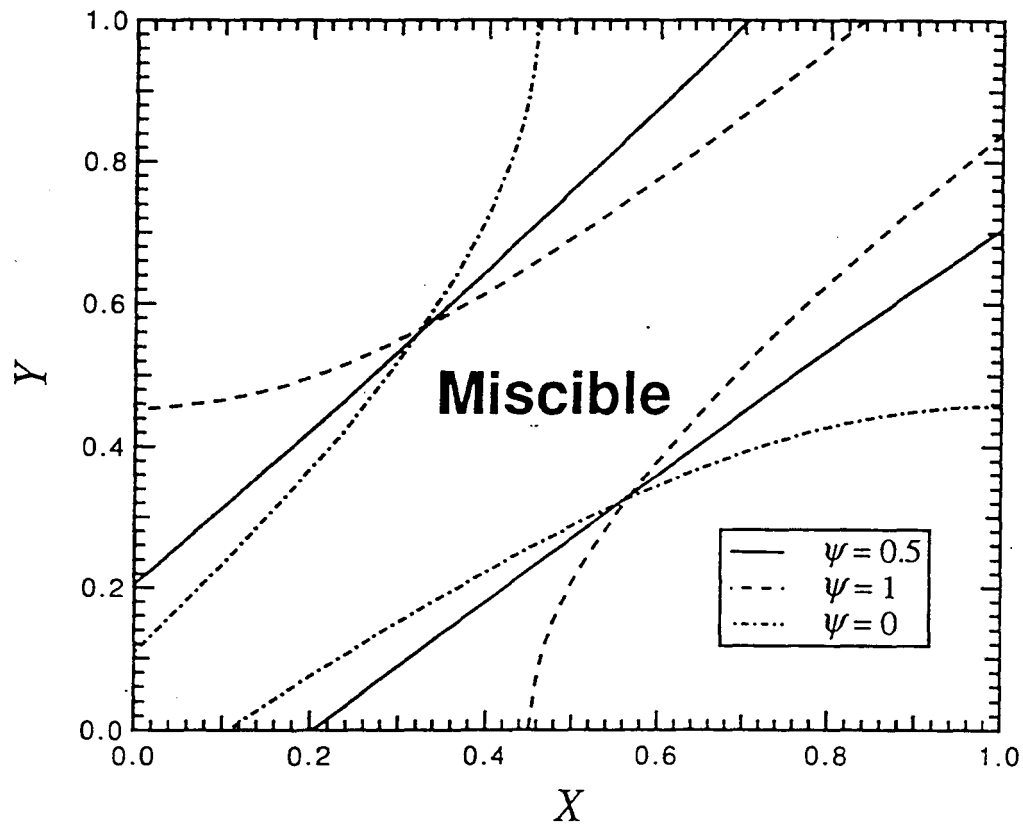


Figure 3

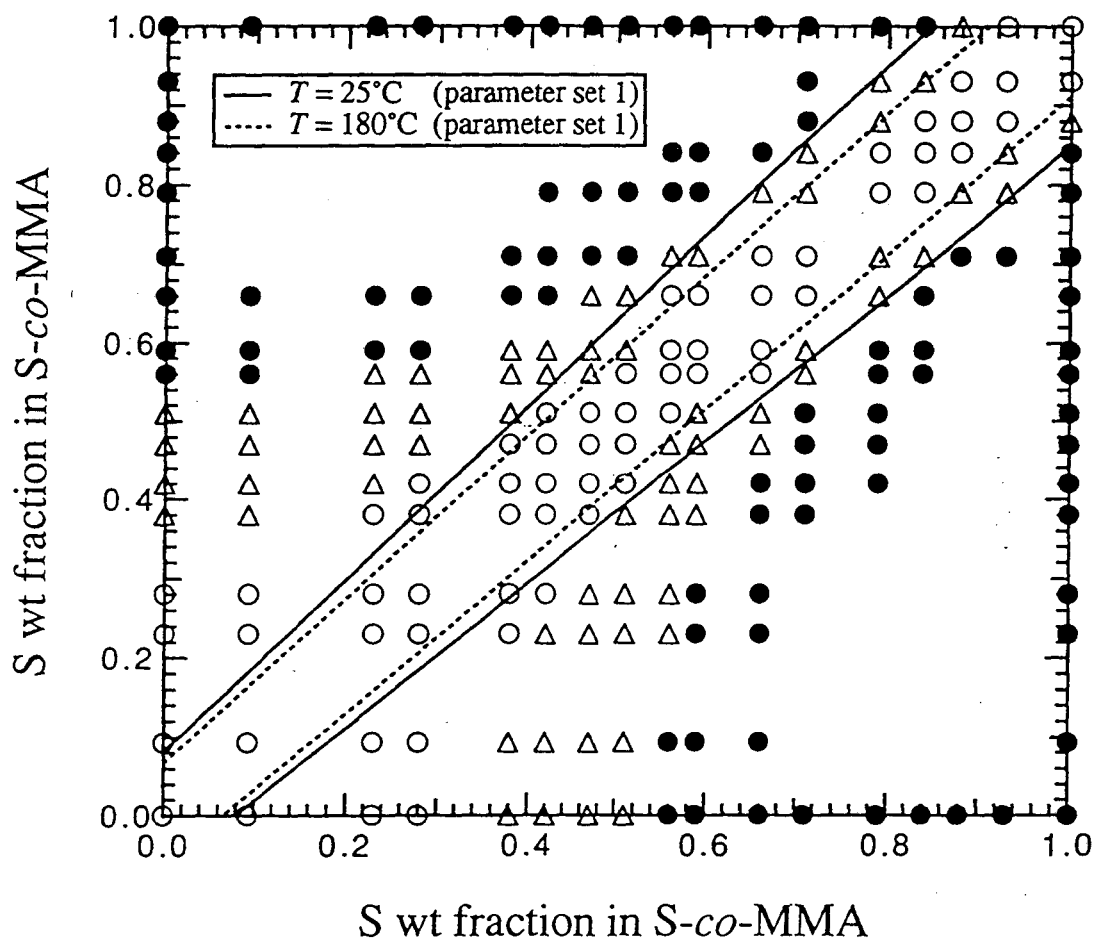
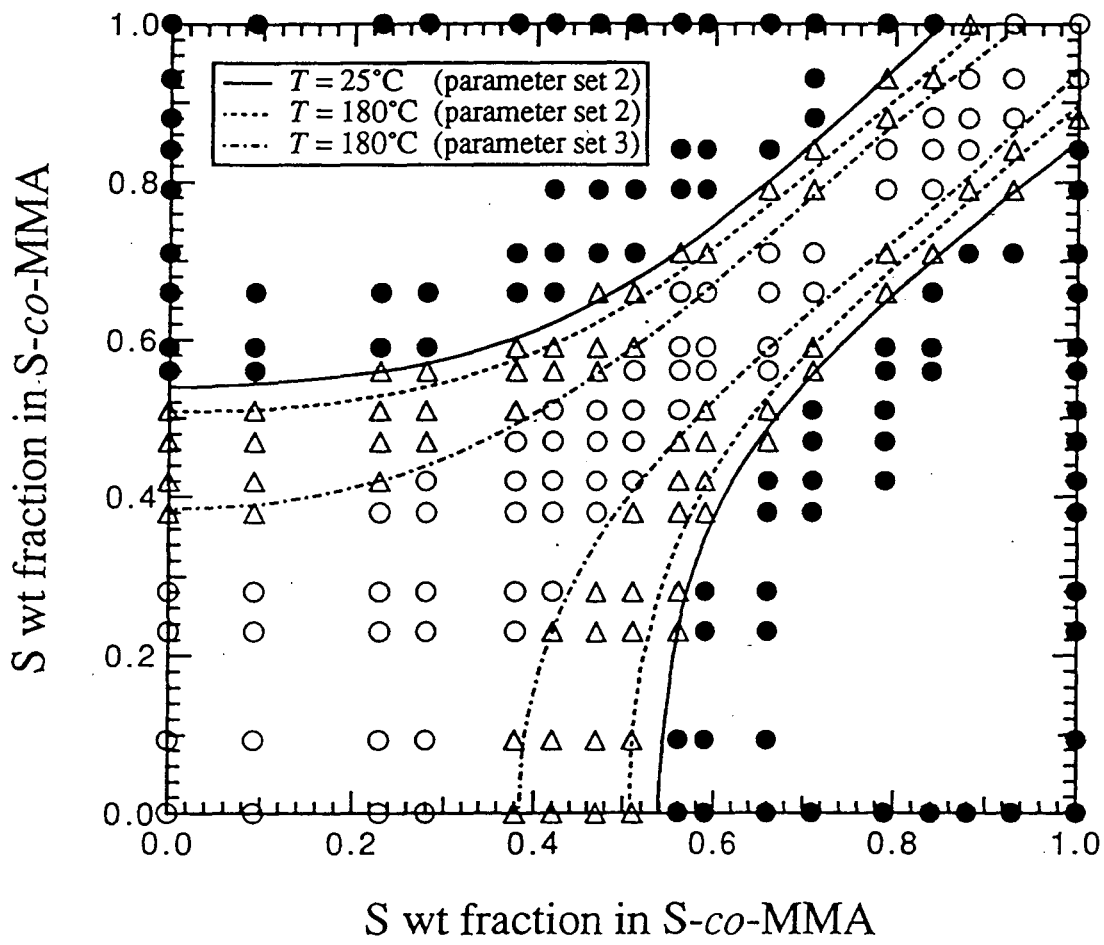


Figure 4



AN EQUATION-OF-STATE ANALYSIS OF BINARY COPOLYMER SYSTEMS 2. HOMOPOLYMER AND COPOLYMER MIXTURES

*Toshiaki Hino, Yuhua Song, and John M. Prausnitz **

Department of Chemical Engineering
University of California, Berkeley
and
Chemical Sciences Division
Lawrence Berkeley Laboratory
Berkeley, CA 94720

ABSTRACT

The perturbed hard-sphere-chain (PHSC) equation of state for copolymer systems is applied to binary homopolymer blends and to mixtures of homopolymer and copolymer. Theoretical results for the effect of copolymer composition on lower critical solution temperature (LCST) are compared with experiment for homopolymer/copolymer mixtures containing poly(methyl methacrylate-*co*-styrene) (MMA-*co*-S) and poly(acrylonitrile-*co*-styrene) (AN-*co*-S) random copolymers. The intersegmental parameters for the MMA-S and AN-S pairs are obtained from the miscibility maps containing MMA-*co*-S and AN-*co*-S random copolymers, respectively, differing in copolymer compositions. The homopolymer/copolymer systems studied in this work exhibit LCSTs in the experimentally accessible temperature range as the copolymer approaches 100% polystyrene. The PHSC equation of state predicts that the LCST of a homopolymer/copolymer system exhibits a maximum as the copolymer composition varies. Unique values are assigned to the intersegmental parameters for a given pair of segments.

(Keywords: copolymer blend; equation-of-state; lower critical solution temperature; phase equilibria)

* To whom correspondence should be addressed.

INTRODUCTION

Phase behavior of copolymer mixtures at constant temperature and pressure depends primarily on copolymer composition and molecular weight. It is well known that, without introducing favorable interactions such as hydrogen bonding between unlike molecules^{1,2}, a mixture of a homopolymer and a copolymer or a pair of copolymers can be miscible over only a restricted copolymer composition range. Several authors have reported the so-called miscibility window in binary mixtures, where miscibility changes from immiscible→miscible→immiscible as the copolymer composition of one component varies³⁻⁶. The miscibility window occurs because intramolecular interactions become more unfavorable as the copolymer composition varies, leading to more favorable intermolecular interactions relative to intramolecular interactions. In addition to the miscibility window, some experimental evidence exists for the immiscibility window where miscibility changes from miscible→immiscible→miscible as the copolymer composition of one component varies⁷⁻⁸.

Many miscible polymer blends exhibit lower-critical-solution temperature (LCST) phase behavior at elevated temperature. In the absence of specific interactions, LCST behavior is caused by the free-volume effect arising from different compressibilities of components in the mixture. Equation-of-state theories are necessary to represent immiscibility caused by LCST behavior due to the free-volume effect. Equation-of-state theories are also able to represent immiscibility caused by upper-critical-solution-temperature (UCST) phase behavior.

Recently, several attempts have been made to generalize the existing equations of state for homopolymer systems to copolymer systems. In principle, equations of state for copolymer systems can be obtained by replacing the characteristic parameters of homopolymers by those of copolymers averaged over copolymer compositions. Among several equations of state applicable to homopolymer systems, the lattice-fluid model⁹⁻¹¹ was generalized for copolymer systems by Panayiotou¹² and by Kim *et al.*¹³⁻¹⁵. Models

based on the Prigogine-Flory-Patterson theory¹⁶⁻¹⁸ were developed by Kammer *et al.*^{19,20} and by Jo and Lee^{21,22}. In addition to the free-volume effect, the model by Kammer *et al.*²⁰ also includes the effect of differences in segmental sizes. Generalization of Flory's equation of state for homopolymer systems^{17,23} to copolymer systems was made by Shiomi *et al.*^{24,25}. Koningsveld *et al.*^{26,27} also introduced the mean-field lattice-gas approach into their incompressible lattice-based theory for copolymer systems such that the model can predict LCST phase behavior arising from the free-volume effect. All of these equations of state are capable of representing the LCST caused by the free-volume effect. For copolymer systems, however, there has been little extensive comparison of equation-of-state theory with experiment.

Recently, Song *et al.*²⁸⁻³¹ and Hino *et al.*³² presented a perturbed hard-sphere-chain (PHSC) equation of state applicable to mixtures of heteronuclear chain molecules. The PHSC equation of state for copolymer systems was *not* obtained by simply replacing the characteristic parameters of homopolymers by those of copolymers averaged over copolymer compositions. The PHSC equation of state for real copolymer mixtures³² is based on a modified form of Chiew's equation of state³³ for athermal mixtures of heteronuclear hard-sphere chains by Song *et al.*²⁸ and a van-der-Waals perturbation whose parameters are related to the intermolecular potential as suggested by Song and Mason²⁹. The screening effect, an effect of sequence distribution in the copolymer, was introduced into the PHSC equation of state in the first paper of this series³⁴.

For copolymer systems, the most challenging task in the calculation of phase equilibria is to represent the phase behavior of various copolymer mixtures using only one consistent set of intersegmental parameters. For utility, the intersegmental parameters of a thermodynamic model for copolymer systems need to be independent of the type of mixtures. In this work we compare the theoretical miscibility windows computed from the PHSC equation of state by Hino *et al.*³² with experiment, using the same set of intersegmental parameters. The systems studied are homopolymer blends,

homopolymer/copolymer mixtures, and a mixture of random copolymers containing two kinds of segments; these mixtures are denoted as A_{r_1}/B_{r_2} , $A_{r_1}/(C_Y B_{1-Y})_{r_2}$, and $(A_X B_{1-X})_{r_1}/(A_Y B_{1-Y})_{r_2}$, respectively, where r_i is the number of effective hard spheres per molecule of component i and X and Y are segment number fractions for segments A, B, and C, in components 1 and 2, respectively. The systems $A_{r_1}/(C_Y B_{1-Y})_{r_2}$ studied in this work exhibits LCSTs in the experimentally accessible temperature range as $Y \rightarrow 0$. The intersegmental parameters obtained here are used to analyze the more complicated copolymer systems in the third publication of this series.

THEORY

Details of the perturbed hard-sphere-chain (PHSC) equation of state for copolymer systems are given in References 32 and 34.

Equation-of-State Parameters. The PHSC equation of state requires three parameters to describe homopolymers: number of effective hard spheres per molecular weight of polymer (M), r/M ; segmental diameter, σ ; and non-bonded segment pair-interaction energy, ϵ . These parameters were regressed from available pressure-volume-temperature (PVT) data for several homopolymers; they are tabulated in Reference 29. The PHSC equation-of-state parameters of the homopolymers used in this work are given in Table I.

For a copolymer of type $(A_X B_{1-X})_r$, the copolymer composition in weight fraction and the weight-average molecular weight, M_w , gives the total mass of segment A per mole of copolymer, Ω_A ; Ω_A is then multiplied by r/M of the homopolymer consisting of segment A to obtain r_A , the number of effective hard spheres of type A per hard-sphere chain. A similar calculation is performed to obtain r_B , the number of effective hard spheres of type B per hard-sphere chain. The weight-average molecular weight is used to compute the equation-of-state parameters as discussed previously³⁴. In this work, M_i ($i=1,2$) is the weight-average molecular weight of component i used to compute equation-of-state parameters.

Equation-of-state parameters are not unique. Although the PHSC equation of state fits the pure-component *PVT* data of homopolymers very well, the set of equation-of-state parameters which gives the best fit of *PVT* data does not produce the phase diagrams consistent with experiment for the systems polystyrene/poly(vinyl methyl ether) (PS/PVME) and PS/tetramethyl bisphenol A polycarbonate (TMPC) which show LCST phase behavior. The theoretical phase diagrams in these mixtures are sensitive to the ratios of equation-of-state parameters. It was therefore necessary to adjust the equation-of-state parameters of one component (PVME and TMPC) by first presetting r/M and then regressing for ε_A and σ_A . With the adjusted equation-of-state parameters, however, the PHSC equation of state still gives a much better fit of the homopolymer *PVT* data than the lattice-fluid equation of state⁹⁻¹¹.

Intersegmental Parameters. For a given pair of dissimilar segments α and β , the PHSC equation of state requires at least one adjustable intersegmental parameter, $\kappa_{\alpha\beta}$:

$$\varepsilon_{\alpha\beta} = \sqrt{\varepsilon_\alpha \varepsilon_\beta} (1 - \kappa_{\alpha\beta}) \quad (\alpha, \beta = A, B, C; \alpha \neq \beta) \quad (1)$$

where ε_α is the minimum potential energy of the non-bonded segment-segment pair potential between similar segments α . Similarly, $\varepsilon_{\alpha\beta}$ is the minimum potential energy between dissimilar segments α and β . An additional adjustable intersegmental parameter, $\zeta_{\alpha\beta}$, can also be introduced to relax the additivity of effective hard-sphere diameters of unlike segments α and β :

$$b_{\alpha\beta} = \frac{(b_\alpha^{1/3} + b_\beta^{1/3})}{2} (1 - \zeta_{\alpha\beta}) \quad (\alpha, \beta = A, B, C; \alpha \neq \beta) \quad (2)$$

where b_α and $b_{\alpha\beta}$ represent the van der Waals covolumes for effective hard spheres between similar and dissimilar segments, respectively; b_α and $b_{\alpha\beta}$ account for the

excluded volume due to repulsive forces. The intersegmental parameters are obtained from experimental phase boundaries such as the critical point of the mixture and the boundary between miscible and immiscible regions on the miscibility map.

Calculation Procedure. The expressions for the spinodal and critical conditions as well as the chemical potential are required to perform phase equilibrium calculations; they are given in References 32 and 34.

The theoretical miscibility map at constant temperature gives the boundary between total miscibility and partial miscibility. When immiscibility is caused by LCST behavior, the LCST of a miscible pair of copolymers in the theoretical miscibility map is higher than the temperature of system. Conversely, when immiscibility is caused by UCST behavior, the UCST of a miscible pair of copolymers is lower than the temperature of system. The theoretical miscibility map tells us that if the copolymer compositions of a pair of copolymers are in the miscible region, these copolymers form a single homogeneous phase in all proportions.

Experimental miscibility maps are usually obtained for equi-mass mixtures. The difference between the miscibility map which gives the boundary between total and partial miscibilities and the miscibility map for a fixed mixture composition, however, is small because the phase diagrams of copolymer blends are flat near the critical point. As a first approximation, the measured phase separation temperature of an equi-mass mixture can be taken as the critical temperature of the mixture.

All theoretical calculations reported here were performed for liquids at zero pressure, an excellent approximation when the systems of interest are in the liquid state near atmospheric pressure.

RESULTS AND DISCUSSION

System Poly(Vinyl Methyl Ether) / Polystyrene. We first obtain the intersegmental parameters for the vinyl methyl ether-styrene (VME-S) pair from the phase diagrams of the system poly(vinyl methyl ether) / polystyrene (PVME/PS) which shows LCST type phase behavior. Using a fluorescence emission technique, Walsh *et al.*³⁵ reported a detailed analysis of molecular-weight dependence of phase separation temperatures in the system PVME/PS. When the molecular weights of both PS and PVME are high, the system PVME/PS has a critical composition of about 80 ~ 90 wt% PVME.

The pure-component *PVT* data of PVME are reported in a figure in Reference 36; they are, however, not tabulated. The *PVT* data of PVME were therefore simulated in the range 100 to 200 °C and 100 to 300 bar by the Simha and Somcynsky equation-of-state³⁷ using the parameters listed in Reference 37. The PHSC equation-of-state parameters for PVME were then obtained by regressing the simulated *PVT* data. It was, however, necessary to preset one of three equation-of-state parameters because theory predicts an UCST in the system PVME/PS when the equation-of-state parameters for PVME obtained by three-parameter regression are used. Using only one adjustable parameter κ , PHSC theory, using the equation-of-state parameters for PVME obtained by presetting r/M to 0.018, gives satisfactory agreement with experiment for the system PVME/PS. Additional intersegmental parameter ζ was later introduced such that the dependence of LCST on the molecular weight of PS is correctly predicted. Equation-of-state parameters for PVME are given in Table I.

Figure 1a shows experimental phase diagrams for the system PVME/PS with various molecular weights of PS reported by Walsh *et al.*³⁵ Theoretical coexistence curves for the systems shown in Figure 1a are given in Figure 1b. The intersegmental parameters for the VME-S pair are obtained such that the molecular-weight dependence of LCSTs in Figure 1a is correctly represented by the model; they are given in Table II. Figure 1c shows experimental phase diagrams of the system PVME/PS with various

molecular weights of PVME by Walsh *et al.*³⁵ and Chien *et al.*³⁸. Theoretical coexistence curves for the systems shown in Figure 1c are calculated using parameters identical to those used in Figure 1b; they are shown in Figure 1d. Theory slightly overestimates the molecular-weight dependence of LCST for the systems in Figure 1c, perhaps because of polydispersity in PVME. The characteristics of polymer samples used by Walsh *et al.*³⁵ and Chien *et al.*³⁸ are given in Table III.

Systems Containing Vinyl Methyl Ether, Styrene, and Methyl Methacrylate. The copolymer-composition dependence of phase-separation temperatures of the system PVME / poly(methyl methacrylate-*co*-styrene) (MMA-*co*-S) was first measured by Chien *et al.* by cloud-point measurement³⁸ and later by Halary *et al.* using a fluorescence-quenching technique³⁹. The results by Chien *et al.* agree very well with those by Halary *et al.* The mixture of PVME and PS used by those authors is miscible up to about 120 °C. As the methyl methacrylate content rises, the LCST of the copolymer systems first increases and then decreases, going through the maximum LCST of about 150 °C when the copolymer contains about 20 % MMA by weight.

To describe the phase behavior of the mixture of type $A_{r_1}/(C_Y B_{1-Y})_{r_2}$, three sets of intersegmental parameters are required. The parameters for the S-MMA pair, $\kappa_{S-MMA} = -0.02125$ and $\zeta_{S-MMA} = -0.02$, were obtained in the first paper of this series³⁴ from the miscibility map of the mixture of type $(A_X B_{1-X})_{r_1}/(A_Y B_{1-Y})_{r_2}$ containing S-*co*-MMA random copolymers. Although the system $(A_X B_{1-X})_{r_1}/(A_Y B_{1-Y})_{r_2}$ containing S-*co*-MMA random copolymers exhibits the screening effect, theoretical miscibility map and experiment show good agreement in the styrene-rich region without introducing the screening effect into the theory³⁴. The intersegmental parameters for the VME-S pair were obtained in Figure 1b from experimental phase diagrams of the mixture of type A_{r_1}/B_{r_2} containing PVME and PS. With these two sets of intersegmental parameters, we use the phase diagram of the system PVME/(MMA-*co*-S) at a fixed copolymer

composition reported by Chien *et al.*³⁸ to obtain the remaining intersegmental parameters for the VME-MMA pair. The polymer samples used by Chien *et al.*, however, are polydisperse; $M_w/M_n=1.9$ for PVME and $M_w/M_n=1.6$ for MMA-*co*-S copolymers where M_n is the number-average molecular weight. Therefore, it was first necessary to adjust slightly the $\kappa_{\text{VME-S}}$ obtained in Figure 1b to 0.01101 such that the theoretical LCST agrees with experiment in the system PVME/PS studied by Chien *et al.*³⁸

Figure 2 compares theoretical coexistence and spinodal curves with cloud points for the system PVME/(MMA-*co*-S) containing 29.2 % methyl methacrylate by weight in the copolymer. The intersegmental parameters for the VME-MMA pair were obtained by assuming that the critical temperature and mixture composition are 127 °C and 79 wt% PVME, respectively; they are given in Table II. Agreement between the theoretical coexistence curve and experimental cloud points is good. To examine how the choice of critical composition affects the prediction of LCST at different copolymer compositions, we also obtain the second set of intersegmental parameters for the VME-MMA pair ($\kappa_{\text{VME-MMA}}=-0.02879$, $\zeta_{\text{VME-MMA}}=-0.01685$) assuming that the critical composition is 60 wt% PVME.

Figure 2b compares the calculated copolymer-composition dependence of LCST for the system PVME/(MMA-*co*-S) with experiment determined by cloud-point measurements³⁸. Theoretical LCSTs are for $M_1=35200$ and $M_2=130000$, respectively. The model underestimates the methyl methacrylate composition at which the LCST is the maximum. Because our calculations neglect the possible screening effect in MMA-*co*-S copolymers³⁴, theory and experiment are in surprisingly good agreement. The maximum LCST is slightly lower for the second set of intersegmental parameters for the VME-MMA. However, it is clear that the choice of critical composition in Figure 2a does not have a significant effect on the prediction of LCST.

In the system PVME/(MMA-*co*-S), LCST increases as the methyl methacrylate content rises because intramolecular interactions of copolymers become more

unfavorable, leading to more favorable intermolecular interactions relative to intramolecular interactions. The maximum LCST therefore depends primarily on the magnitude of interaction energies between methyl methacrylate and styrene segments. Figure 2b shows that the previously determined intersegmental parameters for the S-MMA pair can be used as the parameters for the S-MMA pair in the system PVME/(MMA-*co*-S). These intersegmental parameters were obtained from the mixture containing S-*co*-MMA random copolymers differing in copolymer compositions, Figure 3 of Reference 34.

Systems Containing Vinyl Methyl Ether, Styrene, and Acrylonitrile. The LCST in the system PVME/(MMA-*co*-S) increases as much as about 30 °C relative to that in the system PVME/PS. An interesting question is how much the LCST increases if methyl methacrylate in the MMA-*co*-S copolymer is replaced by acrylonitrile which has more unfavorable interactions with styrene. For the mixture of PVME with poly(acrylonitrile-*co*-styrene) (AN-*co*-S) random copolymer, the copolymer-composition dependence of cloud-point temperatures at a fixed mixture composition was measured by Min and Paul⁴⁰. The mixture composition was chosen to be 80 % PVME by weight because the minimum in the cloud points occurs near this composition. The data by Min and Paul may be taken as the LCST of the system PVME/(AN-*co*-S).

Pure-component *PVT* data of polyacrylonitrile (PAN) are not available. The PHSC equation-of-state parameters for PAN were obtained as follows. We first regress the equation-of-state parameters (ϵ , σ , and r/M) of AN-*co*-S random copolymers¹⁵ at various acrylonitrile contents using the PHSC equation of state for homopolymers²⁹. A plot of equation-of-state parameters obtained in this manner against the mole fraction of acrylonitrile in the copolymer roughly follows straight lines. Equation-of-state parameters for PAN were then obtained by linear extrapolation to zero styrene content in the copolymer; they are given in Table II.

Only limited information is available for the phase behavior of the mixture containing acrylonitrile and styrene segments from which the intersegmental parameters for the S-AN pair can be obtained. An experimental miscibility map of a mixture of type $(A_X B_{1-X})_{r_1} / (A_Y B_{1-Y})_{r_2}$ containing AN-co-S random copolymers in the styrene-rich region was obtained by Molau⁴¹. Schmitt *et al.*⁴² also reported the molecular-weight dependence of the partial-miscibility map at a fixed acrylonitrile composition of one component. Unfortunately, References 41 and 42 do not report the temperatures at which those miscibility maps represent the phase behavior of the mixture. Molau^{41,43}, however, implied that the experiment was carried out at temperatures above the glass-transition temperature of the mixture.

To obtain the intersegmental parameters for the S-AN pair, we use the data by Molau⁴¹ assuming that the miscibility map was obtained at 170 °C. Figure 3 compares the theoretical miscibility map with experiment for the mixture of type $(A_X B_{1-X})_{r_1} / (A_Y B_{1-Y})_{r_2}$ containing AN-co-S random copolymers ($M_w=140000-170000$, $M_w/M_n=1.3-2.0$). Theoretical miscibility maps were computed at 170 °C for $M_1=M_2=150000$ using only one intersegmental parameter, κ_{S-AN} ($\zeta_{S-AN}=0$). Because it is difficult to identify the boundary between miscible and immiscible regions and because the temperature is not known precisely, we obtain two intersegmental parameters; $\kappa_{S-AN}=0.05055$ and 0.085 . The theoretical miscibility map with $\kappa_{S-AN}=0.05055$ gives a slightly wider miscible area than that with $\kappa_{S-AN}=0.085$. The theory with $\kappa_{S-AN}=0.085$ also seems to underestimate slightly the miscible area. With these parameters, theory predicts that immiscibility is caused by UCST behavior.

It is possible to estimate the intersegmental parameters which predict immiscibility due to LCST behavior. To obtain LCST behavior in the system shown in Figure 3, it is necessary to use an unreasonably large ζ_{S-AN} (e.g., -0.1). Such a large ζ_{S-AN} , however, is physically unrealistic because with this value the second virial cross coefficient for acrylonitrile and styrene segments deviates more than 30 % from that

obtained with the assumption of additivity of effective hard-sphere diameters. The measured densities of AN-co-S random copolymers indicate that the AN-co-S random copolymer essentially exhibits volume additivity⁴.

The remaining intersegmental parameters for the VME-AN pair are obtained using the LCST of the system PVME/(AN-co-S) at a fixed copolymer composition reported by Min and Paul⁴⁰. Although Min and Paul did not report the polydispersity indices of the polymers, these polymers may be polydisperse. It was therefore necessary to adjust slightly the $\kappa_{\text{VME-S}}$ obtained in Figure 1b to 0.01096 such that the theoretical LCST agrees with experiment in the system PVME/PS studied by these authors. Experiment shows that for the system PVME/(AN-co-S) containing 80 % PVME by weight, the cloud-point temperature is approximately 128 °C when the copolymer contains 11.5 % acrylonitrile by weight. We take this point as the LCST of the mixture and obtain the intersegmental parameters for the VME-AN pair from the LCST. Intersegmental parameters for the VME-AN pair are given in Table II.

Figure 4 compares the copolymer-composition dependence of theoretical LCST for the system PVME/(AN-co-S) with the cloud points of the mixtures containing 80 wt% PVME. Theoretical LCSTs are for $M_1=99000$ and $M_2=200000$. Although the copolymer composition at which the LCST is the maximum is smaller for the system PVME/(AN-co-S) (7 % AN by weight) than that for the system PVME/(MMA-co-S) (20 % MMA by weight), the increase in the LCST for the system PVME/(AN-co-S) is higher than that for the system PVME/(MMA-co-S). This observation follows because the interactions between acrylonitrile and styrene segments are more unfavorable than those between methyl methacrylate and styrene.

In Figure 4, the curve with $\kappa_{\text{S-AN}}=0.05055$ gives lower LCST than that with $\kappa_{\text{S-AN}}=0.085$ which represents more unfavorable interactions between acrylonitrile and styrene segments. The maximum LCST appears to be sensitive to the choice of intersegmental parameter $\kappa_{\text{S-AN}}$.

Systems Containing Tetramethyl Bisphenol A Polycarbonate, Styrene, and Methyl Methacrylate. The copolymer-composition dependences of LCST in the system $A_{r_1}(C_Y B_{1-Y})_{r_2}$ are also reported for mixtures of tetramethyl bisphenol A polycarbonate (TMPC) and MMA-co-S and for the system TMPC/(AN-co-S) studied by Kim and Paul¹⁵. The phase-separation temperatures in these systems are about 120 °C higher than those in the systems PVME/(MMA-co-S) and PVME/(AN-co-S). TMPC and polystyrene (PS) are miscible up to about 240 °C¹⁵.

Pure-component *PVT* data for TMPC are reported by Kim and Paul in Reference 14 together with the phase diagram of the system TMPC/PS. These authors determined the phase separation temperatures by the d.s.c. method. In this technique, the polymer blends of known proportions were first annealed for 5 min at temperatures near the expected phase-separation temperature. The breadth of the glass-transition region in the d.s.c. scans was then determined as a function of annealing temperature; the onset of a large change in this plot was identified as the phase-separation temperature.

The PHSC equation-of-state parameters ϵ and σ of TMPC were regressed by presetting r/M to 0.012. To obtain good agreement of theory with the experimental phase diagram in the system TMPC/PS, it was necessary to use the equation-of-state parameters obtained by presetting r/M to this value. The equation-of-state parameters ϵ and σ for TMPC which give the best fit of pure-component *PVT* data are about 30 % smaller than those of PS. When the optimum equation-of-state parameters of TMPC are used, theory predicts an UCST in the system TMPC/PS where experiment shows a LCST. Probably because the difference in equation-of-state parameters is large. By presetting r/M to 0.012, the equation-of-state parameters of TMPC are comparable to those of PS. The adjusted PHSC equation-of-state parameters for TMPC are given in Table II.

Figure 5 compares theoretical coexistence and spinodal curves with the phase-separation temperatures determined by the d.s.c method for the system TMPC/PS¹⁴. The weight-average molecular weight determined by light-scattering measurements and the

polydispersity index determined by gel permeation chromatography (GPC) measurements of TMPC are reported to be $M_w=33000$ and $M_w/M_n=2.1$, respectively. For polystyrene, $M_w=330000$ and $M_w/M_n=3.3$, determined by GPC measurements. Theoretical curves are for $M_1=33000$ and $M_2=330000$. The intersegmental parameters for the TMPC-S pair were obtained by assuming that the critical temperature and mixture composition are 242 °C and 55 wt% PS, respectively; they are given in Table III. With these parameters, the calculated spinodal curve agrees very well with experiment. In addition, theory predicts that the LCST in the system TMPC/PS is insensitive to the molecular weight of PS. For example, the theoretical LCST increases only 2.2 °C when the molecular weight of PS decreases from 330000 to 100000. The analysis by Guo and Higgins⁴⁴, who determined the cloud points of the system TMPC/PS with various molecular weights of polydisperse PS, also shows that the LCST in the system TMPC/PS is insensitive to the molecular weight of PS. It is, however, not clear that the phase-separation temperatures determined by the d.s.c. method represent the spinodal curve.

Figure 6 compares the theoretical copolymer composition dependence of LCST with experiment for the systems TMPC/(MMA-co-S)¹⁵. Theory is for $M_1=33000$ and $M_2=200000$. The intersegmental parameters for the S-MMA pair are the same as those used in the systems PVME/(MMA-co-S). The critical compositions in the system TMPC/(MMA-co-S) do not vary significantly with the copolymer composition¹⁵. The intersegmental parameters for the TMPC-MMA pair were obtained by assuming that in the system TMPC/(MMA-co-S) containing 35 % methyl methacrylate by weight in the copolymer, the critical temperature and mixture composition are 210 °C and 45 wt% TMPC, respectively. The copolymer-composition dependence of LCST in the system TMPC/(MMA-co-S) is similar to that in the system PVME/(MMA-co-S) shown in Figure 2. The phase-separation temperatures for the former system, however, are about 120 °C higher than those in the latter system. Using the same set of intersegmental parameters for

the S-MMA pair, theory gives fair agreement with experiment over a wide temperature range.

Systems Containing Tetramethyl Bisphenol A Polycarbonate, Styrene, and Acrylonitrile. Figure 7a compares theoretical coexistence and spinodal curves with cloud points for the system TMPC/(AN-co-S) containing 18 % acrylonitrile by weight in the copolymer. In Figure 7a, the intersegmental parameter for the S-AN pair is $\kappa_{S-AN}=0.085$. The critical mixture composition in the system TMPC/(AN-co-S) shifts toward the copolymer-rich composition as the acrylonitrile content in the copolymer rises¹⁵. The intersegmental parameters for the TMPC-AN pair were obtained by assuming that in the system shown in Figure 7a, the critical temperature and mixture composition are 180 °C and 60 wt% TMPC, respectively; they are given in Table II. Theoretical curves are for $M_1=33000$ and $M_2=200000$. The second set of intersegmental parameters is also obtained using $\kappa_{S-AN}=0.05055$ and $\zeta_{S-AN}=0$ for the S-AN pair.

Figure 7b compares the theoretical copolymer-composition dependence of LCST with experiment for the system TMPC/(AN-co-S)¹⁵. Theoretical curves are for $M_1=33000$ and $M_2=200000$. Similar to the system PVME/(AN-co-S) in Figure 4, the theory with $\kappa_{S-AN}=0.05055$ underestimates the LCST. Theoretical LCST with $\kappa_{S-AN}=0.085$ and experiment show good agreement.

Systems Containing Cyclohexyl Methacrylate, Styrene, and Acrylonitrile. Copolymer-composition dependence of LCST, similar to that in the systems PVME/(AN-co-S) and TMPC/(AN-co-S), is also available for mixtures of poly(cyclohexyl methacrylate) (PCHMA) and AN-co-S random copolymers⁴⁵. PCHMA and polystyrene (PS) are reported to be miscible to about 240 °C. Unfortunately, Reference 45 does not report the detailed characteristics of polymer samples and the complete phase diagram of the system TMPC/PS. The intersegmental parameters for the CHMA-S pair were

obtained by assuming that the critical temperature and mixture composition in the system PCHMA/PS are 240 °C and 70 wt% PS, respectively, for $M_1=M_2=200000$.

Figure 8 compares the theoretical LCST with the phase-separation temperature for the system PCHMA/(AN-co-S). The open and solid circles are for blends which are clear and cloudy, respectively, after annealing for 15 min at the indicated temperature. The open squares represent the blends which are clear to the thermal decomposition temperature (270 °C). The mixture composition is 50 wt% PS for all measurements. Theory is for $M_1=M_2=200000$.

The solid curve is calculated using the intersegmental parameter $\kappa_{S-AN}=0.085$ for the S-AN pair. The semi-broken curve is for the theory with $\kappa_{S-AN}=0.05055$. The intersegmental parameters for the CHMA-AN pair were obtained by assuming that the critical temperature and mixture composition are 185 °C and 70 wt% PS for the AN-co-S copolymer containing 14.7 % acrylonitrile by weight. The predicted maximum LCST with $\kappa_{S-AN}=0.085$ is about 30 °C higher than that predicted with $\kappa_{S-AN}=0.05055$. Theory and experiment are in good agreement. In the subsequent paper of this series, the intersegmental parameters obtained here are used to analyze the miscibility map of the system poly(cyclohexyl methacrylate-co-methyl methacrylate) / poly(acrylonitrile-co-styrene), a system containing four kinds of segments which requires six sets of intersegmental parameters.

Intersegmental Parameters for the Styrene-Acrylonitrile Pair. For mixtures of type $A_{r_1}/(C_Y B_{1-Y})_{r_2}$ containing AN-co-S random copolymers shown in Figures 4 and 7b, the measured copolymer-composition dependences of LCST agree better with the theoretical LCSTs with $\kappa_{S-AN}=0.085$ than those with $\kappa_{S-AN}=0.05055$. The theory with $\kappa_{S-AN}=0.085$, however, seems to underestimate the miscible area in the miscibility map of the mixture of type $(A_X B_{1-X})_{r_1}/(A_Y B_{1-Y})_{r_2}$ containing AN-co-S random copolymers shown in Figure

3.

These observations may be explained by the effect of nonrandom mixing. Since the interactions between acrylonitrile and styrene segments are highly unfavorable, the number of contacts between AN-*co*-S copolymers in the real mixture is likely to be smaller than that predicted by random mixing. Consequently, the number of contacts between homopolymer and AN-*co*-S copolymer in the real mixture can be larger than that in the random mixture, leading to enhanced solubility of AN-*co*-S copolymers. If the same intersegmental parameters are used for the S-AN pair, the theory which takes nonrandom mixing into account may give a higher LCST than that given by a theory which assumes random mixing. In the present theory, the perturbation term for attractive interactions assumes the random mixing of molecules.

As a first approximation, however, a value between 0.05055 and 0.085 can be used as the intersegmental parameter for the S-AN pair, κ_{S-AN} , with $\zeta_{S-AN}=0$. In the subsequent paper of this series, we use $\kappa_{S-AN}=0.05055$ to analyze miscibility maps of systems containing styrene and acrylonitrile segments.

CONCLUSIONS

The perturbed hard-sphere-chain (PHSC) equation of state is able to represent immiscibility caused by lower critical solution temperature (LCST) phase behavior in copolymer systems. The PHSC equation of state is applied to homopolymer/copolymer mixtures containing poly(methyl methacrylate-*co*-styrene) (MMA-*co*-S) and poly(acrylonitrile-*co*-styrene) (AN-*co*-S) random copolymers where the mixture of homopolymer and polystyrene exhibits a LCST. The intersegmental parameters for the S-MMA and S-AN pairs were obtained from experimental miscibility maps for mixtures of type $(A_X B_{1-X})_{r_1} / (A_Y B_{1-Y})_{r_2}$ containing S-*co*-MMA and S-*co*-AN random copolymers, respectively. Using these intersegmental parameters for the S-MMA and S-AN pairs, the theoretical copolymer-composition dependence of LCST shows fair agreement with experiment.

Intersegmental parameters are obtained for ten pairs of segments. In the systems studied in this work, unique values are assigned to the intersegmental parameters for a given pair of segments.

ACKNOWLEDGMENT

This work was supported by the Director, Office of Energy Research, Office of Basic Energy Sciences, Chemical Sciences Division of the U.S. Department of Energy under Contract No. DE-AC03-76SF0098. Additional funding was provided by E.I. du Pont de Nemours & Co. (Philadelphia, PA) and Koninklijke Shell (Amsterdam, The Netherlands). The authors thank S.M. Lambert for performing the regression of pure-component parameters. The authors also thank Professor D.R. Paul and Dr. C.K. Kim for providing pure-component *PVT* data of several homopolymers and copolymers.

References

1. Coleman, M.M.; Graf, J.F.; Painter, P.C. *Specific Interactions and the Miscibility of Polymer Blends*; Technomic Publishing Company, Inc.: Lancaster, P.A., 1991.
2. Hino, T.; Lambert, S.M.; Soane, D.S.; Prausnitz, J.M. *Polymer* **1993**, *34*, 4756.
3. Suess, M.; Kressler, J.; Kammer, H.W. *Polymer* **1987**, *28*, 957.
4. Fowler, M.E.; Barlow, J.W.; Paul, D.R. *Polymer* **1987**, *28*, 1177.
5. Kressler, J.; Kammer, H.W.; Schmidt-Naake, G.; Herzog, K. *Polymer* **1988**, *29*, 686.
6. Kammer, H.W.; Piglowski, J. *Acta Polymerica* **1989**, *40*, 363.
7. Fernandes, A.C.; Barlow, J.W.; Paul, D.R. *J. Appl. Polym. Sci.* **1986**, *32*, 5481.
8. Shiomi, T.; Suzuki, M.; Tohyama, M.; Imai, K. *Macromolecules* **1989**, *22*, 3578.
9. Sanchez, I.C.; Lacombe, R.H. *Macromolecules* **1978**, *11*, 1145.
10. Sanchez, I.C.; Lacombe, R.H. *J. Polym. Sci. Polym. Lett. Edn.* **1977**, *15*, 71.
11. Pañayiotou, C.G. *Macromolecules* **1987**, *20*, 861.
12. Panayiotou, C.G. *Makromol. Chem.* **1987**, *188*, 2733.
13. Kim, J.H.; Barlow, J.W.; Paul, D.R. *J. Polym. Sci. Polym. Phys. Edn.* **1989**, *27*, 223.
14. Kim, C.K.; Paul, D.R. *Polymer* **1992**, *33*, 1630.
15. Kim, C.K.; Paul, D.R. *Polymer* **1992**, *33*, 2089.

16. Prigogine, I. *The Molecular Theory of Solutions*; North-Holland Publishing: Amsterdam, 1957.
17. Flory, P.J. *Discuss. Faraday. Soc.* **1970**, *49*, 7.
18. Patterson, D.; Robard, A. *Macromolecules* **1978**, *11*, 690.
19. Kammer, H.W. *Acta Polymerica* **1986**, *37*, 1.
20. Kammer, H.W.; Inoue, T.; Ougizawa, T. *Polymer* **1989**, *30*, 888.
21. Jo, W.H.; Lee, M.S. *Macromolecules*, **1992**, *25*, 842.
22. Lee, M.S.; Lee, S.C.; Chae, S.H.; Jo, W.H. *Macromolecules* **1992**, *25*, 4339.
23. McMaster, L.P. *Macromolecules* **1973**, *6*, 760.
24. Shiomi, T.; Ishimatsu, H.; Eguchi, T.; Imai, K. *Macromolecules* **1990**, *23*, 4970.
25. Shiomi, T.; Eguchi, T.; Ishimatsu, H.; Imai, K. *Macromolecules* **1990**, *23*, 4978.
26. Koningsveld, R.; Kleintjens, L.A. *Macromolecules* **1985**, *18*, 243.
27. Koningsveld, R.; Kleintjens, L.A.; Leblans-Vinck, A.M. *Ber. Bunsenges. Phys. Chem.* **1985**, *89*, 1234.
28. Song, Y.; Lambert, S.M.; Prausnitz, J.M. *Macromolecules* **1994**, *27*, 441.
29. Song, Y.; Lambert, S.M.; Prausnitz, J.M. *Ind. Eng. Chem. Res.* **1994**, *33*, 1047.
30. Song, Y.; Lambert, S.M.; Prausnitz, J.M. *Chem. Eng. Sci.* **1994**, *49*, 2765.
31. Song, Y.; Lambert, S.M.; Prausnitz, J.M. paper presented at AIChE meeting in St. Louis, November 1993.
32. Hino, T.; Song, Y.; Prausnitz, J.M. *Macromolecules* **1994**, *27*, 5681.
33. Chiew, Y.C. *Mol. Phys.* **1990**, *70*, 129.
34. Hino, T.; Song, Y.; Prausnitz, J.M. submitted to *Macromolecules* **1995**.
35. Walsh, D.J.; Dee, G.T.; Halary, J.L.; Ubiche, J.M.; Millequant, M.; Lesec, J.; Monnerie, L. *Macromolecules* **1989**, *22*, 3395.
36. Ougizawa, T.; Dee, G.T.; Walsh, D.J. *Macromolecules* **1991**, *24*, 3834.
37. Rodgers, P.A. *J. Appl. Polym. Sci.* **1993**, *48*, 1061.
38. Chien, Y.Y.; Pearce, E.M.; Kwei, T.K. *Macromolecules* **1988**, *21*, 1616.
39. Halary, J.L.; Leviet, M.H.; Kwei, T.K.; Pearce E.M. *Macromolecules* **1991**, *24*, 5939.
40. Min, K.E.; Paul, D.R. *J. Polym. Sci. Polym. Phys. Ed.* **1988**, *26*, 2257.
41. Molau, G.E. *Polym. Lett.* **1965**, *3*, 1007.
42. Schmitt, B.J.; Kirste, R.G.; Jelenic, J. *Makromol. Chem.* **1980**, *181*, 1655.
43. Traylor, P.A. *Anal. Chem.* **1961**, *33*, 1629.
44. Guo, W.; Higgins, J.S. *Polymer* **1990**, *31*, 699.
45. Nishimoto, M.; Keskkula, H.; Paul, D.R. *Macromolecules* **1990**, *23*, 3633.

TABLE I. PHSC Equation-of-State Parameters for Homopolymers²⁹

polymer	r/M (mol/g)	σ (Å)	ϵ/k_B (K)
polystyrene	0.01117	5.534	724.7
poly(methyl methacrylate)	0.01432	4.850	655.9
poly(vinyl methyl ether) ^a	0.018	4.659	489.5
polyacrylonitrile ^a	0.01057	5.414	769.5
tetramethyl bisphenol A polycarbonate ^a	0.012	5.249	631.6
poly(cyclohexyl methacrylate)	0.01482	4.889	607.2

M = molecular weight (g/mol); ^a this work.

TABLE II. Intersegmental Parameters

binary pair	κ	ζ
styrene–methyl methacrylate ^a	-0.02125	-0.02
styrene–acrylonitrile	0.05055 (0.085)	0 (0)
vinyl methyl ether–styrene	0.01093	0.0003
vinyl methyl ether–methyl methacrylate	-0.0253	-0.01464
vinyl methyl ether–acrylonitrile	0.05598 (0.08974) ^c	0.00286 (0.00425) ^c
TMPC–styrene ^b	-0.004402	-0.003166
TMPC–methyl methacrylate	-0.02703	-0.01810
TMPC–acrylonitrile	0.05687 (0.08492) ^c	0.00832 (0.00747) ^c
cyclohexyl methacrylate–styrene	0.001936	-0.001718
cyclohexyl methacrylate–acrylonitrile	0.04217 (0.06327) ^c	-0.00317 (-0.00770) ^c

^a Ref. 34; ^b tetramethyl bisphenol A polycarbonate; ^c for $\kappa_{S-AN}=0.085$.

TABLE III. Characterization of Polymer Samples Used in Reference 35

sample	mol wt (M_w)	M_w/M_n
PS233	233000	1.06
PS106	106000	1.06
PS90 ^a	90000	1.05
PS67	67000	1.08
PS36	35700	1.05
PVME152	152000	1.13
PVME95	95000	1.27
PVME77	77000	1.24
PVME56	56000	1.47
PVME45	45000	2.05
PVME35 ^a	35200	1.91

M_n = number-average molecular weight (g/mol); M_w = weight-average molecular weight (g/mol); ^a Ref. 50.

Figure Captions

Figure 1. (a) Experimental phase diagrams for the system PVME/PS with various molecular weights of PS³⁵, (b) Theoretical coexistence curves for the systems shown in Figure 1a, (c) Experimental phase diagrams for the system PVME/PS with various molecular weights of PVME^{35, 38}, (d) Theoretical coexistence curves for the systems shown in Figure 1c. In all calculations $\kappa_{\text{VME-S}}=0.01093$ and $\zeta_{\text{VME-S}}=0.0003$. M_w and M_w/M_n of polymers are given in Table III.

Figure 2. (a) Comparison of theoretical coexistence and spinodal curves with cloud points for the system PVME/(MMA-co-S) containing 29.2 % MMA by weight in the copolymer³⁸. Theoretical curves are for $M_1=35200$ and $M_2=130000$: $\kappa_{\text{VME-S}}=0.01101$, $\zeta_{\text{VME-S}}=0.0003$, $\kappa_{\text{VME-MMA}}=-0.0253$, $\zeta_{\text{VME-MMA}}=-0.01464$, $\kappa_{\text{S-MMA}}=-0.02125$, $\zeta_{\text{S-MMA}}=-0.02$, (b) Copolymer-composition dependence of LCST for the system PVME/(MMA-co-S)³⁸: $M_1=35200$, $M_2=130000$, (—) Theory with the parameters used in Figure 6a; (- · - · -) Theory with $\kappa_{\text{VME-MMA}}=-0.02879$ and $\zeta_{\text{VME-MMA}}=-0.01685$.

Figure 3. Comparison of theoretical miscibility maps with experiment for mixtures of type $(A_X B_{1-X})_{r_1} / (A_Y B_{1-Y})_{r_2}$ containing AN-co-S random copolymers⁴¹: (o) miscible, (●) immiscible. Theoretical miscibility maps are at 170 °C for $M_1=M_2=150000$; (—) $\kappa_{\text{S-AN}}=0.05055$, $\zeta_{\text{S-AN}}=0$; (- · - · -) $\kappa_{\text{S-AN}}=0.085$, $\zeta_{\text{S-AN}}=0$. Theory predicts that immiscibility is caused by UCST behavior. For this system, however, the origin of immiscibility is not reported.

Figure 4. Copolymer-composition dependence of cloud points for the system PVME/(AN-co-S) containing 80 wt% PVME⁴⁰. Solid curve is the calculated LCST for $M_1=99000$ and $M_2=200000$: $\kappa_{\text{VME-S}}=0.01096$, $\zeta_{\text{VME-S}}=0.0003$; (—) $\kappa_{\text{S-AN}}=0.085$, $\zeta_{\text{S-AN}}=0$, $\kappa_{\text{VME-AN}}=0.08974$, $\zeta_{\text{VME-AN}}=0.00425$; (-·-·-) $\kappa_{\text{S-AN}}=0.05055$, $\zeta_{\text{S-AN}}=0$, $\kappa_{\text{VME-AN}}=0.05598$, $\zeta_{\text{VME-AN}}=0.00286$.

Figure 5. Comparison of theory with experimental phase diagram determined by the d.s.c. method for the system TMPC/PS¹⁵. Theory is for $M_1=33000$ and $M_2=330000$ with $\kappa_{\text{TMPC-S}}=-0.004402$ and $\zeta_{\text{TMPC-S}}=-0.003166$.

Figure 6. Copolymer-composition dependence of LCST for the system TMPC/(MMA-co-S)¹⁵. Solid curve is the calculated LCST for $M_1=33000$ and $M_2=200000$: $\kappa_{\text{TMPC-S}}=-0.004402$, $\zeta_{\text{TMPC-S}}=-0.003166$, $\kappa_{\text{TMPC-MMA}}=-0.02703$, $\zeta_{\text{TMPC-MMA}}=-0.01810$, $\kappa_{\text{S-MMA}}=-0.02125$, $\zeta_{\text{S-MMA}}=-0.02$.

Figure 7. (a) Comparison of theoretical coexistence and spinodal curves with the phase-separation temperatures determined by the d.s.c. method for the system TMPC/(AN-co-S) containing 18 % AN by weight in the copolymer¹⁵. Theoretical curves are for $M_1=33000$ and $M_2=200000$: $\kappa_{\text{TMPC-S}}=-0.004402$, $\zeta_{\text{TMPC-S}}=-0.003166$, $\kappa_{\text{TMPC-AN}}=0.08492$, $\zeta_{\text{TMPC-AN}}=0.00747$, $\kappa_{\text{S-AN}}=0.085$, $\zeta_{\text{S-AN}}=0.0$, (b) Copolymer-composition dependence of LCST for the system TMPC/(AN-co-S)¹⁵: $M_1=33000$, $M_2=200000$, (—) Theory with the parameters used in Figure 7a; (-·-·-) $\kappa_{\text{S-AN}}=0.05055$, $\zeta_{\text{S-AN}}=0$, $\kappa_{\text{TMPC-AN}}=0.05687$, $\zeta_{\text{TMPC-AN}}=0.00832$.

Figure 8. Copolymer-composition dependence of LCST for the system PCHMA/(AN-co-S)⁴⁵: $M_1=M_2=200000$, $\kappa_{\text{CHMA-S}}=0.001936$, $\zeta_{\text{CHMA-S}}=-0.001718$, (—) $\kappa_{\text{S-AN}}=0.085$, $\zeta_{\text{S-AN}}=0$, $\kappa_{\text{CHMA-AN}}=0.06327$, $\zeta_{\text{CHMA-AN}}=-0.00770$; (-·-·-) $\kappa_{\text{S-AN}}=0.05055$, $\zeta_{\text{S-AN}}=0$, $\kappa_{\text{CHMA-AN}}=0.04217$, $\zeta_{\text{CHMA-AN}}=-0.00317$.

Figure 1

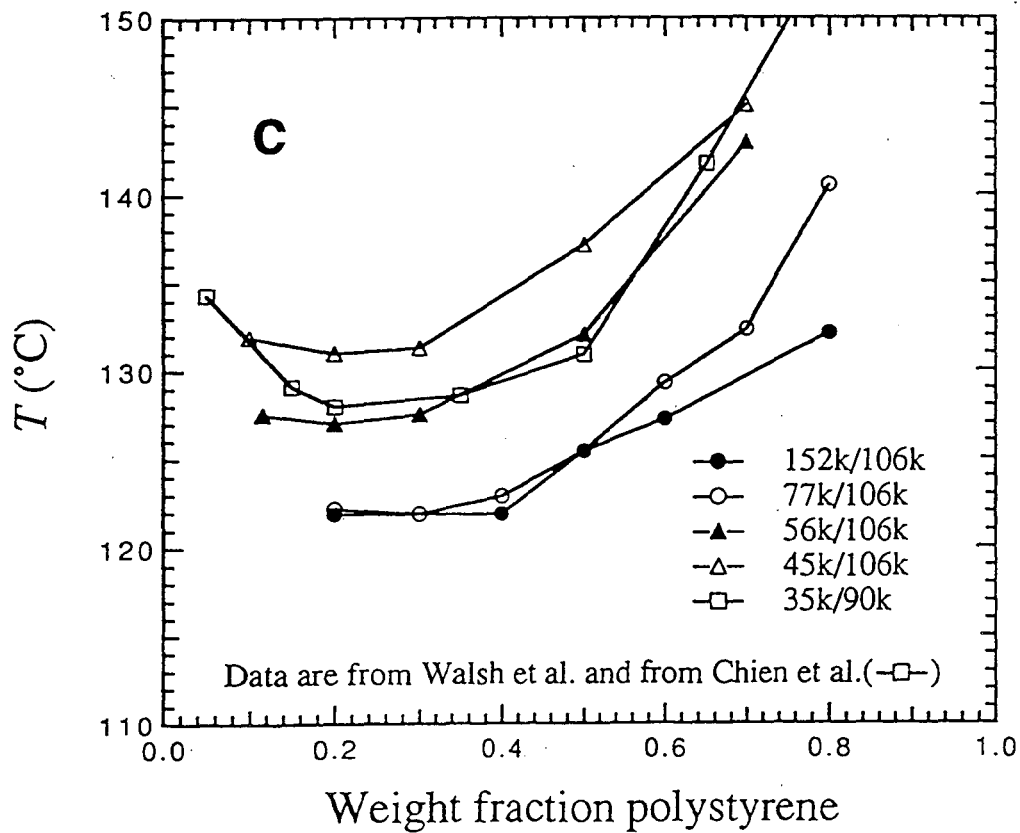
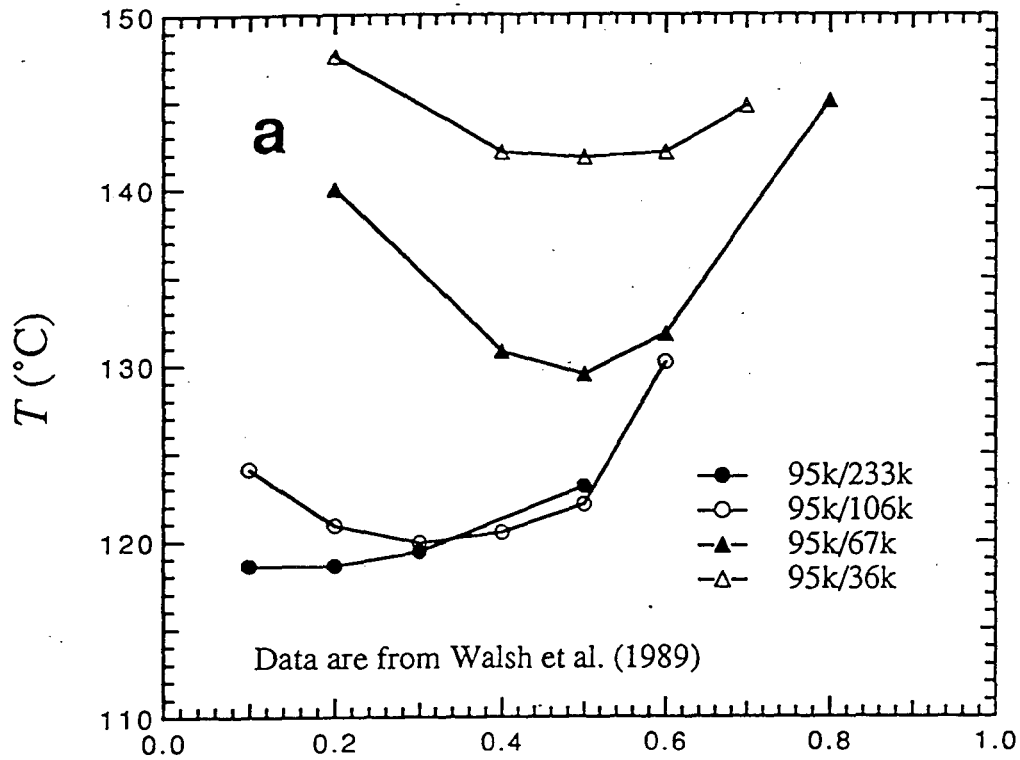


Figure 1

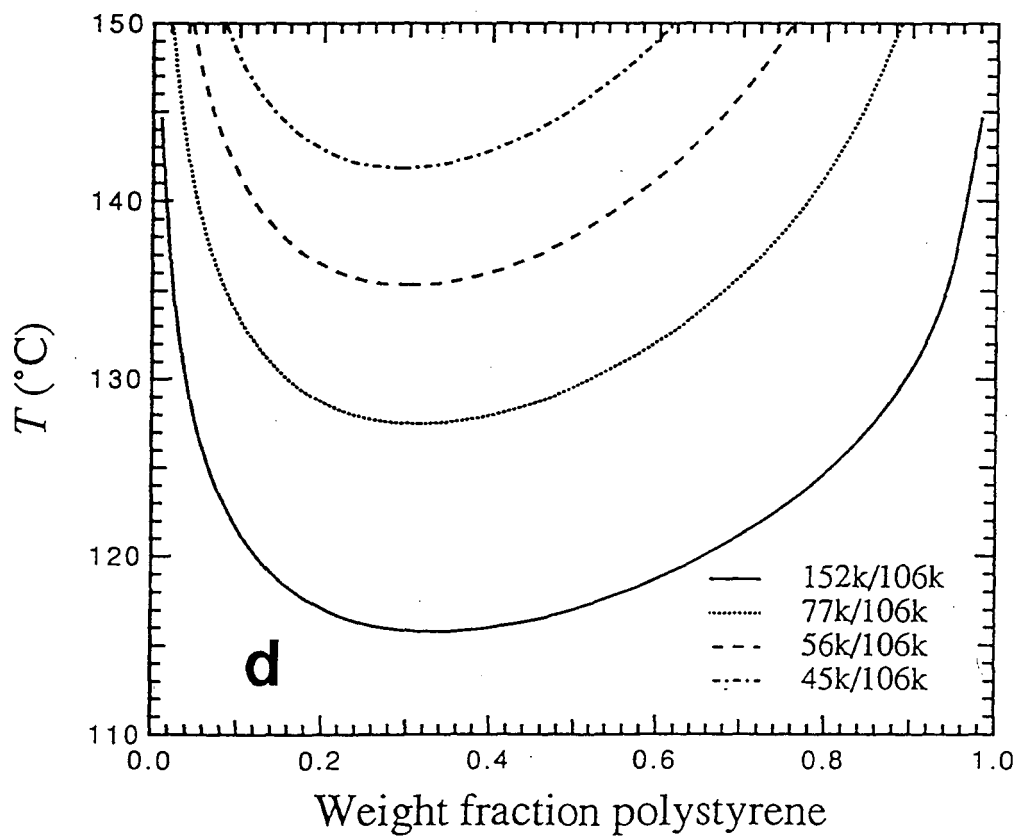
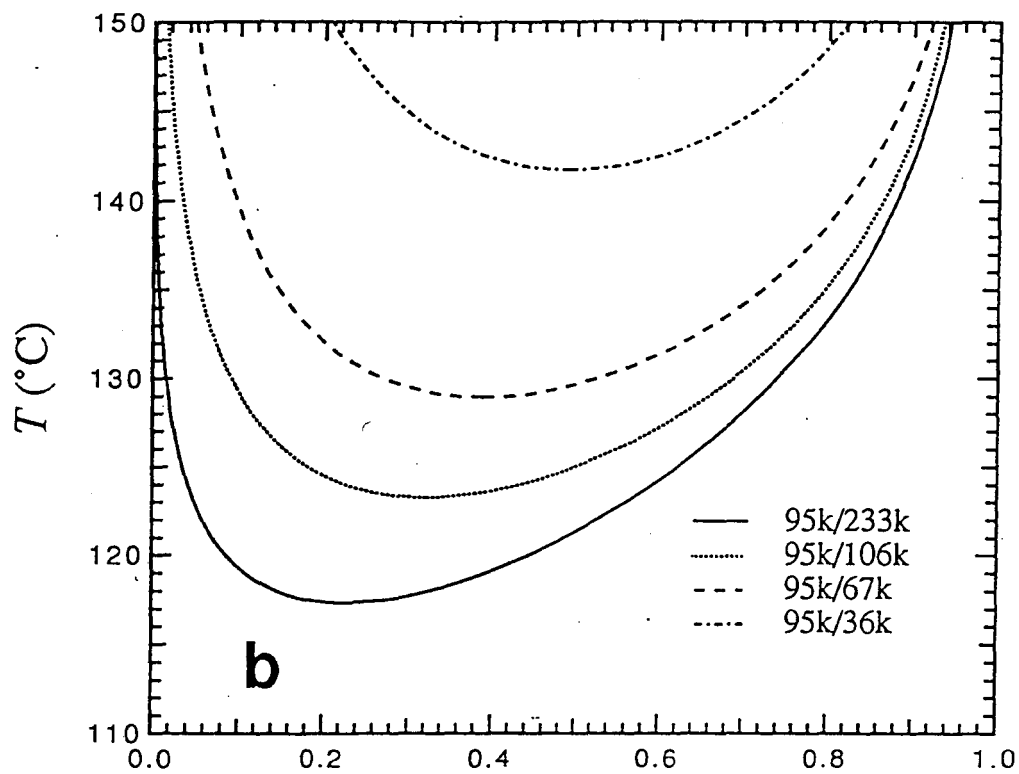


Figure 2

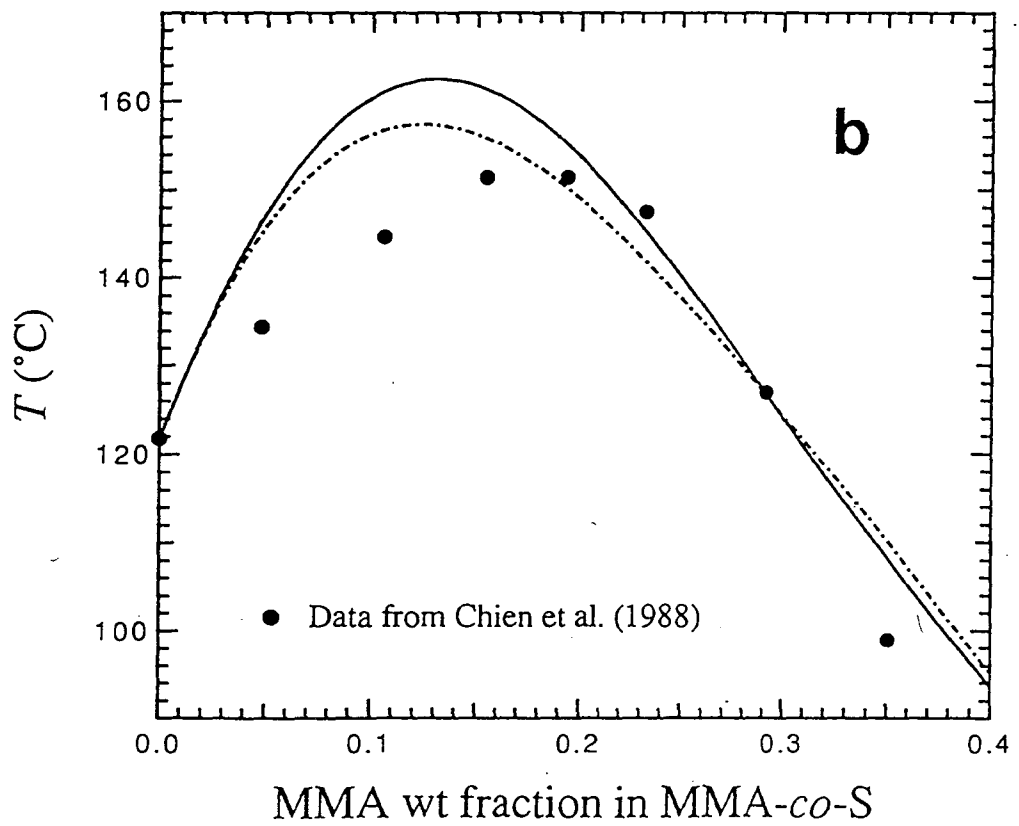
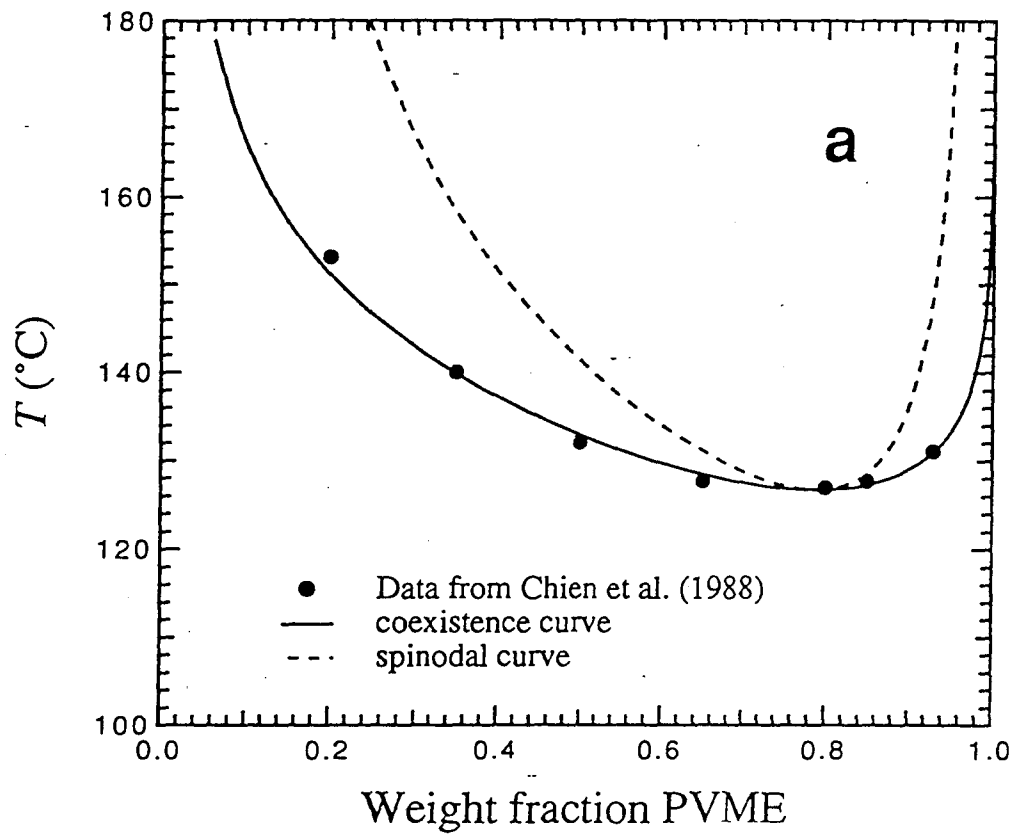


Figure 4

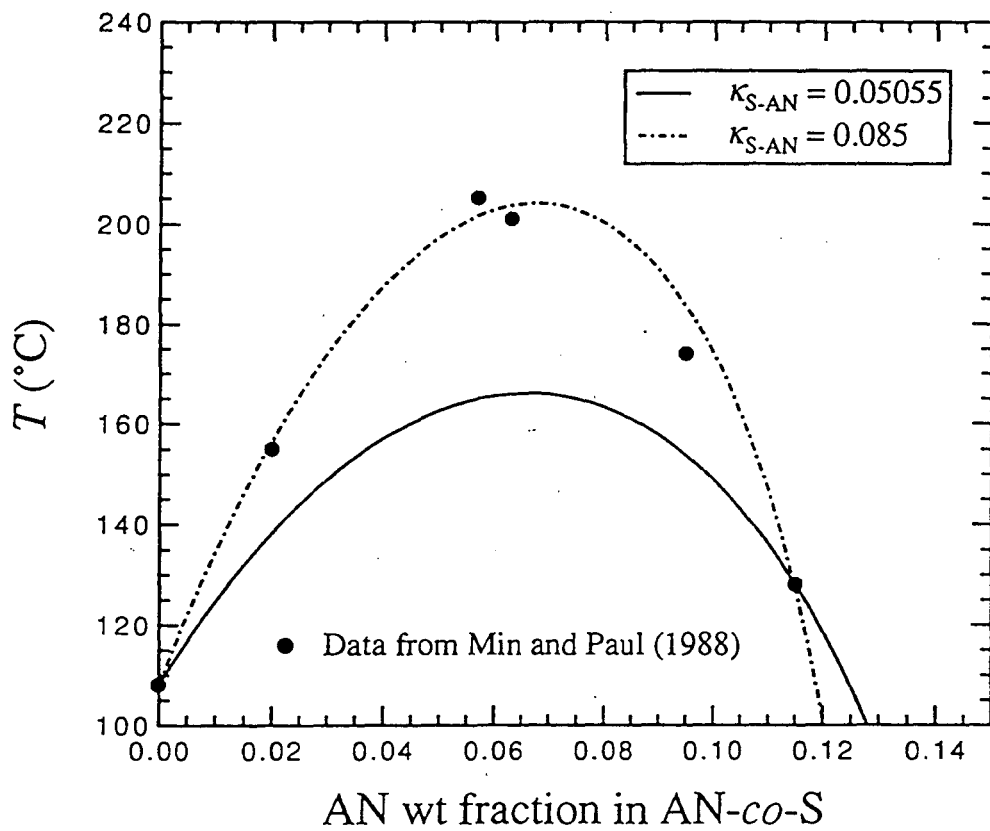


Figure 5

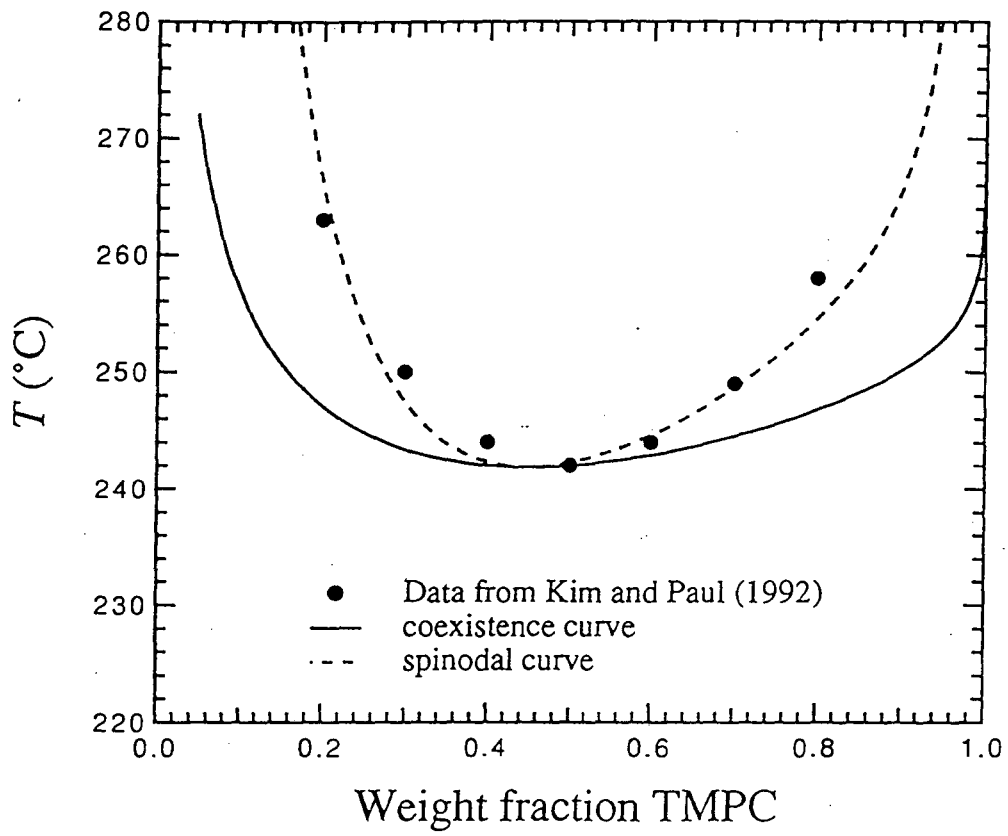


Figure 6

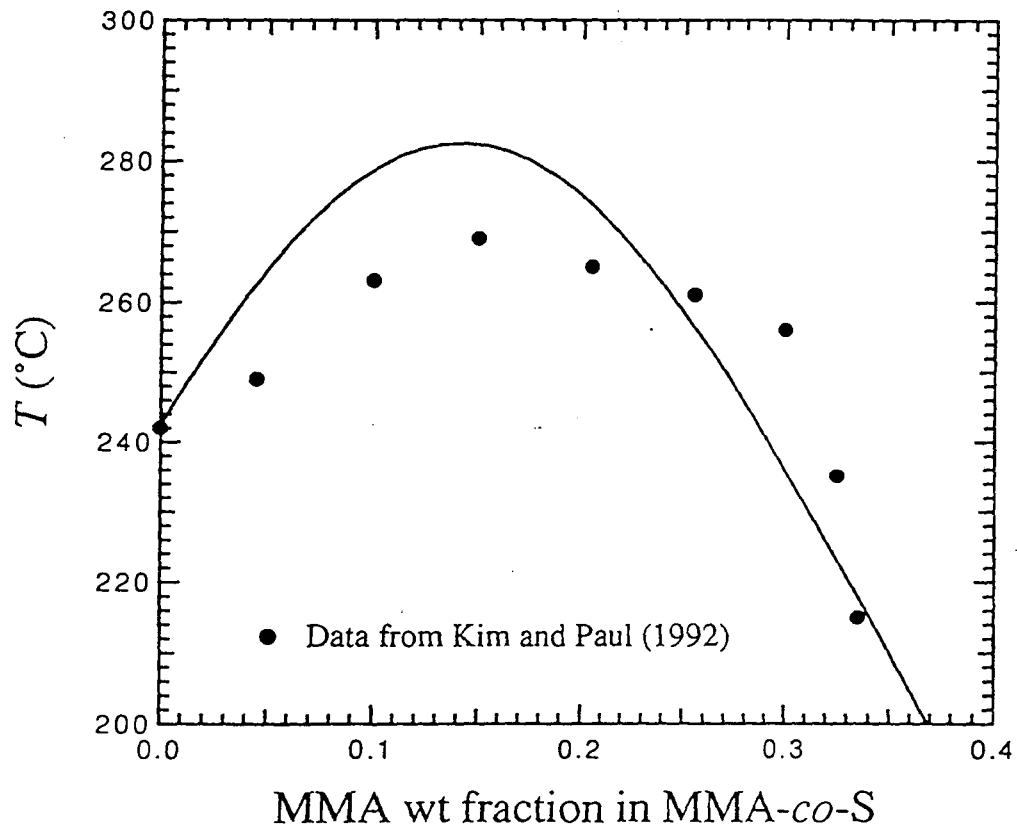


Figure 7

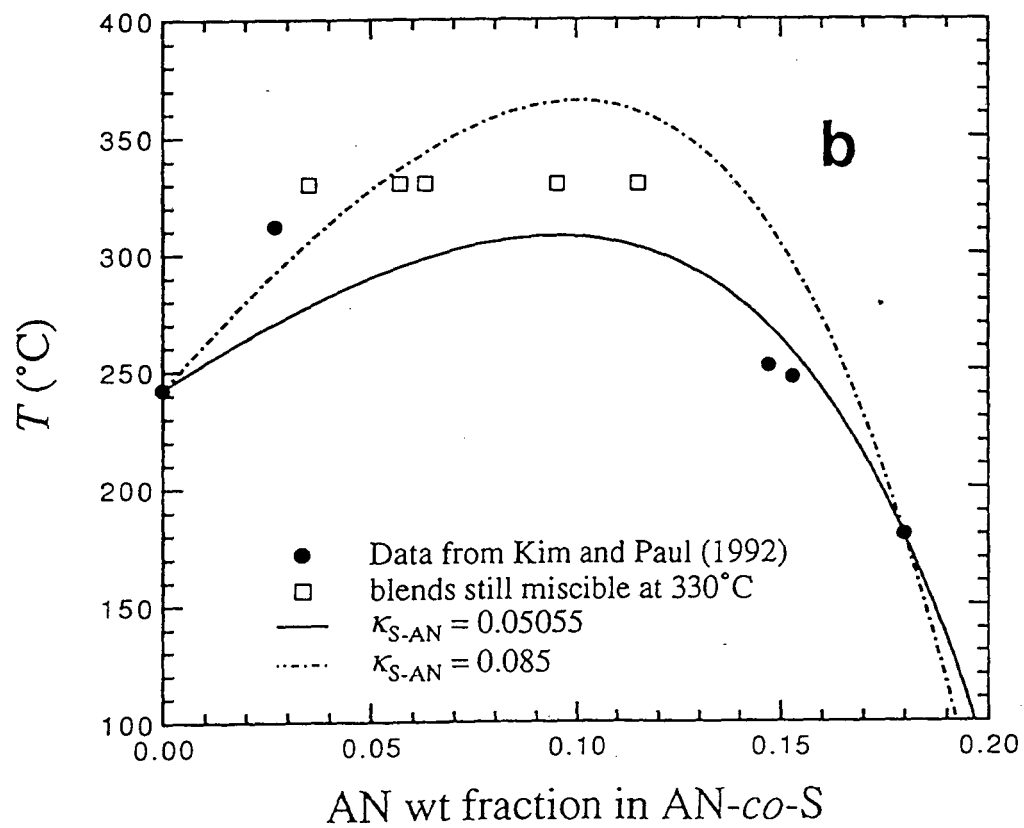
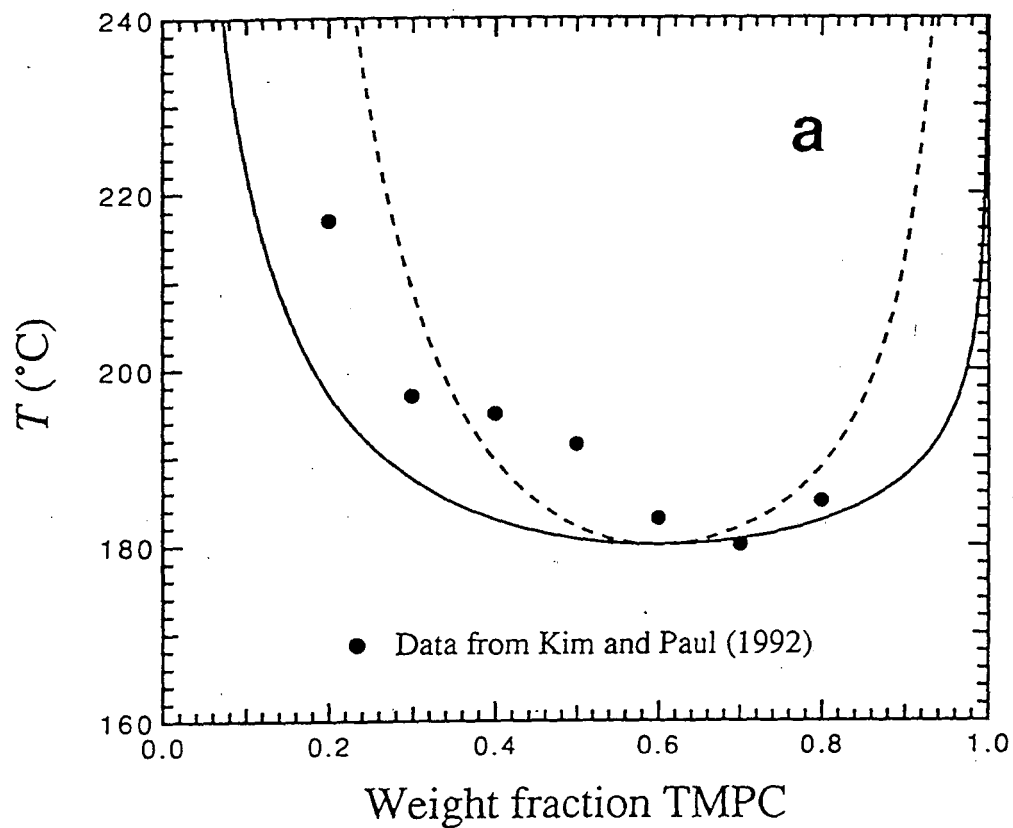
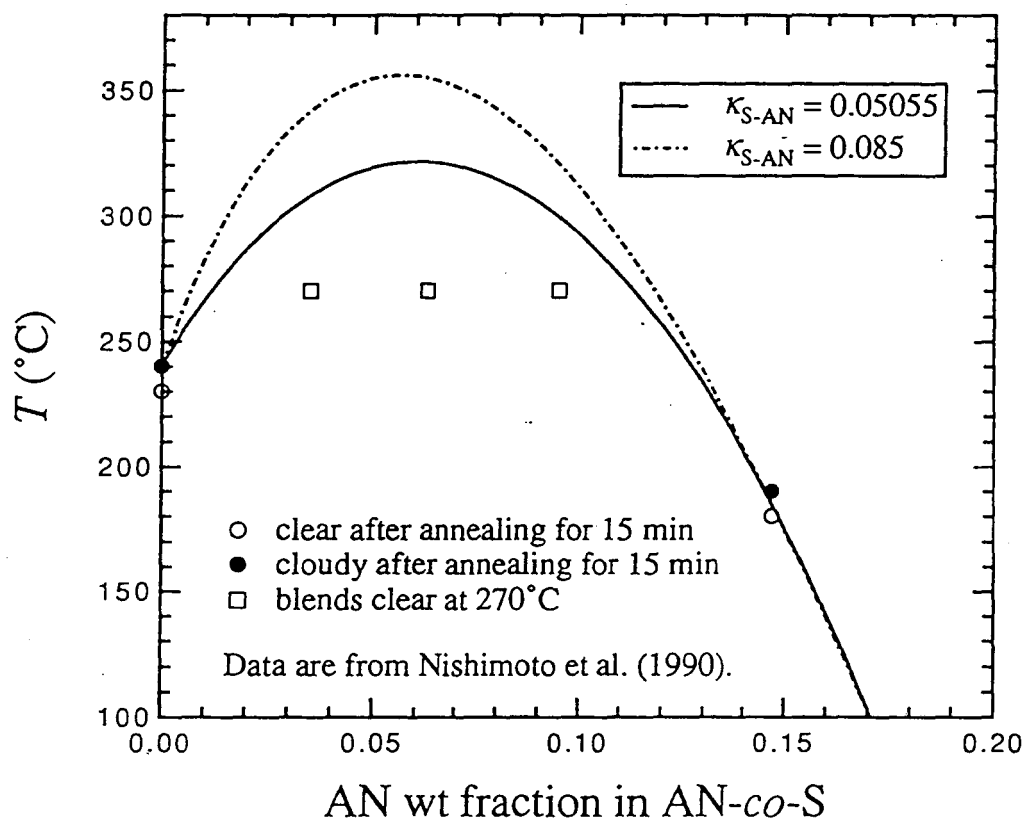


Figure 8



AN EQUATION-OF-STATE ANALYSIS OF BINARY COPOLYMER SYSTEMS 3. MISCIBILITY MAPS

*Toshiaki Hino, Yuhua Song, and John M. Prausnitz **

Department of Chemical Engineering
University of California, Berkeley
and
Chemical Sciences Division
Lawrence Berkeley Laboratory
Berkeley, CA 94720

ABSTRACT

The perturbed hard-sphere-chain (PHSC) equation of state for copolymer systems is applied to binary polymer mixtures containing random copolymers. Intersegmental parameters are obtained for several pairs of segments and theoretical miscibility maps are compared with experiment for systems containing two, three, and four kinds of segments. The PHSC equation of state is able to represent immiscibility caused by lower critical solution temperature (LCST) phase behavior as well as that caused by upper critical solution temperature (UCST) phase behavior. For the system poly(methyl methacrylate) / poly(acrylonitrile-*co*-styrene), theory represents the miscibility window caused by LCST behavior where miscibility changes from immiscible→miscible→immiscible as the composition of poly(acrylonitrile-*co*-styrene) random copolymer becomes rich in acrylonitrile. Using the same set of intersegmental parameters, theoretical miscibility maps and experiment show good agreement for systems containing styrene, acrylonitrile, methyl methacrylate, and cyclohexyl methacrylate.

(Keywords: copolymer blend; equation-of-state; lower critical solution temperature; phase equilibria)

*Correspondence concerning this paper should be addressed to J.M. Prausnitz.

INTRODUCTION

Continuing demand for polymer blends with desired properties has been propelling extensive research on liquid-liquid equilibria of polymer blends¹⁻⁵. One motivation behind these studies is the search for miscible pairs of polymers, including copolymers, which could lead to novel materials.

Miscibilities of copolymer blends have been often analyzed by the classical incompressible Flory-Huggins model⁶⁻⁸, a binary-interaction model where the intramolecular and intermolecular interaction energies are expressed in terms of segmental interaction energies and copolymer compositions. These parameters can be obtained from miscibility/immiscibility boundaries on experimental miscibility maps. Segmental interaction parameters are assumed to be independent of the type of mixtures. In principle, miscibilities of copolymers at constant temperature and pressure can be predicted by the Flory-Huggins model if the relevant segmental interaction parameters are known.

Miscibilities in several binary copolymer mixtures at room temperature⁹⁻¹² were successfully predicted by the classical Flory-Huggins model⁶⁻⁸ using the same set of segmental interaction parameters. In the copolymer systems where miscibilities are sensitive to temperature, however, the temperature dependence of phase behavior is difficult to predict by the classical incompressible Flory-Huggins model. The incompressible Flory-Huggins theory can represent only immiscibility caused by upper critical solution temperature (UCST) type phase behavior. Many copolymer blends, however, exhibit lower critical solution temperature (LCST) phase behavior at elevated temperatures arising from the free-volume effect. In the systems where immiscibility is caused by UCST behavior, the miscible copolymer composition range increases as the temperature rises. In the systems where immiscibility is caused by LCST behavior, however, the miscible copolymer composition range decreases as the temperature rises. Equation-of-state theories, rather than incompressible lattice theories, are appropriate for

representing liquid-liquid equilibria of systems where immiscibility is caused by LCST behavior due to the free-volume effect. However, equation-of-state theories are also able to predict immiscibility caused by UCST behavior.

An equation of state applicable to copolymer systems is the perturbed hard-sphere-chain (PHSC) equation of state¹³⁻¹⁷. The PHSC equation of state¹³⁻¹⁷ has been applied to homopolymer blends, homopolymer/copolymer mixtures, and mixtures of random copolymers containing two kinds of segments; these mixtures are denoted as A_{r_1}/B_{r_2} , $A_{r_1}/(C_Y B_{1-Y})_{r_2}$, and $(A_X B_{1-X})_{r_1}/(A_Y B_{1-Y})_{r_2}$, respectively, where r_i is the number of effective hard spheres per molecule of component i and X and Y are segment number fractions for segments A, B, and C in components 1 and 2, respectively. The screening effect was introduced into the PHSC equation of state for copolymer systems in the first paper of this series¹⁸.

In the second paper of this series¹⁹, the theoretical copolymer-composition dependence of LCST was compared with experiment for mixtures of type $A_{r_1}/(C_Y B_{1-Y})_{r_2}$ containing poly(methyl methacrylate-*co*-styrene) (MMA-*co*-S) and poly(acrylonitrile-*co*-styrene) (AN-*co*-S) random copolymers. These systems exhibit LCSTs in the experimentally accessible temperature range as the copolymer approaches polystyrene (i.e., as $Y \rightarrow 0$). The intersegmental parameters for the S-MMA pair were obtained from the styrene-rich region of the miscibility map for the system $(A_X B_{1-X})_{r_1}/(A_Y B_{1-Y})_{r_2}$ containing MMA-*co*-S random copolymers¹⁸. Similarly, the intersegmental parameters for the S-AN pairs were obtained from the miscibility map for mixtures of type $(A_X B_{1-X})_{r_1}/(A_Y B_{1-Y})_{r_2}$ containing AN-*co*-S random copolymers¹⁹. It was shown that unique intersegmental parameters can be assigned to the S-MMA and S-AN pairs in the systems $A_{r_1}/(C_Y B_{1-Y})_{r_2}$ containing MMA-*co*-S and AN-*co*-S random copolymers, respectively.

In this work we attempt to apply the PHSC equation of state to more complicated systems using the same set of intersegmental parameters. Theoretical miscibility maps are

compared with experiment for mixtures of random copolymers containing two, three, and four kinds of segments; these mixtures are denoted by $(A_X B_{1-X})_{r_1} / (A_Y B_{1-Y})_{r_2}$, $(A_X B_{1-X})_{r_1} / (C_Y B_{1-Y})_{r_2}$, and $(A_X B_{1-X})_{r_1} / (C_Y D_{1-Y})_{r_2}$, respectively. Comparison of a theoretical miscibility window with experiment was made for the system poly(methyl methacrylate) / poly(acrylonitrile-*co*-styrene), a mixture of type $A_{r_1} / (C_Y B_{1-Y})_{r_2}$, where the mixture is miscible over a limited copolymer composition range even though none of the three binary mixtures of relevant homopolymers are miscible. Attention is also given to the screening effect¹⁸ in the system poly(methyl methacrylate-*co*-styrene) / poly(acrylonitrile-*co*-styrene), a mixture of type $(A_X B_{1-X})_{r_1} / (C_Y B_{1-Y})_{r_2}$.

THEORY

Equation of State for Copolymer Mixtures. Details of the perturbed hard-sphere-chain (PHSC) equation of state for copolymer systems are given in References 17 and 18.

The PHSC equation of state requires three parameters to describe normal fluids including homopolymers: number of effective hard spheres per molecule, r ; segmental diameter, σ ; and non-bonded segment pair-interaction energy, ϵ . These parameters were regressed from available pressure-volume-temperature (*PVT*) data for several homopolymers; they are tabulated in References 14 and 19. For a homopolymer, one of the regressed characteristic quantities is r/M , where M is the molecular weight of the polymer. Table I gives PHSC equation-of-state parameters for homopolymers used in this work. The equation-of-state parameters for copolymer systems are computed as discussed in the first¹⁸ and second papers¹⁹ of this series. The weight-average molecular weight of component i , M_i ($i=1,2$ for a binary system), is used to compute equation-of-state parameters.

The PHSC equation of state requires at least one adjustable intersegmental parameter, $\kappa_{\alpha\beta}$, for a given pair of dissimilar segments α and β :

$$\varepsilon_{\alpha\beta} = \sqrt{\varepsilon_\alpha \varepsilon_\beta} (1 - \kappa_{\alpha\beta}) \quad (\alpha, \beta = A, B, C, D; \alpha \neq \beta) \quad (1)$$

where ε_α is the minimum potential energy of the non-bonded segment-segment pair potential between similar segments α and $\varepsilon_{\alpha\beta}$ is that between dissimilar segments α and β . An additional adjustable intersegmental parameter, $\zeta_{\alpha\beta}$, can be introduced to relax the additivity of effective hard-sphere diameters of unlike segments α and β :

$$b_{\alpha\beta} = \frac{(b_\alpha^{1/3} + b_\beta^{1/3})}{2} (1 - \zeta_{\alpha\beta}) \quad (\alpha, \beta = A, B, C, D; \alpha \neq \beta) \quad (2)$$

where b_α and $b_{\alpha\beta}$ represent the van der Waals covolumes for effective hard spheres between similar and dissimilar segments, respectively. The intersegmental parameters are obtained from the phase boundaries such as the critical point of the mixture or the miscibility/immiscibility boundary on an experimental miscibility map.

Screening Effect. A simple method to introduce the screening effect into the PHSC equation of state is discussed in the first paper of this series¹⁸. The model first replaces a copolymer molecule consisting of segments A and B, $(A_x B_{1-x})_r$, by a terpolymer consisting of segments A, B, and C which represent AA, BB, and AB and BA sequences, respectively, of a copolymer. To keep the hard-core volume of a terpolymer equal to that of a copolymer, the diameter of segment C is given by

$$\sigma_C = \left[\frac{\sigma_A^3 + \sigma_B^3}{2} \right]^{1/3} \quad (3)$$

where σ_α ($\alpha = A, B, C$) is the hard-sphere diameter of segment of type α . The fractions ψ and $1-\psi$ of segments C are then replaced by segments B and A, respectively. The

copolymer of type $(A_x B_{1-x})_r$ is therefore assumed to have the number of segments of type A and B given by r_A'' and r_B'' , respectively:

$$r_A'' = n_{AA} + (n_{AB} + n_{BA})(1 - \psi) \left(\frac{\sigma_C^3}{\sigma_A^3} \right). \quad (4)$$

$$r_B'' = n_{BB} + (n_{AB} + n_{BA})\psi \left(\frac{\sigma_C^3}{\sigma_B^3} \right) \quad (5)$$

where $n_{\alpha\beta}$ ($\alpha, \beta = A, B$) is the number of α - β hard-sphere sequences of the copolymer of type $(A_x B_{1-x})_r$ and

$$n_{AA} + n_{AB} + n_{BA} + n_{BB} = r - 1. \quad (6)$$

In this model, $\psi=1$ represents complete screening of segment A by segment B in AB and BA sequences. Conversely, $\psi=0$ represents complete screening of segment B by segment A in AB and BA sequences. When $\psi = (\sigma_B^3 / \sigma_C^3) / 2$, the screening effect vanishes.

Calculation Procedure. To perform phase-equilibrium calculations, expressions for the spinodal and critical conditions as well as those for the chemical potential are required; they are given in References 17 and 18.

As computed here, the theoretical miscibility map at constant temperature computed tells us that, if the copolymer compositions of a pair of copolymers are in the miscible region, these copolymers form a single homogeneous phase in all proportions. On the other hand, experimental miscibility maps are usually obtained for equi-mass mixtures. The difference between the theoretical miscibility map computed here and the experimental miscibility map for equi-mass mixtures, however, is small because the phase diagrams of copolymer blends are flat near the critical point. As a first

approximation, the measured phase separation temperature of an equi-mass mixture can be taken as the critical temperature of the mixture.

All theoretical calculations reported here were performed for liquids at zero pressure, an excellent approximation when the systems of interest are in the liquid state near atmospheric pressure.

RESULTS AND DISCUSSION

Systems Containing Styrene, Acrylonitrile, and α -Methylstyrene. We first consider the miscibility map of the mixture of type $(A_X B_{1-X})_{r_1} (C_Y B_{1-Y})_{r_2}$ containing poly(styrene-co-acrylonitrile) (*S-co-AN*) and poly(α -methylstyrene-co-acrylonitrile) (*MS-co-AN*) random copolymers. Let segments A, B, and C represent styrene, acrylonitrile, and α -methylstyrene, respectively. In the miscibility map of the mixture of type $(A_X B_{1-X})_{r_1} (C_Y B_{1-Y})_{r_2}$, there is always a miscible region near the origin $X=Y=0$. When $X=Y=0$, there is complete miscibility because component 1 is identical to component 2.

For the system (*S-co-AN*)/(*MS-co-AN*), the intersegmental parameters for the S-MS pair can be obtained from the accurate cloud-point curves for the system polystyrene / poly(α -methylstyrene) (PS/PMS). The intersegmental parameters for the S-AN pair were obtained in the second paper of this series¹⁹ from the miscibility map of the mixture of type $(A_X B_{1-X})_{r_1} (A_Y B_{1-Y})_{r_2}$ containing *S-co-AN* random copolymers; they are $\kappa_{S-AN}=0.05055$ and $\zeta_{S-AN}=0$. The remaining intersegmental parameters for the AN-MS pair are determined from the miscibility/immiscibility boundary on the miscibility map of the system (*S-co-AN*)/(*MS-co-AN*).

Figure 1a compares theoretical coexistence curves with measured phase diagrams for the system PS/PMS. Because the pure-component *PVT* data for PMS are not available, we use the equation-of-state parameters of poly(*o*-methylstyrene) as those for PMS. The experimental data are from Lin and Roe²⁰ who used monodisperse polymers. The characterizations of polymer samples used in Reference 20 are given in Table II. The

phase diagram for the system PS58/PMS62 and that for the system PS49/PMS56 were determined by differential scanning calorimetry (d.s.c.) and by cloud-point measurements, respectively. Using the same set of intersegmental parameters, theory is able to represent the molecular-weight dependence of the upper critical solution temperature (UCST). The intersegmental parameters for the S-MS pair are given in Table III.

Figure 1b compares a theoretical miscibility map with experiment for the system (S-co-AN)/(MS-co-AN). Data are from Cowie *et al.*²¹ who used d.s.c. to determine the miscibility of copolymer blends. The open circles are the miscible blends which have only one glass-transition temperature. The blends having two glass-transition temperatures of the components are considered immiscible. The theoretical miscibility map is at 25 °C for $M_1=350000$ and $M_2=8000$. Good agreement between theory and experiment is obtained with the intersegmental parameters $\kappa_{AN-MS}=0.064$ and $\zeta_{AN-MS}=0$ for the AN-MS pair. Theory predicts that immiscibility is caused by UCST type phase behavior. Although experimental data are not available for the entire copolymer-composition range, theory predicts that the system PS/(MS-co-AN) is miscible when the MS-co-AN copolymer contains 78 to 98 % α -methylstyrene by weight.

Systems Containing Styrene, Acrylonitrile, and Butadiene. A miscibility map similar to that shown in Figure 1b is also reported for mixtures of type $(A_xB_{1-x})_{r_1}(C_yB_{1-y})_{r_2}$ containing poly(styrene-co-acrylonitrile) (S-co-AN) and poly(butadiene-co-acrylonitrile) (BD-co-AN) random copolymers.²² In this system, the intersegmental parameters for three pairs of segments can be obtained from the systems containing two kinds of relevant segments. In addition to the intersegmental parameters for the S-AN pair obtained in the second paper of this series¹⁹, those for the BD-S pair are $\kappa_{BD-S}=0.00544$ and $\zeta_{BD-S}=0.00117$, determined from mixtures of oligomers of polystyrene (PS) and polybutadiene (PBD) in Reference 17. The oligomer systems PS/PBD exhibit UCST

phase behavior. The remaining intersegmental parameters for the BD-AN pair are obtained from the miscibility map for mixtures of type $(A_X B_{1-X})_{r_1} (A_Y B_{1-Y})_{r_2}$ containing poly(acrylonitrile-*co*-butadiene) (AN-*co*-BD) random copolymers.

Figure 2a compares a theoretical miscibility map with experiment for the system $(A_X B_{1-X})_{r_1} (A_Y B_{1-Y})_{r_2}$ containing AN-*co*-BD random copolymers. Data are from Cowie *et al.*²² obtained by d.s.c. Unfortunately, the AN-*co*-BD copolymers used by Cowie *et al.* are highly polydisperse ($M_w \approx 284000$, $M_w/M_n = 1.5 \sim 11$; M_n = number-average molecular weight). It is therefore difficult to determine the intersegmental parameter for the BD-AN pair accurately from the data shown in Figure 2a. We obtain two sets of intersegmental parameters $\kappa_{BD-AN} = 0.01222$ and 0.029 assuming $\zeta_{BD-AN} = 0$. Theoretical miscibility maps in Figure 2a are at 25 °C for $M_1 = M_2 = 284000$. The miscible area predicted by the theory with $\kappa_{BD-AN} = 0.029$ is slightly smaller than that predicted by the theory with $\kappa_{BD-AN} = 0.01222$.

Figure 2b compares a theoretical miscibility map with experiment²² for the system (S-*co*-AN)/(BD-*co*-AN). The theoretical miscibility map is at 25 °C for $M_1 = 324000$ and $M_2 = 284000$. Theory predicts that immiscibility is caused by UCST phase behavior. The theoretical miscibility map is very sensitive to the intersegmental parameter for the BD-AN pair, κ_{BD-AN} . Theory predicts that the system (S-*co*-AN)/(BD-*co*-AN) becomes immiscible as κ_{BD-AN} varies from 0.01222 to 0.029, although the miscibility map in Figure 2a does not vary significantly in this range for κ_{BD-AN} . Agreement between theoretical miscibility map and experiment cannot be obtained by simply adjusting κ_{BD-AN} .

In the system (S-*co*-AN)/(BD-*co*-AN), the deviation of theoretical miscibility map from experiment may be caused by the polydispersity effect as well as by the probability that polybutadiene can assume several microstructures. The intersegmental parameters for the BD-S pair may also be inaccurate because they are obtained from data for mixtures of oligomers.

The origin of immiscibility in this system also needs to be clarified. Cowie *et al.*²² mention that in the system (S-*co*-AN)/(BD-*co*-AN), miscible blends exhibit LCST phase behavior at elevated temperatures. In addition, Owgizawa and Inoue²³ report that the system (S-*co*-AN)/(BD-*co*-AN) containing 75 % styrene and 60 % butadiene by weight in S-*co*-AN and BD-*co*-AN, respectively, shows both an UCST and a LCST in the temperature-composition phase diagram with complete miscibility between UCST and LCST. The simultaneous occurrence of an UCST and a LCST is also reported for the high-molecular-weight system polybutadiene/poly(styrene-*co*-butadiene) containing 45 % styrene²⁴ by weight in the copolymer. The phase behavior of the system (S-*co*-AN)/(BD-*co*-AN) appears to be very complicated.

An important conclusion from the theoretical calculations shown in Figures 2a and 2b is that in the system having limited miscibility, the theoretical miscibility map can be very sensitive to slight changes in intersegmental parameters.

System Poly(Methyl Methacrylate) / Poly(Acrylonitrile-*co*-Styrene). The phase behavior of copolymer systems containing methyl methacrylate, styrene, and acrylonitrile has been extensively studied²⁵⁻²⁸. The mixture poly(methyl methacrylate) (PMMA) / poly(acrylonitrile-*co*-styrene) (AN-*co*-S) is known to exhibit a miscibility window caused by LCST phase behavior. In this system miscibility changes from immiscible→miscible→immiscible as the copolymer content of acrylonitrile in AN-*co*-S rises, even though none of the three relevant binary mixtures of homopolymers are miscible. The system PMMA/(AN-*co*-S) is miscible at room temperature when the copolymer contains approximately 9 to 35 % acrylonitrile by weight. Suess *et al.*²⁵ and Cowie *et al.*²⁷ report that the LCST in the system PMMA/(AN-*co*-S) containing approximately 10 to 25 % acrylonitrile by weight lies above the thermal-degradation temperature of the mixture. The exact miscible copolymer composition range and phase separation temperatures, however, may depend on the sample preparation and the heating

rates of cloud-point measurements as well as on the molecular weight and polydispersity of the polymer samples.

Three mixtures of type $(A_X B_{1-X})_{r_1} (C_Y B_{1-Y})_{r_2}$ can be obtained from methyl methacrylate (MMA), styrene (S), and acrylonitrile (AN) segments: the systems (MMA-co-AN)/(S-co-AN), (AN-co-MMA)/(S-co-MMA), and (MMA-co-S)/(AN-co-S). We attempt to fit the miscibility maps of these systems using the same set of intersegmental parameters. The intersegmental parameters for the S-AN pair are $\kappa_{S-AN}=0.05055$ and $\zeta_{S-AN}=0$, obtained from the miscibility map of the mixture of type $(A_X B_{1-X})_{r_1} (A_Y B_{1-Y})_{r_2}$ containing S-co-AN random copolymers¹⁹. Because of the screening effect discussed in the first paper of this series¹⁸, however, the intersegmental parameters for the MMA-S pair cannot be obtained from the miscibility map of the mixture of type $(A_X B_{1-X})_{r_1} (A_Y B_{1-Y})_{r_2}$ containing S-co-MMA random copolymers. We obtain the intersegmental parameters for the MMA-S and MMA-AN pairs from the miscibility window of the system PMMA/(AN-co-S).

Figure 3a compares the theoretical miscibility window with experimental data by Suess *et al.*²⁵ for the system PMMA/(AN-co-S). The solid circles are the LCSTs determined by cloud-point measurements. The open and solid squares are the miscible and immiscible blends, respectively, containing 60 % PMMA by weight at 50 °C. Curves are the theoretical LCSTs for $M_1=43000$ and $M_2=162000$. The intersegmental parameters for the MMA-S and MMA-AN pairs were obtained by assuming that at 166°C, the immiscibility/miscibility and miscibility/immiscibility boundaries lie at 9.4 and 34.6 % acrylonitrile by weight, respectively. For given intersegmental parameters for the S-AN pair, κ_{S-AN} and ζ_{S-AN} it was found that there is only one set of intersegmental parameters κ_{MMA-S} and κ_{MMA-AN} for $\zeta_{MMA-S}=\zeta_{MMA-AN}=0$ which satisfy the above-mentioned conditions. Additional intersegmental parameter ζ_{MMA-S} was introduced to change the width of the miscibility window. The intersegmental parameters for the MMA-AN pair

are the same ($\kappa_{\text{MMA-AN}}=0.03249$ and $\zeta_{\text{MMA-AN}}=0$) in the three curves shown in Figure 3a.

The experimental data in Figure 3a show that the LCST does not vary significantly between 25 to 35 wt% acrylonitrile and that the width of the miscibility window is almost independent of temperature below about 170 °C. On the other hand, the theoretical miscibility window is a smooth curve. It is therefore not possible to obtain good agreement between theory and experiment over a wide temperature range.

A miscibility window for the system PMMA/(AN-co-S) is also reported by Fowler *et al.*²⁶ who used the PMMA of higher molecular weight ($M_w=105400$, $M_w/M_n=2.0$) than that used by Suess *et al.*²⁵ ($M_w=43000$, $M_w/M_n=1.72$). The molecular weight and polydispersity factor of AN-co-S copolymers are roughly the same for both experiments. Figure 3b compares the cloud points by Fowler *et al.*²⁶ with the theoretical spinodal for equi-mass mixtures. The theoretical spinodal is calculated using the intersegmental parameters obtained in Figure 3a with $M_1=100000$ and $M_2=150000$. Theory predicts that in the system PMMA/(AN-co-S) the LCST increases as the molecular weight of PMMA, M_1 , rises. Theory also predicts that the LCST decreases as the molecular weight of AN-co-S copolymer, M_2 , rises. Although the cloud points for $M_1=100000$ by Fowler *et al.*²⁶ are higher than those for $M_1=43000$ by Suess *et al.*²⁵, it is not clear if the LCST indeed increases with rising molecular weight of PMMA in the system PMMA/(AN-co-S) because the measured phase separation temperature could depend on sample preparation and polydispersity. Equation-of-state theories, however, are able to represent such a molecular-weight dependence of LCST because the unfavorable equation-of-state effect, which results from compressibility disparities, decreases as the difference in molecular sizes declines.

We use $\kappa_{\text{MMA-S}}=-0.00273$ and $\zeta_{\text{MMA-S}}=-0.0035$ as the intersegmental parameters for the MMA-S pair. With these parameters, theory slightly overestimates the miscible

copolymer composition range near the immiscibility/miscibility boundary at room temperature.

Systems Containing Methyl Methacrylate, Styrene, and Acrylonitrile. We next compare theoretical miscibility maps with experiment for various systems containing methyl methacrylate, styrene, and acrylonitrile segments using the intersegmental parameters obtained from Figure 3a.

Figure 4 compares a theoretical miscibility map with experiment for mixtures of the type $(A_X B_{1-X})_{r_1} (C_Y B_{1-Y})_{r_2}$ containing MMA-*co*-AN and S-*co*-AN random copolymers. Data at 130 °C are from Nishimoto *et al.*²⁸. A similar miscibility map is also reported at room temperature by Cowie *et al.*²⁷ As expected from the temperature dependence of the miscibility window in the system PMMA/(AN-*co*-S) shown in Figure 3a, the theoretical miscibility map is not sensitive to the temperature between 25 and 130 °C. Theory and experiment are in good agreement.

Figure 5 compares a theoretical miscibility map with experiment for mixtures of the type $(A_X B_{1-X})_{r_1} (C_Y B_{1-Y})_{r_2}$ containing AN-*co*-MMA and S-*co*-MMA random copolymers²⁷. In the theoretical miscibility map, there is a small miscible area near the origin $X=Y=0$. Theory predicts that this system is essentially immiscible, consistent with experiment.

Figure 6 compares a theoretical miscibility map with experiment at room temperature for mixtures of the type $(A_X B_{1-X})_{r_1} (C_Y B_{1-Y})_{r_2}$ containing MMA-*co*-S and AN-*co*-S random copolymers^{29,30}. In this system miscibility changes from immiscible → miscible → immiscible as the acrylonitrile content in component 2 rises from zero wt% acrylonitrile. As expected from Figure 3a, theory overestimates the miscible area near the immiscibility/miscibility boundary. The intersegmental parameters were obtained at 166 °C; better agreement between the theoretical miscibility map and

experiment at 25 °C is obtained if the intersegmental parameters obtained are obtained at 25 °C. The predicted miscibility/immiscibility boundary agrees well with experiment.

An interesting question is whether the system (MMA-co-S)/(AN-co-S) exhibits the screening effect. As discussed in the first paper of this series¹⁸, mixtures of type $(A_X B_{1-X})_{r_1} (A_Y B_{1-Y})_{r_2}$ containing S-co-MMA random copolymers exhibit the screening effect. In this system, a simple model proposed in Reference 18 indicates that the styrene segment is screened by the methyl methacrylate segment in the S-MMA and MMA-S sequences; these sequences behave essentially as MMA-MMA sequences. It is therefore possible that a similar screening effect is observed in the MMA-co-S copolymer in the system (MMA-co-S)/(AN-co-S).

The first paper of this series¹⁸ gives details of the method to include the screening effect into the PHSC equation of state. We replace all of the S-MMA and MMA-S sequences by the MMA-MMA sequences, i.e., $\psi=0$ in Eqs. (4) and (5) with segments A and B representing methyl methacrylate and styrene, respectively. As discussed in Reference 18, to use the number of monomer sequences calculated from the measured reactivity ratios of copolymerization as the number of hard-sphere sequences, $n_{\alpha\beta}$ ($\alpha, \beta=A, B$) in the model, the equation-of-state parameters must be obtained such that one monomer is represented by a single sphere in the model. The equation-of-state parameters used in this work, however, are those that give the best fit to the pure-component *PVT* data; these parameters do not assume that one monomer corresponds to a single sphere in the PHSC equation of state. Therefore, we assume that the number of hard-sphere sequences of a copolymer of type $(A_X B_{1-X})_r$ are given by that of a truly random copolymer:

$$n_{AA} = X^2(r-1), \quad n_{AB} = n_{BA} = X(1-X)(r-1), \quad n_{BB} = (1-X)^2(r-1). \quad (7)$$

The broken curves in Figure 6 are calculated by assuming that the S-MMA and MMA-S hard-sphere sequences of MMA-co-S copolymer behave as the MMA-MMA sequences, i.e., $\psi=0$ in Eqs. (4) and (5) with segments A and B representing methyl methacrylate and styrene, respectively. For a given methyl methacrylate content in the MMA-co-S copolymer, agreement of the theoretical immiscibility/miscibility boundary with experiment seems to be improved as the screening effect is included. The difference between the solid and broken curves, however, is small. In addition, the theory with screening effect clearly overestimates the miscible area near the miscibility/immiscibility boundary. Therefore, the screening effect in the MMA-co-S copolymer in the system (MMA-co-S)/(AN-co-S) is not as apparent as that in the system $(A_X B_{1-X})_{r_1} (A_Y B_{1-Y})_{r_2}$ containing S-co-MMA random copolymers. The screening effect in the system (MMA-co-S)/(AN-co-S) may be important only when the AN-co-S copolymer contains very small amount of acrylonitrile.

The results shown in Figures 4 to 6 imply that the intersegmental parameters do not depend on the type of mixture in the systems (MMA-co-AN)/(S-co-AN), (AN-co-MMA)/(S-co-MMA), and (MMA-co-S)/(AN-co-S). A question, however, still remains regarding the intersegmental parameters for the MMA-S pair obtained in Figure 3a. Figure 7 compares a theoretical miscibility map with screening effect with experiment for mixtures of the type $(A_X B_{1-X})_{r_1} (A_Y B_{1-Y})_{r_2}$ containing S-co-MMA random copolymers³⁰. The screening effect is introduced by the same procedure used to include the screening effect in the system (MMA-co-S)/(AN-co-S); the S-MMA and MMA-S sequences are replaced by the MMA-MMA sequences. The number of specific sequences is given by Eq. (7) with segments A and B representing styrene and methyl methacrylate segments, respectively. The complete screening of styrene by methyl methacrylate in the S-MMA and MMA-S sequences corresponds to $\psi=1$ in Eqs. (4) and (5). The screening effect is included in both components 1 and 2. Although the temperature dependence of

the miscibility map is not correctly predicted, the parameters used in Figure 7 seem to be of the correct order of magnitude.

We next consider mixtures of the type $(A_X B_{1-X})_{r_1} (C_Y D_{1-Y})_{r_2}$ containing four kinds of segments which requires six sets of intersegmental parameters.

Systems Containing Cyclohexyl Methacrylate, Methyl Methacrylate, Acrylonitrile, and Styrene. A miscibility map for mixtures of poly(cyclohexyl methacrylate-*co*-methyl methacrylate) (CHMA-*co*-MMA) and AN-*co*-S random copolymers is reported by Nishimoto *et al.*³¹ In this system all of the necessary six sets of intersegmental parameters can be obtained from the following three mixtures of type $A_{r_1} (C_Y B_{1-Y})_{r_2}$: PMMA/(AN-*co*-S), PCHMA/(AN-*co*-S), and PS/(CHMA-*co*-MMA) where PMMA, PCHMA, and PS denote poly(methyl methacrylate), poly(cyclohexyl methacrylate), and polystyrene, respectively.

The intersegmental parameters for the CHMA-S and CHMA-AN pairs were obtained in the second paper of this series¹⁹; they are given in Table III. The mixture of PCHMA and PS is miscible up to about 240 °C³¹. The mixture of PCHMA and AN-*co*-S copolymer also shows LCST phase behavior. The intersegmental parameters among methyl methacrylate, acrylonitrile, and styrene segments are the same as those used in Figures 4 to 7. The remaining intersegmental parameters for the CHMA-MMA pair are obtained from the copolymer-composition dependence of phase-separation temperatures in the system PS/(CHMA-*co*-MMA)³¹.

Figure 8 compares the copolymer-composition dependence of theoretical LCST with the cloud points of equi-mass mixtures³¹ for the system PS/(CHMA-*co*-MMA). Although the molecular weights of copolymers and complete phase diagrams are not reported, this system is shown to exhibit LCST phase behavior. The theoretical curve is for $M_1=M_2=200000$. The intersegmental parameters for the CHMA-MMA pair were obtained assuming that for the copolymer containing 28.5 % cyclohexyl methacrylate by

weight, the critical temperature and mixture composition are 150 °C and 13 wt% PS, respectively. Under these assumptions, the calculated critical compositions may not agree with the measured critical compositions. The difference between the calculated LCST and the measured phase separation temperature for equi-mass mixtures, however, would be small because the phase diagram in this system is flat near the LCST.

Figure 9 compares a theoretical miscibility map with experiment³¹ for the system (CHMA-*co*-MMA)/(AN-*co*-S). Theory and experiment are in excellent agreement. Theory predicts that the miscible area decreases with temperature because in this system immiscibility is caused by LCST phase behavior.

Systems Containing Butyl Methacrylate, Methyl Methacrylate, Acrylonitrile, and Styrene. A partial miscibility map for mixtures of poly(butyl methacrylate-*co*-methyl methacrylate) (BMA-*co*-MMA) and AN-*co*-S random copolymers is reported by Kammer and Piglowski³². The system (BMA-*co*-MMA)/(AN-*co*-S) is obtained by simply replacing chclohexyl methacrylate segment by butyl methacrylate in the system (CHMA-*co*-MMA)/(AN-*co*-S) shown in Figure 8. Poly(butyl methacrylate) (PBMA) and PS are known to be immiscible. PBMA and AN-*co*-S random copolymer are also reported to be immiscible²⁶. Therefore, it is expected that the miscible area is smaller in the system (BMA-*co*-MMA)/(AN-*co*-S) than in the system (CHMA-*co*-MMA)/(AN-*co*-S).

The intersegmental parameters for the BMA-MMA and BMA-S pairs were obtained in Reference 17 from the miscibility maps of mixtures of type $(A_X B_{1-X})_{r_1} (A_Y B_{1-Y})_{r_2}$ containing BMA-*co*-MMA and S-*co*-BMA random copolymers, respectively, which show LCST type phase behavior. They are: $\kappa_{\text{BMA-MMA}} = -0.00158$, $\zeta_{\text{BMA-MMA}} = -0.001$, $\kappa_{\text{BMA-S}} = 0.01085$, and $\zeta_{\text{BMA-S}} = -0.002$. The system $(A_X B_{1-X})_{r_1} (A_Y B_{1-Y})_{r_2}$ containing S-*co*-BMA random copolymers also exhibits moderate screening effect having the miscibility map similar to that for the system containing S-*co*-

MMA random copolymers shown in Figure 7. Theory, however, was able to obtain semi-quantitative agreement with experiment without introducing the screening effect. All of the necessary intersegmental parameters (except those for the BMA-AN pair) are now obtained. We obtain the intersegmental parameters for the BMA-AN pair by using the partial information of the miscibility map for the system (BMA-*co*-MMA)/(AN-*co*-S).

Figure 10 compares a theoretical miscibility map with experiment at room temperature for the system (BMA-*co*-MMA)/(AN-*co*-S). The intersegmental parameters for the BMA-AN pair were obtained by assuming $\zeta_{\text{BMA-AN}}=0$ and that the miscibility/immiscibility boundary lies at $\omega_{\text{BMA}}=0.5$ and $\omega_{\text{AN}}=0.085$, where ω_{BMA} and ω_{AN} are the weight fraction of butyl methacrylate and that of acrylonitrile in BMA-*co*-MMA and AN-*co*-S copolymers, respectively. With these intersegmental parameters, however, theory (solid curve) underestimates the miscible area. The uncertainty in intersegmental parameters is most likely in those for the BMA-S pair because they were obtained from the miscibility map of the system $(A_X B_{1-X})_{r_1} / (A_Y B_{1-Y})_{r_2}$ containing BMA-*co*-S random copolymers exhibiting the screening effect. Good agreement with experiment is obtained if the same fitting procedure is repeated by slightly adjusting one of the intersegmental parameters for the BMA-S pair, $\kappa_{\text{BMA-S}}$, to 0.0125. In that event, theory predicts that the system PBMA/(AN-*co*-S) is immiscible, consistent with experiment by Fowler *et al.*²⁶

CONCLUSIONS

The perturbed hard-sphere-chain (PHSC) equation of state is able to represent immiscibility caused by lower critical solution temperature (LCST) phase behavior as well as the immiscibility due to upper critical solution temperature (UCST) phase behavior. Theoretical miscibility maps are compared with experiment for binary mixtures of copolymers containing two, three, and four kinds of segments.

For the systems $(A_X B_{1-X})_{r_1} / (C_Y B_{1-Y})_{r_2}$ studied in this work, intersegmental parameters for as many as two pairs of segments are obtained from the systems containing two kinds of relevant segments. The remaining intersegmental parameters are obtained from data for the system $A_{r_1} / (C_Y B_{1-Y})_{r_2}$. For the system $(A_X B_{1-X})_{r_1} / (C_Y B_{1-Y})_{r_2}$, theoretical miscibility maps are in good agreement with experiment except for the system poly(styrene-co-acrylonitrile) / poly(butadiene-co-acrylonitrile). The theoretical miscibility map and experiment show excellent agreement for the system $(A_X B_{1-X})_{r_1} / (C_Y D_{1-Y})_{r_2}$ containing poly(cyclohexyl methacrylate-co-methyl methacrylate) and poly(acrylonitrile-co-styrene) random copolymers, where intersegmental parameters are obtained from three mixtures of type $A_{r_1} / (C_Y B_{1-Y})_{r_2}$.

In the copolymer systems studied in this work, theoretical miscibility maps and experiment show good agreement using the same set of intersegmental parameters. Total prediction using the intersegmental parameters obtained from the system containing two kinds of segments only, however, remains to be carried out together with the measurements of miscibility maps and phase diagrams of relevant copolymer systems using monodisperse copolymers.

ACKNOWLEDGMENT

This work was supported by the Director, Office of Energy Research, Office of Basic Energy Sciences, Chemical Sciences Division of the U.S. Department of Energy under Contract No. DE-AC03-76SF0098. Additional funding was provided by E.I. du Pont de Nemours & Co. (Philadelphia, PA) and Koninklijke Shell (Amsterdam, The Netherlands).

References

1. Paul, D.R.; Newman, S., Eds. *Polymer Blends*; Academic Press: New York, 1978.
2. Olabisi, O.; Robeson, L.M.; Shaw, M.T. *Polymer-Polymer Miscibility*; Academic Press: New York, 1979.

3. Schmitt, B.J. *Angew. Chem. Int. Ed. Engl.* **1979**, *18*, 273.
4. Solc, K., Ed. *Polymer Compatibility and Incompatibility: Principles and Practices*, MMI Press Symposium Series, Vol. 2; Harwood Academic Publishers GmbH: New York, 1982.
5. Krause, S. *Pure Appl. Chem.* **1986**, *58*, 1553.
6. Kambour, R.P.; Bendler, J.T.; Bopp, R.C. *Macromolecules* **1983**, *16*, 753.
7. Paul, D.R.; Barlow, J.W. *Polymer* **1984**, *25*, 487.
8. ten Brinke, G.; Karasz, F.E.; MacKnight, W.J. *Macromolecules* **1983**, *16*, 1827.
9. Cowie, J.M.G.; Lath, D. *Makromol. Chem., Macromol. Symp.* **1988**, *16*, 103.
10. Cowie, J.M.G.; Reid, V.M.C.; McEwen, I.J. *Polymer* **1990**, *31*, 486.
11. Cowie, J.M.G.; Reid, V.M.C.; McEwen, I.J. *Polymer* **1990**, *31*, 905.
12. Bell, S.Y.; Cowie, J.M.G.; McEwen, I.J. *Polymer* **1994**, *35*, 786.
13. Song, Y.; Lambert, S.M.; Prausnitz, J.M. *Macromolecules* **1994**, *27*, 441.
14. Song, Y.; Lambert, S.M.; Prausnitz, J.M. *Ind. Eng. Chem. Res.* **1994**, *33*, 1047.
15. Song, Y.; Lambert, S.M.; Prausnitz, J.M. *Chem. Eng. Sci.* **1994**, *49*, 2765.
16. Song, Y.; Lambert, S.M.; Prausnitz, J.M. paper presented at AIChE meeting in St. Louis, November 1993.
17. Hino, T.; Song, Y.; Prausnitz, J.M. *Macromolecules* **1994**, *27*, 5681.
18. Hino, T.; Prausnitz, J.M. submitted to *Macromolecules* **1995**.
19. Hino, T.; Prausnitz, J.M. submitted to *Macromolecules* **1995**.
20. Lin, J.L.; Roe, R.J. *Polymer* **1988**, *29*, 1227.
21. Cowie, J.M.G.; Elempuru, E.M.; McEwen, I.J. *Polymer* **1992**, *33*, 1993.
22. Cowie, J.M.G.; Harris, J.H.; McEwen, I.J. *Macromolecules* **1992**, *25*, 5287.
23. Ougizawa, T.; Inoue, T. *Polym. J.* **1986**, *18*, 521.
24. Ougizawa, T.; Inoue, T.; Kammer, H.W. *Macromolecules* **1985**, *18*, 2092.
25. Suess, M.; Kressler, J.; Kammer, H.W. *Polymer* **1987**, *28*, 957.
26. Fowler, M.E.; Barlow, J.W.; Paul, D.R. *Polymer* **1987**, *28*, 1177.
27. Cowie, J.M.G.; Lath, D. *Makromol. Chem., Macromol. Symp.* **1988**, *16*, 103.
28. Nishimoto, M.; Keskkula, H.; Paul, D.R. *Polymer* **1989**, *30*, 1279.
29. Kammer, H.W. *Acta Polymerica* **1986**, *40*, 75.
30. Braun, D.; Yu, D.; Kohl, P.R.; Gao, X.; Andradi, L.N.; Manger, E.; Hellmann, G.P. *J. Polym. Sci., Polym. Phys. Edn.* **1992**, *30*, 577.
31. Nishimoto, M.; Keskkula, H.; Paul, D.R. *Macromolecules* **1990**, *23*, 3633.
32. Kammer, H.W.; Piglowski, J. *Acta Polymerica* **1989**, *40*, 363.

TABLE I. PHSC Equation-of-State Parameters for Homopolymers 14,19

polymer	r/M (mol/g)	σ (Å)	ϵ/k_B (K)
polystyrene	0.01117	5.534	724.7
polyacrylonitrile	0.01057	5.414	769.5
poly(α -methyl styrene) ^a	0.01191	5.446	731.4
<i>cis</i> -1,4-polybutadiene	0.01499	5.264	611.8
poly(methyl methacrylate)	0.01432	4.850	655.9
poly(cyclohexyl methacrylate)	0.01482	4.889	607.2
poly(butyl methacrylate)	0.01899	4.550	510.8

M = molecular weight (g/mol); ^a parameters for poly(*o*-methylstyrene).

TABLE II. Characterizations of Polymer Samples Used in Reference 20

sample	mol wt (M_w)	M_w/M_n
PS58	58400	1.07
PS49	49000	1.06
PMS62	62100	1.05
PMS56	56100	1.07

M_n = number-average molecular weight (g/mol); M_w = weight-average molecular weight (g/mol)

TABLE III. Intersegmental Parameters

binary pair	κ	ζ
styrene-acrylonitrile ^a	0.05055	0
styrene- α -methylstyrene	0.000153	0.000110
acrylonitrile- α -methylstyrene	0.064	0
butadiene-styrene ^b	0.00544	0.00117
butadiene-acrylonitrile	0.01222 (0.029)	0 (0)
methyl methacrylate-styrene	-0.00273	-0.0035
methyl methacrylate-acrylonitrile	0.03249	0
cyclohexyl methacrylate-styrene ^a	0.001936	-0.001718
cyclohexyl methacrylate-acrylonitrile ^a	0.04217	-0.00317
cyclohexyl methacrylate-methyl methacrylate	0.01507	0.00806
butyl methacrylate-methyl methacrylate ^b	-0.00158	-0.001
butyl methacrylate-styrene	0.01085 ^b (0.0125)	-0.002 ^b -0.002
butyl methacrylate-acrylonitrile	0.06395 (0.04508)	0 0

^a Ref. 19; ^b Ref. 17.

Figure Captions

Figure 1. (a) Comparison of theoretical coexistence curves with experimental phase diagrams for the system PS/PMS²⁰: (—) PS58/PMS62; (- · - · -) PS49/PMS56; $\kappa_{S-MS}=0.000153$, $\zeta_{S-MS}=0.000110$, (b) Miscibility map for the system (S-co-AN)/(MS-co-AN)²¹: (o) miscible, (●) immiscible. Theoretical miscibility map is at 25 °C for $M_1=350000$ and $M_2=8000$: $\kappa_{S-AN}=0.05055$, $\zeta_{S-AN}=0$, $\kappa_{S-MS}=0.000153$, $\zeta_{S-MS}=0.000110$, $\kappa_{AN-MS}=0.064$, $\zeta_{AN-MS}=0$.

Figure 2. (a) Miscibility map for mixtures of type $(A_X B_{1-X})_{r_1} / (A_Y B_{1-Y})_{r_2}$ containing AN-co-BD²²: (o) miscible, (●) immiscible. Theoretical miscibility map is at 25 °C for $M_1=M_2=284000$: (—) $\kappa_{BD-AN}=0.01222$, $\zeta_{BD-AN}=0$; (- - - -) $\kappa_{BD-AN}=0.029$, $\zeta_{BD-AN}=0$, (b) Miscibility map for the system (S-co-AN)/(BD-co-AN)²²: (o) miscible, (Δ) partially miscible, (●) immiscible. Theory is at 25 °C for $M_1=324000$ and $M_2=284000$: $\kappa_{S-AN}=0.05055$, $\zeta_{S-AN}=0$, $\kappa_{BD-S}=0.00544$, $\zeta_{BD-S}=0.00117$; $\zeta_{BD-AN}=0$.

Figure 3. Miscibility window for the system PMMA/(AN-co-S)^{25,26}: $\kappa_{MMA-AN}=0.03249$, $\zeta_{MMA-AN}=0$, $\kappa_{S-AN}=0.05055$, $\zeta_{S-AN}=0$. (—) $\kappa_{MMA-S}=0.00273$, $\zeta_{MMA-S}=-0.0035$; (- - - -) $\kappa_{MMA-S}=-0.00431$, $\zeta_{MMA-S}=-0.0045$; (- · - · -) $\kappa_{MMA-S}=-0.00669$, $\zeta_{MMA-S}=-0.006$, (a) Theoretical LCST for $M_1=43000$ and $M_2=162000$: (●) LCST¹⁵, (\square) miscible¹⁵, (\blacksquare) immiscible¹⁵, (b) Theoretical spinodal for equi-mass mixtures of $M_1=100000$ and $M_2=150000$: (●) cloud points of equi-mass mixtures¹⁶.

Figure 4. Comparison of theoretical miscibility map with experiment for the system (MMA-co-AN)/(S-co-AN)²⁸: (o) miscible at 130 °C, (●) immiscible at 130 °C. Theory is for $M_1=M_2=150000$: $\kappa_{\text{MMA-S}}=-0.00273$, $\zeta_{\text{MMA-S}}=-0.0035$, $\kappa_{\text{MMA-AN}}=0.03249$, $\zeta_{\text{MMA-AN}}=0$, $\kappa_{\text{S-AN}}=0.05055$, $\zeta_{\text{S-AN}}=0$.

Figure 5. Comparison of theoretical miscibility map with experiment at room temperature²⁷ for the system (AN-co-MMA)/(S-co-MMA): (●) immiscible. Theory is at 25 °C for $M_1=M_2=150000$. Intersegmental parameters are the same as those used in Figure 4.

Figure 6. Comparison of theoretical miscibility map with experiment at room temperature for the system (MMA-co-S)/(AN-co-S)^{29,30}: (o,Δ) miscible, (●,Δ) immiscible. Theory is at 25 °C for $M_1=43000$ and $M_2=162000$. The screening effect is introduced by replacing the MMA-S and S-MMA sequences by the MMA-MMA sequence as discussed in the text. Intersegmental parameters are the same as those used in Figures 4 and 5.

Figure 7. Miscibility maps with screening effect for mixtures of type $(A_X B_{1-X})_{r_1} (A_Y B_{1-Y})_{r_2}$ containing S-co-MMA random copolymers³⁰ ($M_w \approx 150000$, $M_w/M_n \approx 1.7$): (o) miscible at 25 and 180 °C, (Δ) miscible at 25 °C but immiscible at 180 °C, (●) immiscible at 25 and 180 °C. Theoretical miscibility maps are for $M_1=M_2=150000$ with $\kappa_{\text{S-MMA}}=-0.00273$ and $\zeta_{\text{S-MMA}}=-0.003$. The screening effect is introduced by replacing the MMA-S and S-MMA sequences by the MMA-MMA sequences as discussed in the text.

Figure 8. Comparison of theoretical LCST with the phase-separation temperatures of equi-mass mixtures for the system PS/(CHMA-co-MMA)³¹: $M_1=M_2=200000$, $\kappa_{S-MMA}=-0.00273$, $\zeta_{S-MMA}=-0.0035$, $\kappa_{CHMA-S}=0.001936$, $\zeta_{CHMA-S}=-0.001718$, $\kappa_{CHMA-MMA}=0.01507$, $\zeta_{CHMA-MMA}=0.00806$.

Figure 9. Comparison of theoretical miscibility map with experiment for the system (CHMA-co-MMA)/(AN-co-S)³¹: (o) miscible at 130 °C, (•) immiscible at 130 °C. Theory is for $M_1=M_2=200000$. Intersegmental parameters are given in Table III.

Figure 10. Comparison of theoretical miscibility map with experiment at room temperature for the system (BMA-co-MMA)/(AN-co-S)^{25,32}: (o) miscible, (•) immiscible. Theory is at 25 °C for $M_1=100000$ and $M_2=150000$: (—) $\kappa_{BMA-S}=0.0125$, $\zeta_{BMA-S}=-0.002$, $\kappa_{BMA-AN}=0.06395$, $\zeta_{BMA-AN}=0$; (- - -) $\kappa_{BMA-S}=0.01085$, $\zeta_{BMA-S}=-0.002$, $\kappa_{BMA-AN}=0.04508$, $\zeta_{BMA-AN}=0$.

Figure 1

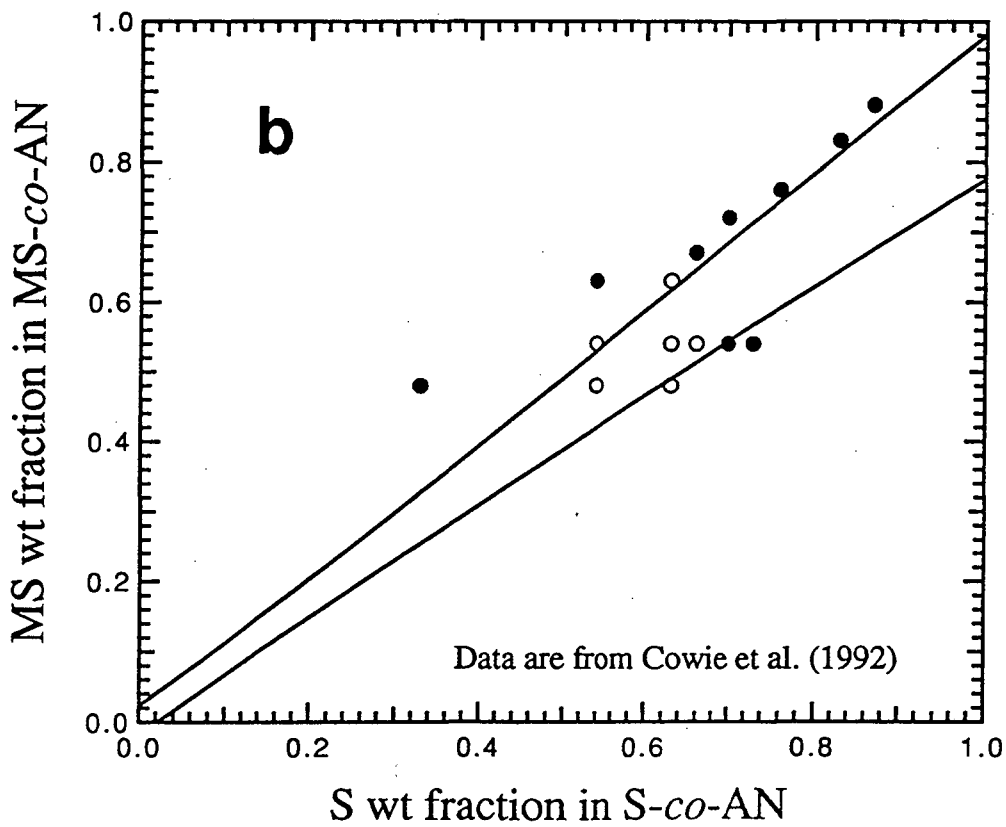
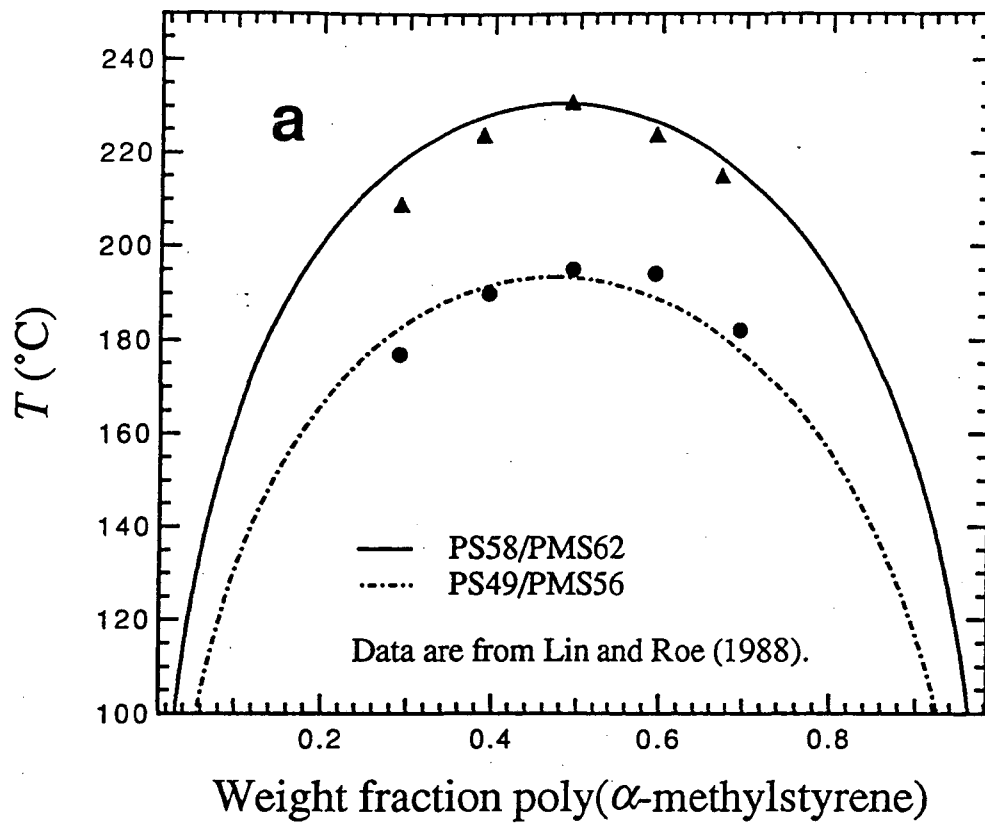


Figure 2

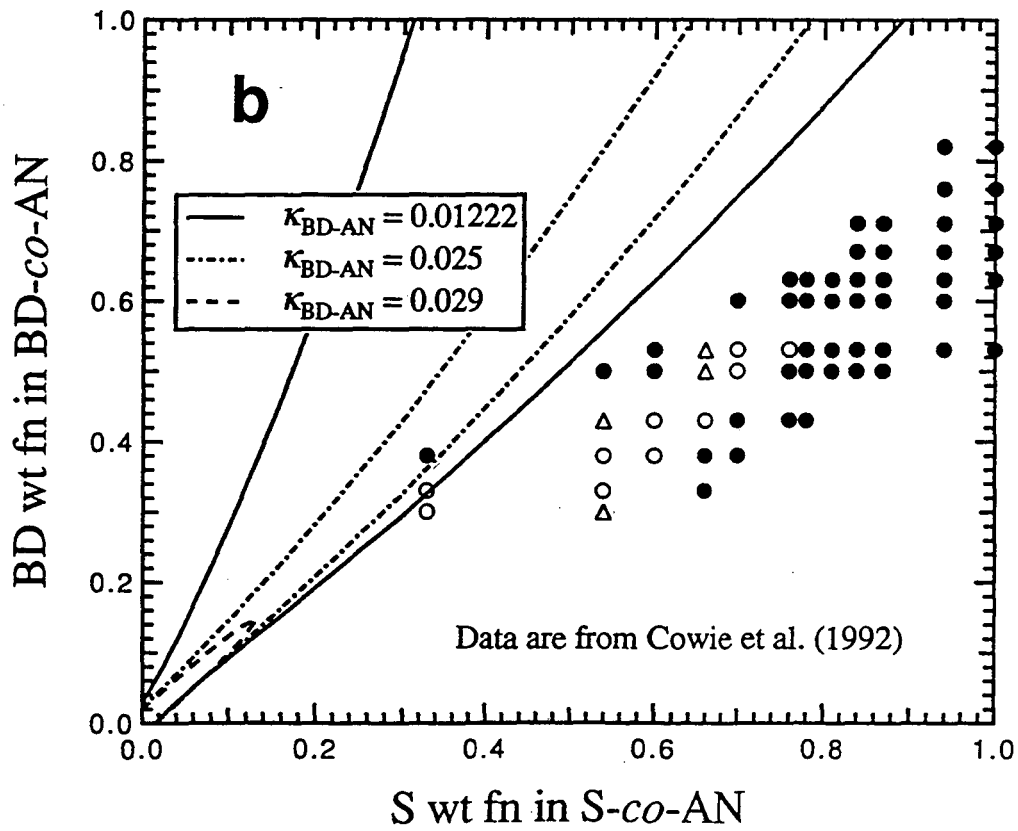
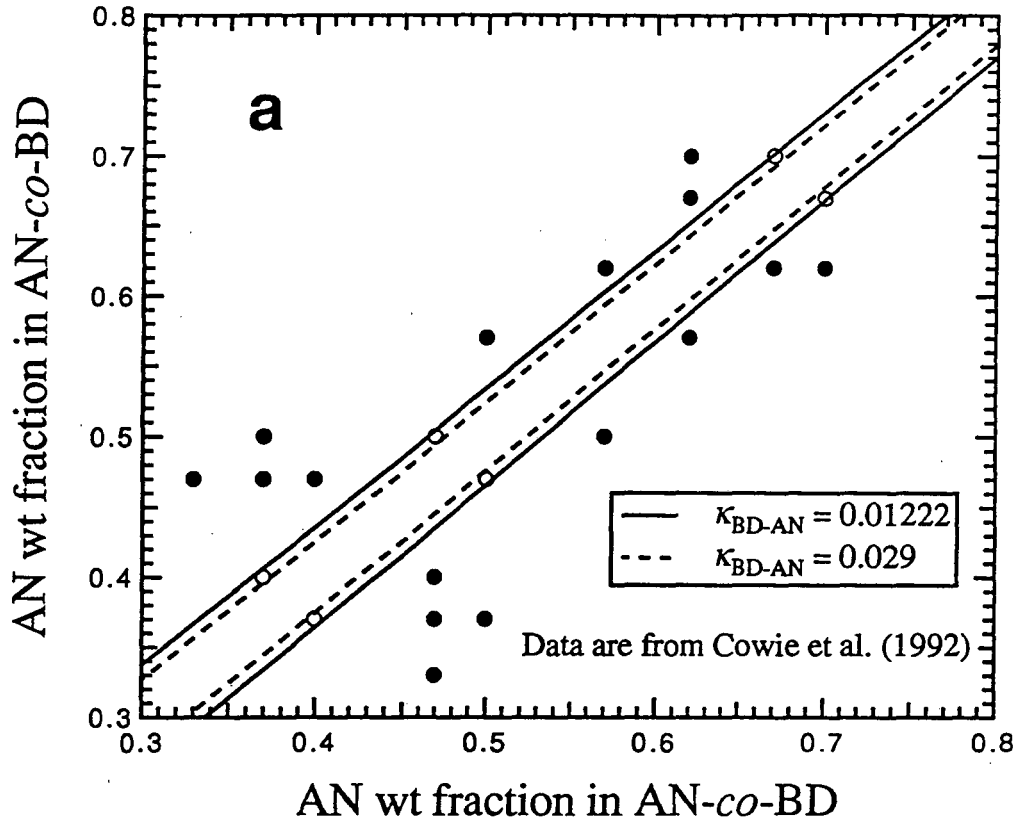


Figure 3

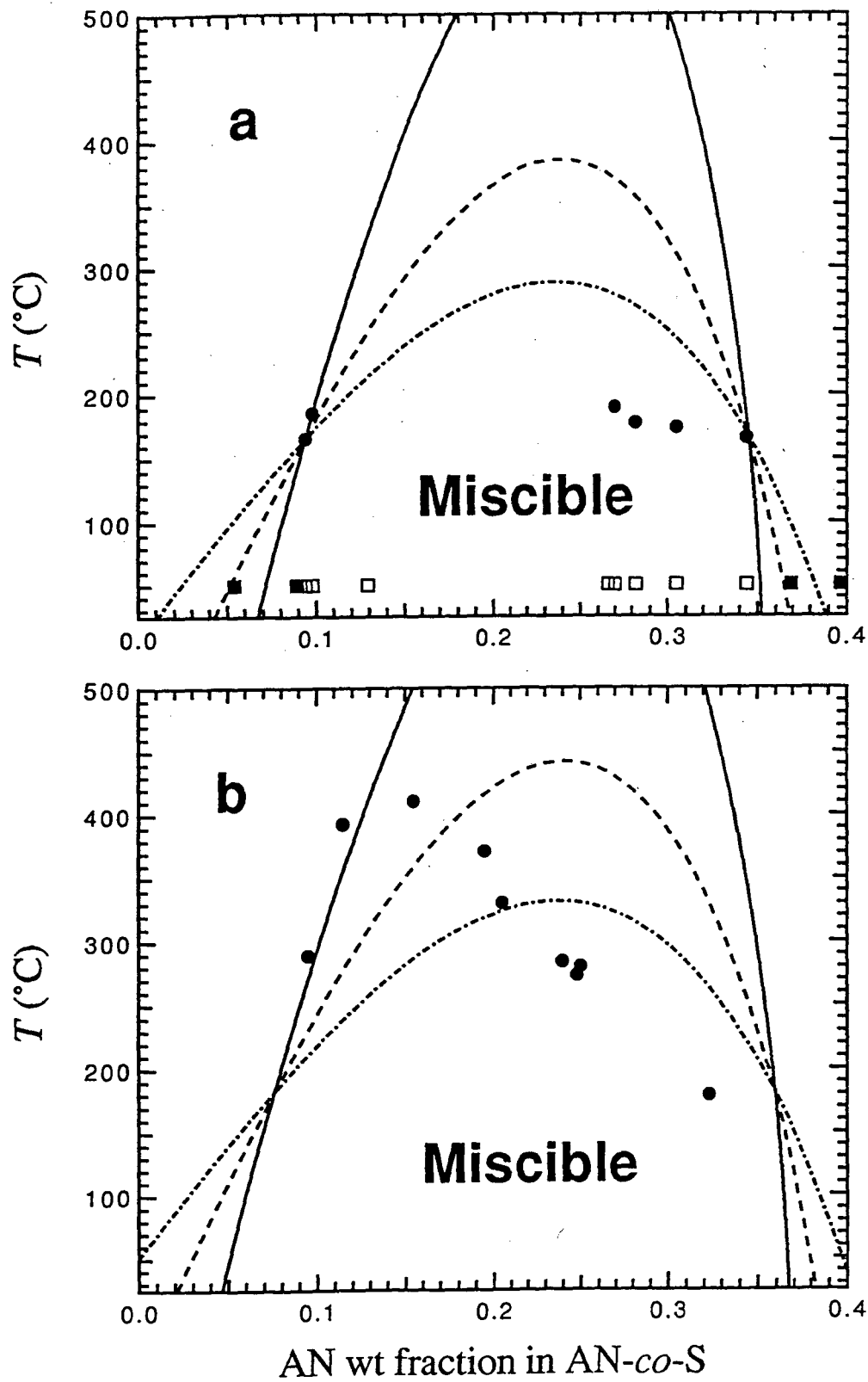


Figure 4

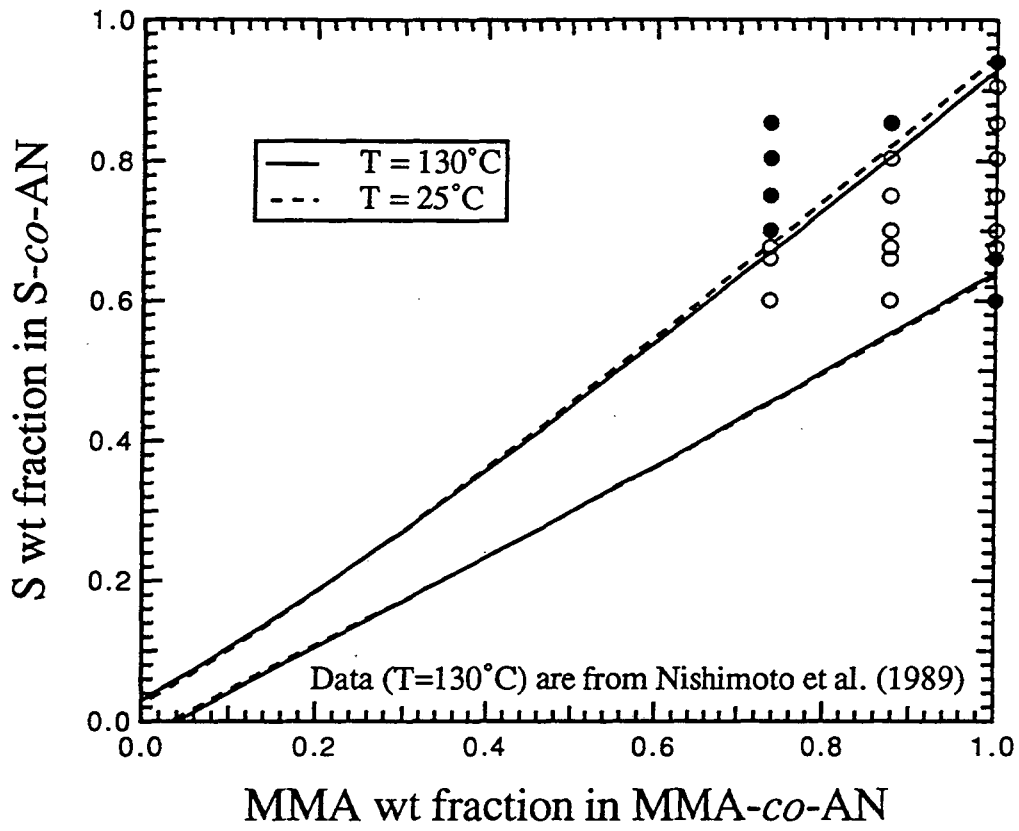


Figure 5

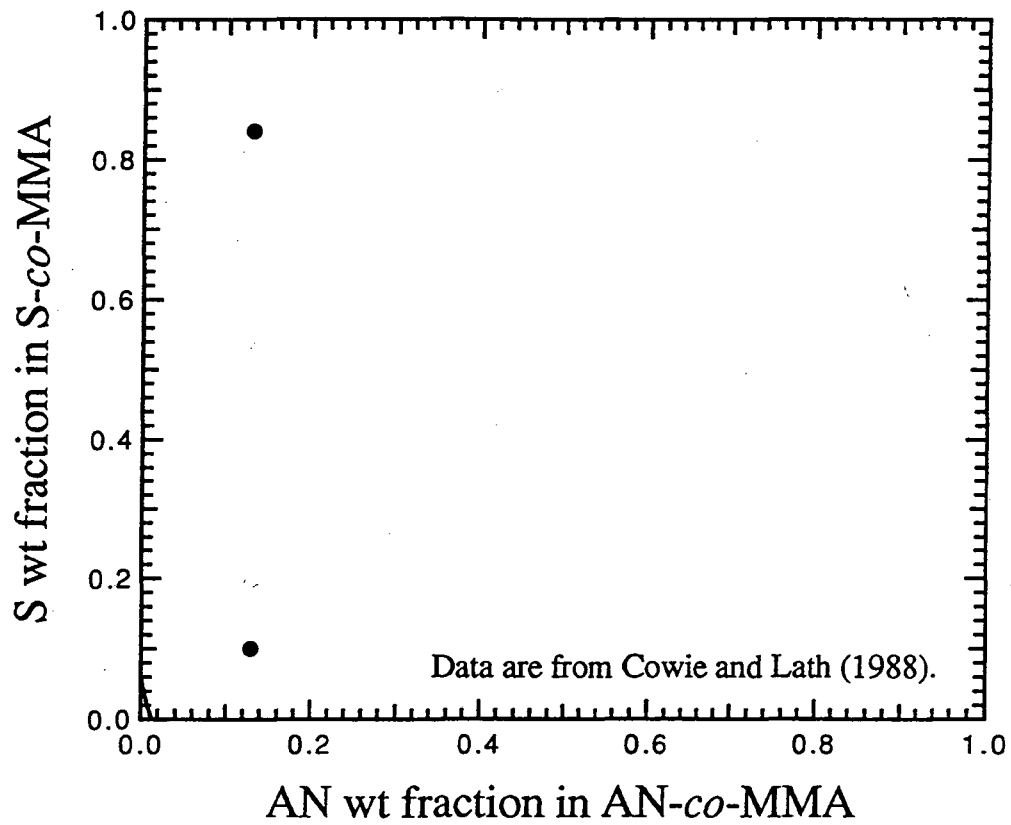


Figure 6

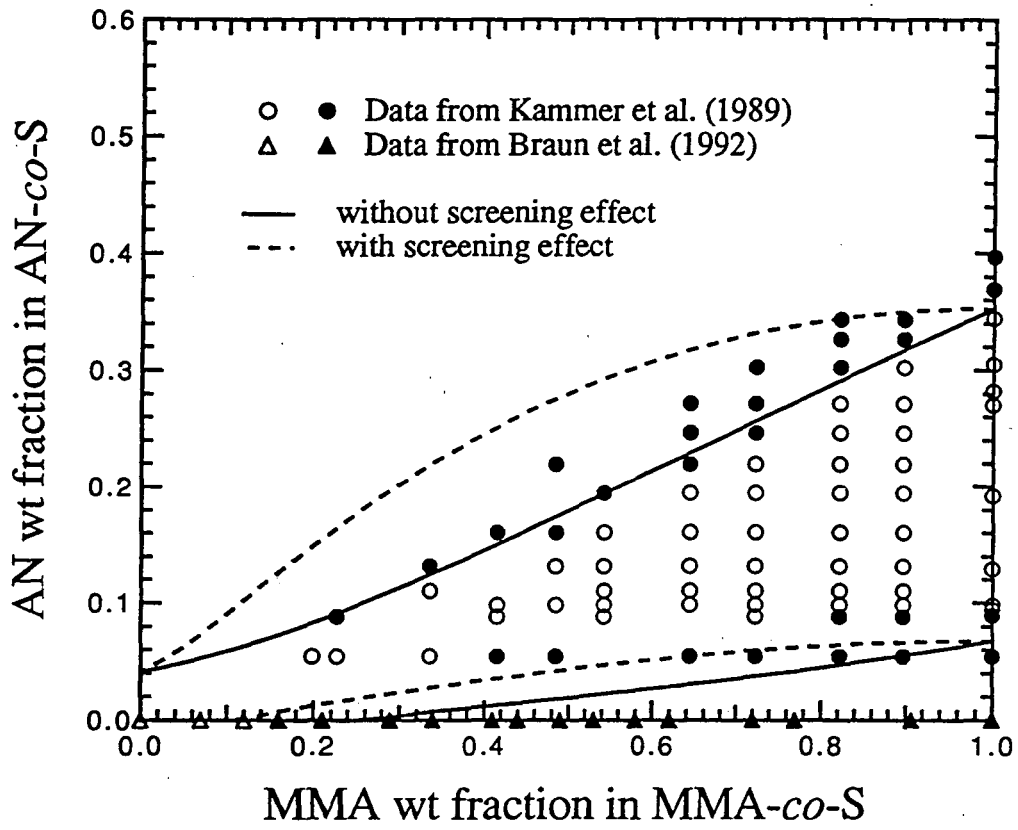


Figure 7

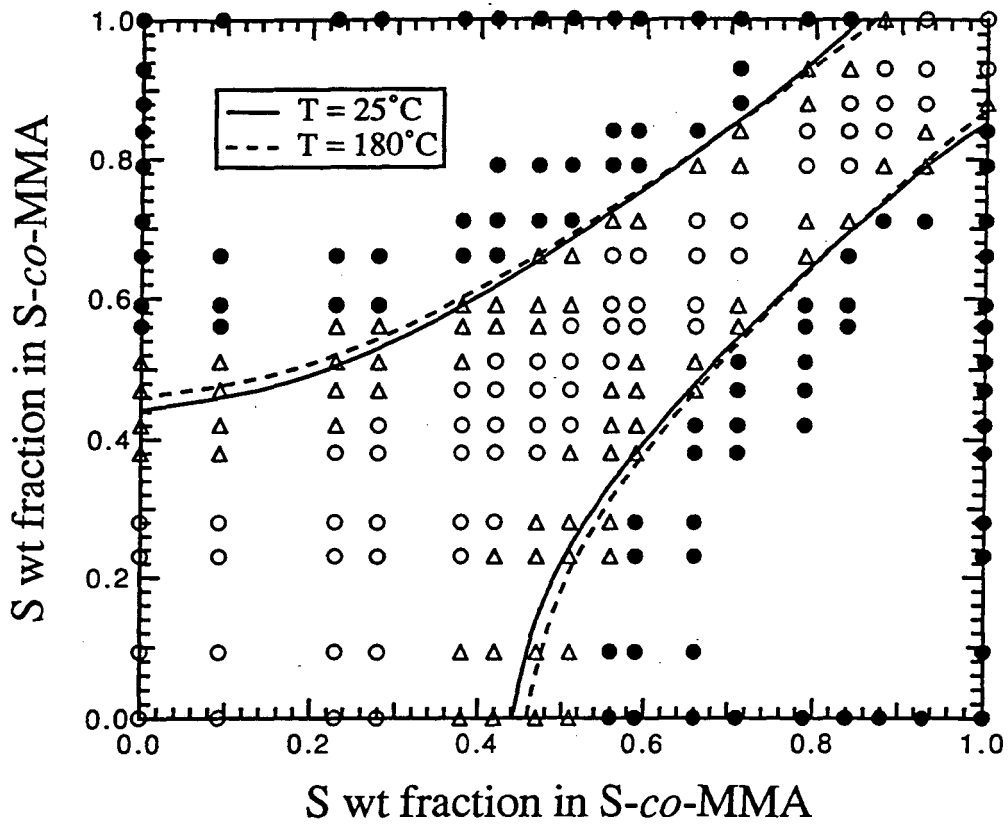


Figure 8

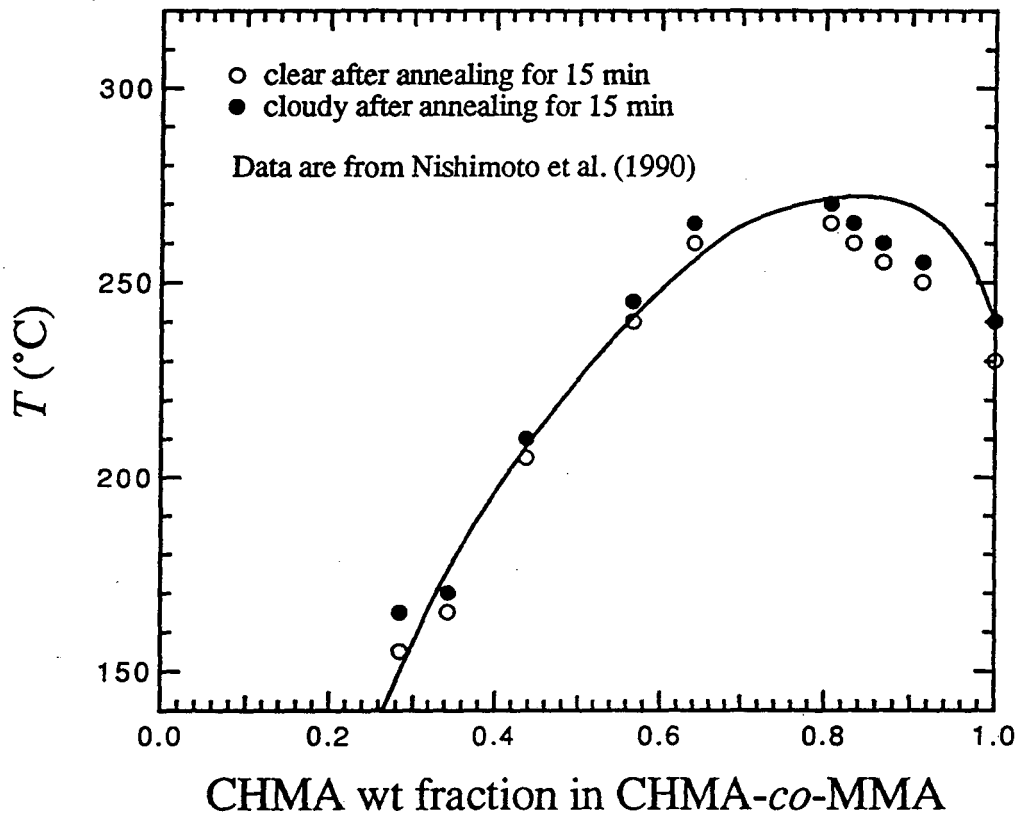


Figure 9

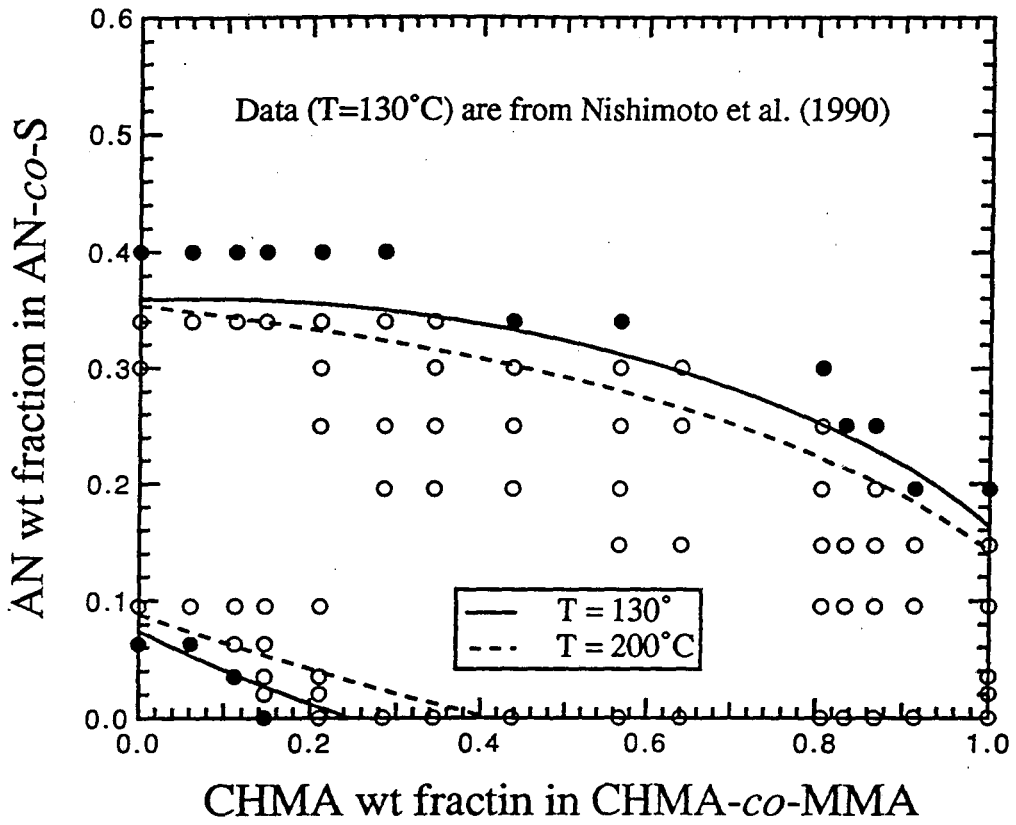
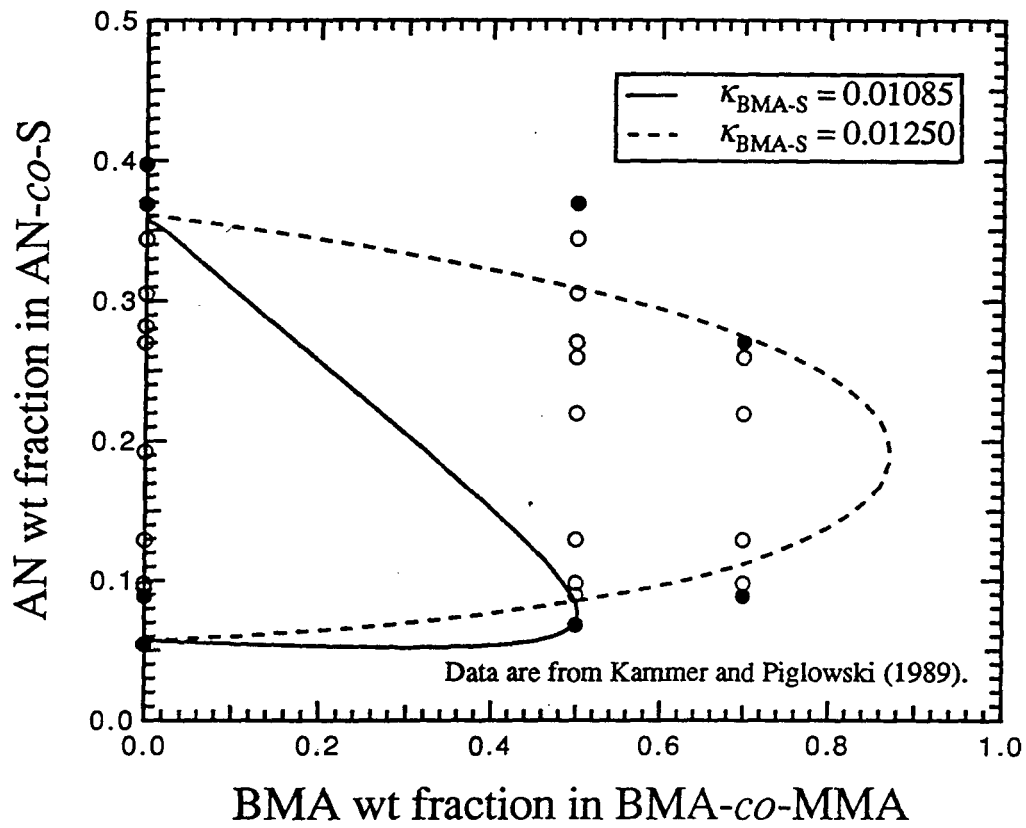


Figure 10



LAWRENCE BERKELEY LABORATORY
UNIVERSITY OF CALIFORNIA
TECHNICAL INFORMATION DEPARTMENT
BERKELEY, CALIFORNIA 94720